ADAPTIVE OUT-OF-STEP RELAYING WITH PHASOR MEASUREMENT

by

Virgilio Antonio Centeno Zaldivar

Dissertation submitted to the Faculty of the

Virginia Polytechnic Institute and State University

in partial fulfillment of the requirements for the degree of

Doctor of Philosophy

in

Electrical Engineering

APPROVED BY

Prof. Arun G. Phadke, Chairman

Prof. Robert P. Broadwater

Prof. Jaime De La Ree

Prof. Werner Kohler

Prof. Yilu Liu

August 1995

Blacksburg, Virginia

ADAPTIVE OUT-OF-STEP RELAYING WITH PHASOR MEASUREMENT

by

Virgilio Antonio Centeno Zaldivar

Prof. Arun G. Phadke, Chairman

(ABSTRACT)

This work describes the development of an adaptive out-of-step relay, from the formulation of its concept to its field implementation and one year testing at the Florida-Georgia interface. This dissertation describes the theory of such a relay, its hardware configuration, the system as it was installed in the field, the major results and improvements obtained after the one year field test, and the adaptive features developed after the analysis of the collected data. Most of the adaptive concepts applied on this relay were used on field application for the first time and proved their value through the one year field test. Synchronized phasor measurements were used for the first time for relaying application, proving their ability to detect and analyze system disturbances through the measurement of angle differences between any two points in a system. It is shown that for a system that behaves primarily as a two-machine power system, the out-of-step relay could be enhanced and made more secure by applying the principle of equal area criterion.

The main contribution of this dissertation is the use and application of old and new adaptive concepts as well as new technology to the solution of the out-of-step problem for a system that behaves like a two machine system. This work provides a solution for the basic stability problem with currently available technology and knowledge. In addition, the data collected during this research has been and will be of great help for those studying the power system stability problem and those developing new adaptive relaying techniques.

Dedicación

Dedico esta disertación a mis padres:

Virgilio Centeno Köelpin quien me enseño a dar mi mejor esfuerzo, enfrentar mis temores y perseguir mis sueños. Su devoción, sacrificio y amor me dieron la oportunidad y motivación para llegar a este momento. Muchas son las memorias, consejos y ejemplos que le matienen a mi lado a pesar de su partida. Que Dios le bendiga papá y le mantenga en su gloria.

Gloria Irma Zaldivar Centeno quien fue mi primera maestra y motivo mi mente y mi alma a buscar el conocimiento en todas sus formas. No existen las palabras para agradecerle por sus sacrificios, consejos, apoyo, ejemplo, devoción y amor. Que Dios le bendiga mamá y le de mucha felicidad.

Acknowledgments

I would like to thank my academic advisor, Professor Arun G. Phadke, for his support, patience, and guidance during the duration of this research work. I thank Professors Jaime De La Ree and Yilu Liu for their continuos support, and Professors Robert Broadwater and Werner Kohler for their genuine interest in this research work. The help, patience, and continuos support of Doctor Robert J. Murphy is also truly appreciated.

I also wish to thank Nora Castro, Steve Turner, Kang Kong, Sharon Anderson, and Pat Manning for their contributions to the research work for this project. The cooperation of Jim Benton, Robert Burnett, Madan Gaudi, Gary Michel, Abdel-Aty Edris, and Melvin Deallerd are thankfully acknowledged.

The financial support for this project by the Electric Research Institute, EPRI, and my financial support from Macrodyne Inc. are gratefully acknowledged.

The direct and indirect help and support of all my friends and lab partners, through all this time, is greatly appreciated. Last but not least I thank my parents, sisters, and brother for their continuos love and support.

TABLE OF CONTENT

LIST OF FIGURES

LIST OF TABLES

1

INTRODUCTION

1.1 Introduction

The development of new technology provides solutions to old problems, creates problems of its own, and forces the engineer to review established practices in search of old and new concepts that could be improved the use of the latest technology. Real time prediction of power system instability is an old and unsolved problem for the relay engineers even for the most simple cases. Newly developed techniques such as synchronized phasor measurements and the improved efficiency and reliability of digital relays allow the application of the old concepts of equal area criterion and adaptive relaying to the solution of the simplest real time stability problem: a system that behaves like a two machine system.

This dissertation begins by introducing one such system and reviewing the techniques used to provide a solution to one class of problems. The developments in adaptive relaying concepts are reviewed and the new technology of synchronized phasor measurement is introduced. The theories of the swing equation and the equal area criterion are reviewed and algorithms for stability prediction using these concepts are described.

The hardware and software used for the relay implementation are presented as well as the results of the laboratory tests used to confirm proper operation under realistic conditions.

Without proper field testing the developed algorithms and hardware are of little use to the relaying engineer. The results obtained in a one-year field test of the system are presented as well as the algorithm modifications suggested by the experience gained in the field. Conclusion as to what was learned and what still needs to be improved for solving the problem of adaptive out-of-step relaying with phasor measurements for a two machine system are given. Some ideas are discussed on the application of this technology for power system models with three or four machines.

1.2 Outline of the Dissertation

Chapter 1, Introduction, the remaining sections of this chapter introduce the key concepts, present the scope of this dissertation, and provide information on the bibliography review.

Chapter 2, Florida-Georgia Power Systems and Out-of-Step Relaying, presents a brief history of the development of the Florida-Georgia interconnection and its stability problem. The latest unstable cases recorded are discussed together with the steps taken for their solution, their limitations, and the problems that still need to be solved. The concepts and applications of out-of-step relaying presently used by electric utilities are reviewed with emphasis on their limitations.

Chapter 3, Adaptive Relaying and Phasor Measurement, reviews the evolving concept of adaptive relaying with the use of computer relays. The possible adaptive applications to the out-of-step relaying problem are discussed. A brief history of the new technology of synchronized phasor measurement is presented reviewing the key concepts and the capabilities of the available equipment.

Chapter 4, The Swing Equation and The Equal Area Criterion, presents the derivation of the swing equation based on the assumptions of classical stability and a two machine model. The equal area criterion for stability is explained for a one machine infinite bus system and for a two machine system. The concept is later applied to the solution of stability swings for faults and loss of generation cases, as they apply to the Florida-Georgia system.

Chapter 5, Relay Implementation and Laboratory Testing, the hardware used to implement the relay unit is functionally described. The software implementation of the algorithms is discussed in detail based on the equations derived in chapter 4. Flowcharts are given for the most important subroutines.

Chapter 6, Field Installation and Results, presents the complete structure of the adaptive out-of-step relay system and describes its field installation. This chapter also reviews the most significant cases detected and recorded by the system during its 15 months of field testing. The results obtained by the relaying algorithms are presented and discussed for each the major cases.

Chapter 7, Algorithm Changes, discusses the model problems discovered during field testing, especially those caused by the occurrence of unexpected compound swings. Solutions to these problems are discussed, and tested with the collected field data. All the solutions presented in this chapter are based on the analysis of the data collected during the field tests.

Chapter 8, Conclusions and Future Work, contains a list of conclusions derived from the experience obtained from the implementation of the out-of-step relay. A list is also given for recommended future work that will enhance the knowledge obtained from this application.

1.3 Key Concepts

i. ***Adaptive Relaying***: "is a protection philosophy which permits and seeks to make adjustments to various protection functions in order to make them more attuned to prevailing power systems conditions."[1]

ii. ***Out-of-Step Condition***: A condition by which a transient swing brings the generator rotor angle past its unstable equilibrium point, where an increase in the angular

[1] S.H. Horowitz, A.G. Phadke, J.S. Thorpe."Adaptive Transmission System Relaying", IEEE Transactions on Power Delivery, Vol. 3, No. 4, October 1988, p. 1463.

displacement results in torques which move the rotor further from its equilibrium point [78].

iii. ***Synchronized Phasor Measurement***: Is a procedure by which the fundamental frequency component of positive sequence phasor is measured from a given three phase input [10].

iv. ***Transient Stability***: Sudden changes in the power system that affect the short time stability of the generators as they move with respect to the center of inertia. A system is considered transient stable if following a disturbance the rotor angles of all its generators settle at an acceptable steady state angle [78].

v. ***Equal Area Criterion***: A direct energy method for a two machine system that predicts system stability based on the behavior of the kinetic energy during a system transient [77], [78].

1.4 Scope of this Dissertation

The goal of this work is the application of synchronized phasor measurement and adaptive relaying to the solution of the stability problem for a system which can be accurately modeled by a two machine system. The classical model for stability is adopted for the developments of the key assumptions for the system model. The developed relaying system is considered to be a learning tool where concepts are tested and valuable field data is collected for the testing and improvement of adaptive out-of-step relaying

algorithms. No action was taken on the system by the relaying units and all the results were recorded for post-disturbance analysis and evaluation.

1.5 Bibliography Review

A list of the most significant references on the concepts and topics related to the out-of-step relay system is presented in Appendix B. This list, consisting of more than one hundred references, is classified by subject as follows: General Knowledge, Phasor Measurement, General Relaying, Out-of-step Relaying, Adaptive Relaying, Florida Georgia Interconnection, Stability, and System Model. The references in each subject are listed in chronological order. These references form the base of knowledge from which the work presented here has arisen. References for direct quotes taken from specific sources are given at the end of the page where they appear. References to Appendix B are given at the end of a paragraph when the general ideas presented in the references are discussed.

The core of this dissertation comes from the information and concepts in references [3] and [78] on equal area criterion, [10] and [17] on phasor measurement, [36] and [42] on out-of-step relaying, [47] and [52] on adaptive relaying, and [64], [70], [107], and [108] on the Florida-Georgia model.

2

FLORIDA-GEORGIA POWER SYSTEMS AND OUT-OF-STEP RELAYING

2.1 Introduction

The electric power systems in the Florida peninsula are unique in the sense that they are tied to the rest of the country at their northern boundary and their major loads are located in the south and center of the peninsula. Although large amounts of energy are generated in these systems, imported energy is required to meet load demand. The relatively low inertia constant of the system makes it vulnerable to stability swings whenever a disturbance occurs in the major interconnecting links, or when a large amount of generation is lost in Florida. Although less severe at present, this situation has always existed in the Florida system. The nature of the power system in Florida makes it possible to model the Florida-Georgia interconnection as a two machine model allowing the application of an out-of-step relay scheme based on the equal area criterion for the determination of stability.

Out-of-step relays were developed to protect groups of generators from the effects of severe swings caused by disturbances in the system which make the generators lose synchronism with the rest of the system. Unfortunately the parameters of out-of-step relay

schemes are set for specific system conditions which may result in unnecessary trips or blocks when the system state is not sufficiently close to the assumed conditions.

In this chapter a brief history of the Florida Georgia interface is given, followed by a proposed two machine model for the interconnection. The basic concepts of out-of-step relaying are reviewed with a brief discussion on current practices. Finally an adaptive out-of-step relaying scheme is proposed which is expected to provide significant improvements over the traditional out-of-step schemes.

2.2 Recent History of the Florida Interface

Twenty years ago the Florida-Georgia interface consisted of one 230 kV line, two 115 kV lines, one 69 kV line, and a transfer capability between Georgia Power Company, (GAPCo.), and Florida Power and Light, (FPL), of 75 MW [67]. The fast growth of the Florida system in the early 1970's resulted in the addition of large generating units in Florida to meet the growing demand. As these units were added to the system the number of loss of generation cases in the Florida systems increased resulting in increased number of splits between Florida and the eastern United States. These system separations created problems not only for the utilities in Florida but also for GAPCo., which suffered from low voltage problems in its southern area due to the demand produced by the addition of the northern Florida load after system separation. Line protections in Georgia were changed to detect swings between the two systems and force an early split in Florida for those swings which were considered severe enough to cause instability [71]. The relay settings

for this application were fixed and were based on worst case condition. This protection system managed to improve the low voltage problem in southern Georgia but did nothing to reduce the number of separations between the two systems.

In 1979 the first 230kV line connecting FPL and GAPCo. was added between Kingsland substation in southern Georgia and Duval substation in northern Florida. This line increased the interface capacity of Florida to 400MW. Due to the lower price of the coal-fired generation in Georgia compared to the oil-fired generation in Florida, the interconnection operated near its limit most of the time [70]. Twenty system separations occurred during 1980, triggered by loss of generation in Florida [71].

In 1982 the first 500kV line connecting Florida and Georgia was completed between Plant Hatch in Georgia and Duval in Florida. A parallel line was completed a few months later increasing the interface capacity to 1500MW, and was limited by the capacity of the 500/230 kV transformer at Duval. Although the system splits were drastically reduced, the problem still existed. In 1983 a second 500/230kV transformer was added at Duval. This addition and other improvements in the system raised the transfer capacity to 1925MW. Although 1983 was the first year in a decade when no splits due to loss of generation occurred between Florida and Georgia, two system splits did occur during 1984 [71].

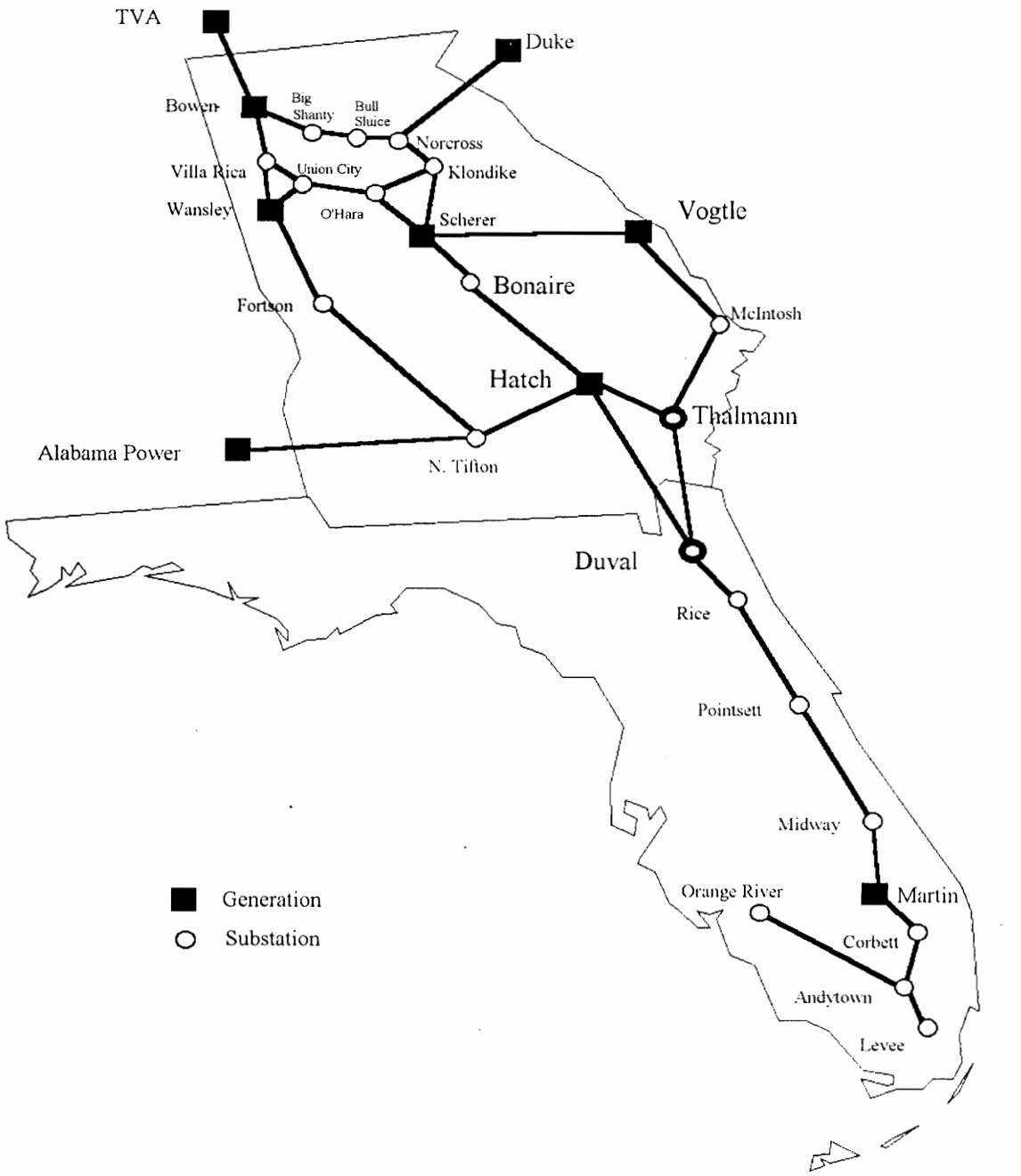

Figure 2.1 *Florida-Georgia 500kV System.*

In 1986 FPL completed its 500kV lines between Duval and southern Florida at the same time Georgia Power completed the 500kV substation at Thalmann. These improvements increased the power transfer capacity to 2900MW and greatly reduced the possibility of separation due to loss of generation in Florida. But in 1987 and 1989 mis-operation of the protective relays at Hatch and Duval caused system separations [73], [74]. In 1993 the power transfer capacity was increased to 3600MW by upgrading the disconnect switches at Thalmann. Figure 2.1 shows the present interconnecting 500kV system between Florida and Georgia.

Simulation studies by the Southern Company show that the interface is stable for the loss of the two largest units in Florida (1200MW) or for a fault on one of the 500kV lines. Due to the strong 500kV ties out-of-step protection in Florida is limited to the 230kV system for the cases when both 500kV lines are lost.

The events of 1987 and 1989 showed that the possibility of stability problems still existed and that it was greater when one of the two 500kV lines into Duval goes out of service, or when the loss of generation in Florida involves more than two of its largest units. To try to reduce the possibility of a system separation a Fast Acting Load Shedding (FALS) program has been implemented to shed load in Florida and maintain stability when [75]:

a) Any of the 500kV transmission lines operates above its rating.
b) The system voltage is too low.
c) A heavy reactive power demand is placed on the generators.

When any of the above conditions is detected the FALS program sheds 80MW of load to stop any problem before it results in a stability swing. FALS also detects loss of generation in Florida and differentiates between losses of 1200MW or greater, in which case complete load shedding of designated distribution stations is performed to avoid a system separation [75].

The FALS system has limited adaptability resulting in several problems which make it vulnerable to mis-operation:

a) Its scan rate of two seconds may cause it miss swings caused by severe loss of generation.

b) Its effect is very limited when one of the 500kV lines is out-of service.

c) It may shed load when it is not necessary to do so.

Due to these shortcomings a protection scheme is needed to perform an early determination of stability swings for severe loss of generation cases, and to block unnecessary trips of the 500kV lines if a stable swing occurs when one of the 500kV lines is out of service. To operate properly such a system should continuously adapt to the changing conditions at the interface and it should give early prediction for unstable swing to enhance the ability for orderly separation of the Florida system into islands with matched generation and load, so that the system could be promptly restored after the separation.

2.3 Florida-Georgia Model

When a severe loss of generation occurs in the Florida system the percentage of the deficiency picked up by the remaining generators in Florida is small due to the lower inertia constant of the system as compared to that of the eastern United States. The rest of the energy demanded by the system tries to come through the 500kV tie lines connecting Florida to Georgia. This demand produces a power swing between the two systems which can be modeled correctly by a two machine system.

In the case of a fault on one of the interconnecting 500kV lines the amount of energy delivered to Florida from the eastern United States is suddenly reduced and it is limited to the transmission capacity of the remaining line. This type of event causes a swing between the two systems as the generators in Florida try to provide part of the energy demanded by the system and the system in Georgia tries to increase its energy delivery through the remaining interconnection. For this case a two machine system can also be used to model the behavior of the Florida system [108].

In order to take into consideration all the possible fault cases in the interconnecting 500kV lines, these lines must be part of the two machine system model used for stability analysis. Figure 2.2 shows the two machine model proposed for the analysis of the stability swings in the Florida system.

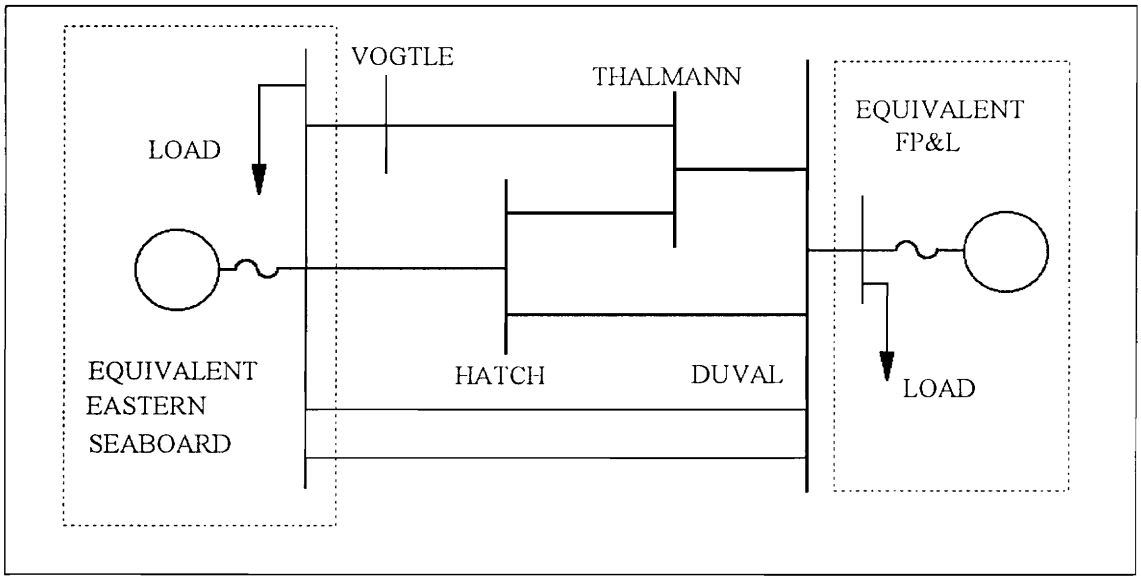

Figure 2.2 *Two Machine Model for Florida Georgia Systems.*

The impedance values for the elements of the six-bus network are given in table 2.1. The darker lines in Figure 2.2 represent actual lines in the system and the lighter lines represent equivalents used to model the remaining 500kV and 230kV lines connecting the system equivalents to the reduced network. The impedances that connect the equivalent systems to the reduced impedance model were obtained by a short circuit analysis of the system at the Duval interconnection; these calculation were performed by FPL.

Table 2.1 Impedances for 6 Bus Model[1]

From	To	Line Length	R	X	B/2
Duval	Hatch	126.18	0.0016	0.0268	1.2782
Duval	Thalmann	78.51	0.0010	0.0166	0.7953
Thalmann	Hatch	65.00	0.0008	0.0138	0.6585
Fla. Eqv	Duval	NA	0.0004	0.0044	0.0000
Hatch	E. Eqv	NA	0.0003	0.0080	0.3816
Thalmann	E. Eqv	NA	0.0026	0.0441	2.0424
Duval	E. Eqv	NA	0.0375	0.3780	0.5005

The machine constant for the two equivalents were computed by paralleling all major generators in Florida and in the Eastern United States. The values of the inertia constants and transient reactances for the proposed model are given in Table 2.2. A large amount of fixed load is assumed for the Eastern equivalent to more closely simulate an infinite bus [108]. The load for the Florida model comes from actual load curves of the Florida system.

Table 2.2 Machine Data for System, 500kV and 100MW Base.[1]

Machine	H Constant Seconds	Transient Reactance X'_d in PU
Fla. Eqv	948.98	0.0010
E. Eqv	3758.82	0.0003

[1] S.L. Aderson, "Reduced Order Power System Models", Master Thesis, Virginia Tech, Blacksburg, VA, December 1993, pp. 29-30.

Simulations have been run comparing the two machine model to a full system model. The simulations show that the two machine model is adequate for the analysis of the stability swings in the Florida system. A better model could be obtained by using a three or four machine system which will show the modes of oscillation inside Florida [108]. Such models although more accurate, require more complex algorithms for their analysis and additional measurement units and system information, which makes their implementation impossible with the presently available hardware and communication system.

2.4 Out-Of-Step Relaying

When a stability swing occurs between two machines, their angle difference increases as the power flow between them increases. If the angular difference increases monotonically the units are said to go out-of-step and an unstable swing develops. Protection against these kinds of swings is known as out-of-step relaying or loss of synchronism relaying.

In addition to detecting unstable swings, out-of-step relaying schemes must take action to prevent or minimize the unstable swings. Such actions involve:

1. Block tripping of lines for stable swings.
2. Selective tripping of lines for unstable swings. Line tripping should leave a satisfactory generation and load balance in the separated systems.
3. Block line reclosing on unstable swings.

4. Minimize breaker stress by initiating tripping before the angles are too far apart.

In the following paragraph the traditional methods of out-of-step relying are explained and some of the new approaches are briefly discussed.

2.4.1 Present practice on Out-Of-Step Relaying

Two different criteria are used for the determination of stability by traditional out-of-step relays. These criteria are dependent on the specific application. For out-of-step protection of individual generators against three phase faults on the transmission line connecting the generator to the system, a critical clearing time criterion is used to protect the generator against three phase faults. The critical clearing time is computed off-line by equal area calculations and is the minimum time available to clear a three phase fault before the generator loses synchronism with the rest of the system [36],[66]. This criterion is for a specific contingency and for the protection of an individual generator.

The second criterion is based on the movement in the R-X plane of the angle difference between the generators due to the swing in the power flow [42]. This criterion will be explained in more detail since it is more applicable to the stability problem between systems that can be modeled as a two machine system.

Traditionally protection of transmission lines is performed with distance relays. It is therefore not a surprise that distance relay characteristics are widely used for out-of-step relay applications. The impedance variation, as observed by distance relays, is a function of the system voltage and the angular difference between the systems, equation 2.1.

$$Z_{12} = \frac{E_1 \angle \delta_1}{Y_{12}(E_1 \angle \delta_1 - E_2 \angle \delta_2)} \tag{2.1}$$

By proper interpretation of the movement of the impedance in the R-X plane as shown in Figure 2.3, the angular displacement of a generator with respect to the system can be monitored and out-of-step conditions can be detected.

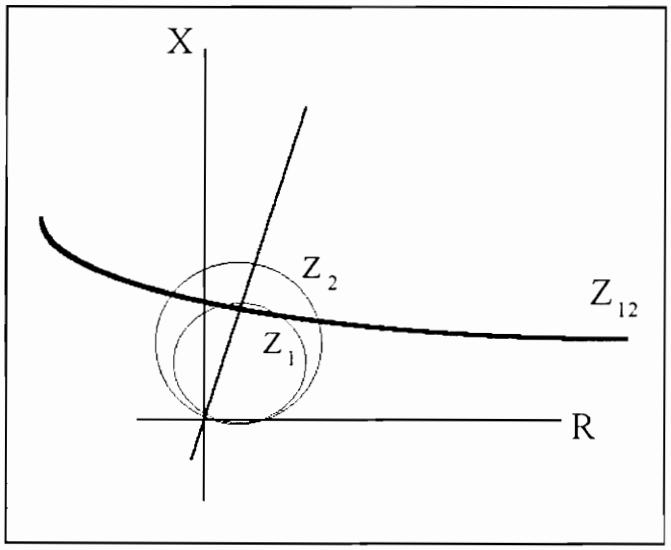

Figure 2.3 *Impedance Plot in R/X plane*

The increase in the angle difference during system swings reduces the impedance seen by the distance relays, and may produce apparent impedance values similar to those seen during high resistance faults. But unlike the almost instantaneous change seen during a fault the changes seen during a swing occur gradually. This different reaction of the impedance seen by the relay for faults and swings is used by the traditional out-of-step relays to differentiate between faults and stability swings. This is accomplished by using a timing mechanism and two distance relays having vertical or circular characteristics in the

R-X plane [43]. When the time used by the impedance to cross the two characteristics exceeds a pre-set value an out-of-step detection is initiated and if the second characteristic is crossed the swing is considered unstable.

An out-of-step relay with vertical characteristics is called a blinder scheme and can be performed with a single or a double blinder as shown in Figure 2.4. A single blinder scheme is appropriate for out-of-step tripping while a two blinder scheme is appropriate for line tripping and reclose-blocking for unstable swings, and trip-blocking for stable swings [36].

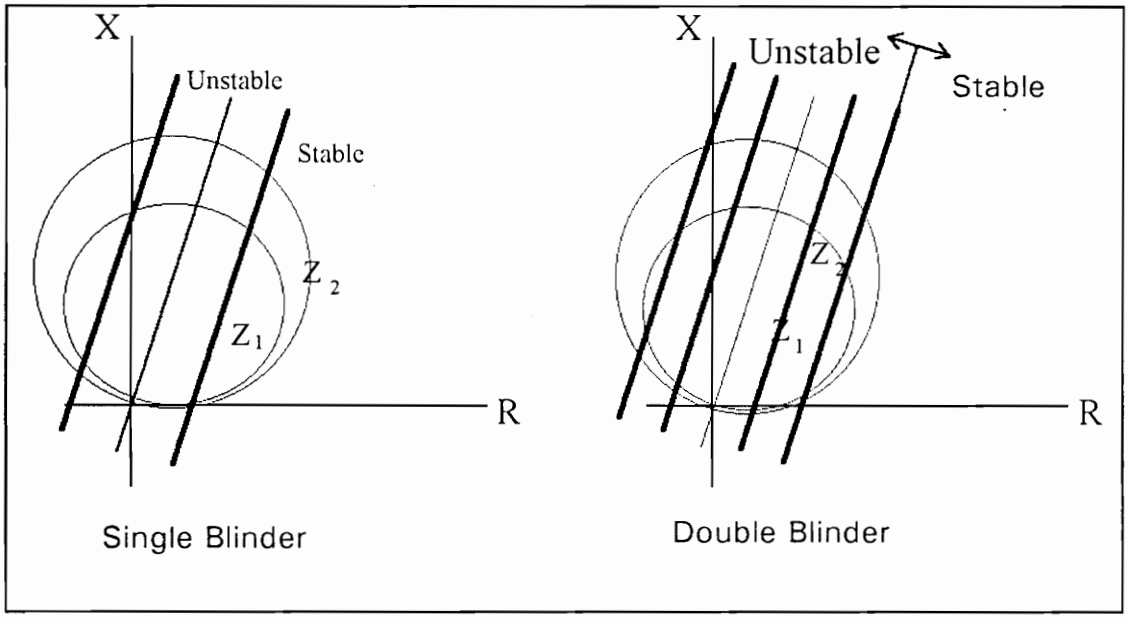

Figure 2.4 *Blinder Type Out-of-Step Relaying Scheme*

A circular characteristic out-of-step relay is known as the mho element scheme (Figure 2.5) which is more appropriate to block the tripping of lines for an stable swing or

block re-closing for an unstable swing. It may be used to initiate tripping on unstable swings [36].

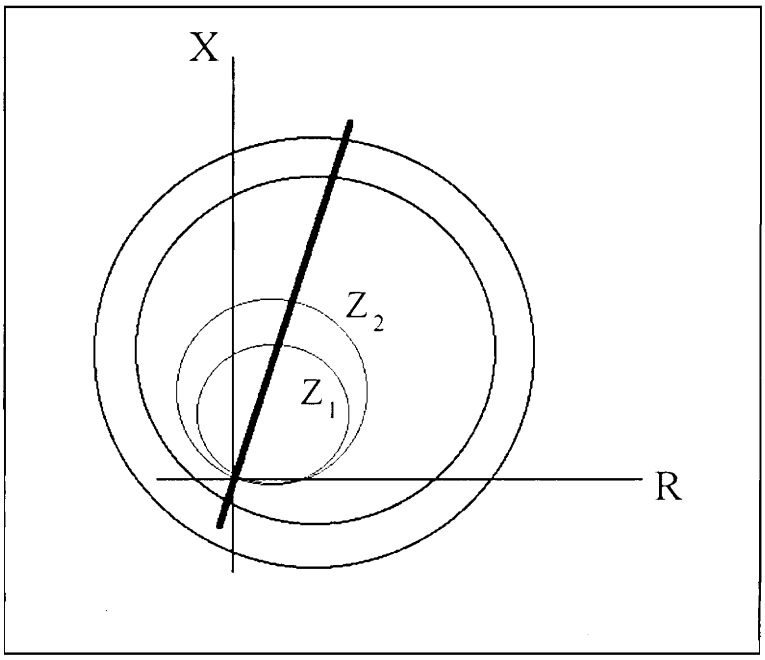

Figure 2.5 *Mho Element Out-of-Step Relaying Scheme*

The determination of the impedance value that differentiates between a stable and an unstable swings is achieved by simulation of faults at different load levels and different system conditions. By running several simulations a region is found in the R-X plane beyond which all the oscillations are always unstable. By setting a zone of protection equal to this region (with a safety margin) any swing entering the protection zone will be considered unstable and all swings outside this zone will be considered stable [43].

2.5 Proposed Out-of-Step Scheme

Traditional out-of-step relaying is characterized by its lack of adaptability to changing system conditions, since its parameters are usually set for specific system conditions that define the worst case scenario. In addition, it uses the line impedance loci of equation 2.1, which is an indirect function of the angle difference, to detect swings and determine if these swing are unstable.

A new out-of-step relaying scheme is proposed for the Florida-Georgia interface relay that is not only adaptable to the system conditions, but uses angle measurement instead of impedance loci to detect swings and determine the degree of stability of the angle swings between Florida and the eastern united States.

To accomplish this out-of-step relaying scheme the new technology provided by the synchronized Phasor Measurement Unit (PMU) is required to directly measure the angle difference between any two points in the system. By measuring the angle difference at the interconnection, angle swings can be easily detected. The reduced network model of Figure 2.2 can then be used to determine the angle difference between the two system equivalents.

The use of a specially designed digital relays with communication capability allows the detection of events in the system that change the system parameters. The two machine model used must be updated to properly determine the system stability. This feature makes

the proposed out-of-step relaying scheme adaptable to critical system conditions. Some of the most important features of the proposed relay system are:

a) Detection of opening or closing of critical transmission lines to update the impedance used in the system model.

b) Use of actual load curves from the Florida system to more closely reflect the load changes in the Florida model.

c) Use of an accurate two machine model of the system to determine the angle difference between system equivalents.

d) Use of PMUs to obtain a measurement of the angle difference used to detect angle swings.

e) Use of the equal area criterion to determine the degree of stability of the angle swings.

It is also proposed that this out-of-step relay system be implemented, tested and installed in the field. The testing of this new concept with actual field data helps validate and improve the system models and relaying algorithms. In addition the recording ability of the digital relays allows the storage of valuable field information that could be used for future development and testing.

3

ADAPTIVE RELAYING AND PHASOR MEASUREMENT

3.1 Introduction

The increased reliability, speed, and computational power of digital computers have made digital relays a feasible option for power system protection. Digital relays have the ability to receive external information, store it in memory, and change the relay software logic based on this new information. These characteristics of digital relays allow the application of innovative concepts and numerical techniques for the protection of the different elements of a power system.

Adaptive relaying is an old concept that has been taken to a new level by digital relays that adapt to the prevailing power system conditions. Digital relaying has also made possible the use of new techniques like synchronized phasor measurements in which the Discrete Fourier Transforms, DFT, are used to obtain a phasor representation of the fundamental frequency component of voltages and currents in the power system.

In this chapter the adaptive relaying concept is explained underlining the adaptive features used in the out-of-step relay system. Phasor measurement algorithms and Global Positioning System, GPS, synchronization are briefly explained and a short history of phasor measurement is given from the initial relay units to the presently available commercial units.

3.2 Adaptive Relaying

Adaptive relaying has been defined as the ability of relays to change their parameters, operation, or logic to adapt to prevailing system conditions [52]. This concept has reached a new level with the use of digital relays but is clearly not a new concept. Adaptive features have been present in relays for a long time: directional relays change their operation based on the direction of the fault current, time-delay overcurrent relays vary their operating time according to the fault current magnitude, and transformer differential relays use harmonic restraint to differentiate between fault and inrush currents [31]. But these adaptive abilities of electromagnetic and solid state relays are very limited compared to those available in digital relays. Three features make digital relays more suitable for adaptive operation: communication, software logic, and digital memory. External communication gives the relay the ability to detect changes in the surrounding system elements, while software logic allows the relay to change its operation based on the external information. Memory gives the relay the ability to store models and parameters for all possible contingencies, and to save event information for post disturbance study of the relay operation which could later be used to improve the relay algorithms.

For the adaptive out-of-step relay system four adaptive features were planned from the beginning and others where added after some experience was gained with the relay units and system models. The first adaptive feature is that of changing the impedance matrix of the reduced system model based on changes in the status of key transmission

lines. The relay system receives external information on the status of the circuit breakers of four critical transmission lines. When the external status indicates a change in one of these lines the current magnitude of the specific line is compared to its previous value to confirm that the state of the line has changed. If the change in magnitude of the current in the line agrees with the status of the circuit breakers the relay updates the impedance matrix used by the relay algorithms. Impedance matrices for every possible line outage including compound cases are stored in the relay memory. Besides changing the impedance matrix of the model, the relay predicts the stability of the swing caused by the line switching.

The second adaptive feature of the relay system is that of changing the system load used in the Florida model to reflect a normal load curve in the Florida system. Three load curves were included in the relay memory for weekday, Saturday and Sunday loads. The relay uses the system date and time to update the load value hourly from the stored load curves. The date of the year is checked to determine if a weekday or weekend curve should be used. Load adaptability can be improved by using seasonal load curves or by periodically updating the load curves using more recent data.

The third adaptive feature of the relay is that of increased security on the stability prediction for fault cases. When a fault occurs the relay predicts two stability solutions: one assuming a successful line re-close after thirty cycles and one assuming no re-close. If the stability prediction is the same for both cases the relay trip or block signal is given in

the minimum time. If the outcome will change with a successful re-closing a special output signal is given to indicate that the swing will become stable if the line re-closes after 30 cycles. The relay then waits thirty cycles for a possible re-close before issuing a trip signal; if a successful re-close occurs a block signal is issued.

The last adaptive feature of the relay is the ability to record phasor data from angle swings and line faults in the monitored substations. This data was used to monitor the performance of the relay, update parameters, and change the relay algorithms based on the results obtained during actual swings. This feature proved to be of greates importance in the out-of-step relay application giving the relay the ability to learn from the collected data.

3.3 Phasor Measurement

Phasors are numerical representations of the state of the system where voltages and currents are expressed as RMS magnitudes with a referenced phase angle. Figure 3.1 shows two sinusoidal signals with their respective phasor representations. The use of a common reference for the calculation of the phase angles allows the calculation of the angle difference between any two phasors.

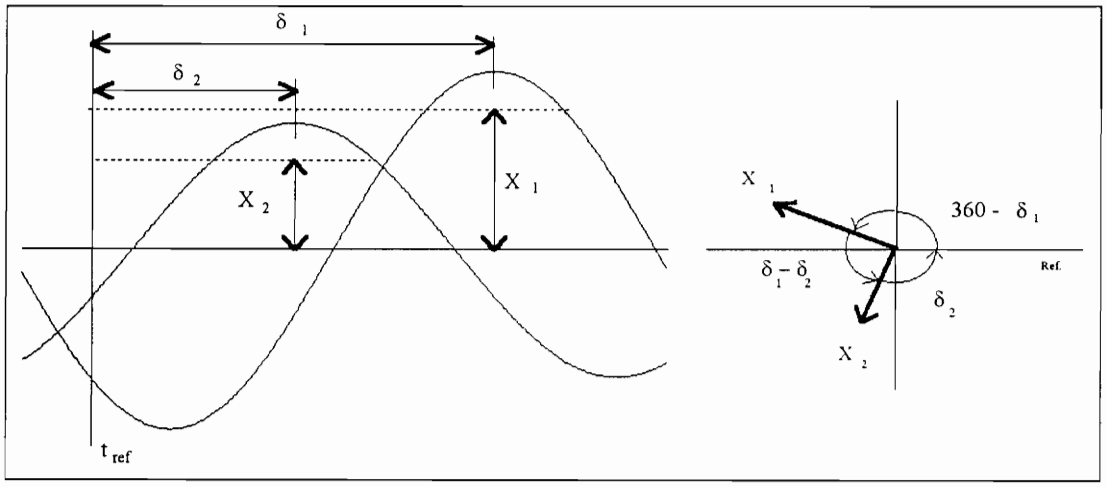

Figure 3.1. *Phasor Representation of Two Sinusoidal Signals.*

3.3.1 Phasor algorithm

As Fourier discovered in 1822, any periodic signal can be represented as an infinite sum of all its frequency components including a DC offset, equation 3.1.

$$f(t) = a_0 + \sum_{n=1}^{\infty} a_n \cos(n\omega t) + \sum_{n=1}^{\infty} b_n \sin(n\omega t) \qquad (3.1)$$

where $a_n = \frac{2}{T}\int_{\frac{-T}{2}}^{\frac{T}{2}} f(t)\cos(n\omega t)dt$, $b_n = \frac{2}{T}\int_{\frac{-T}{2}}^{\frac{T}{2}} f(t)\sin(n\omega t)dt$ and T = period

The a_n and b_n terms are known as the Fourier coefficients and together represent the magnitude and phase angle of the different frequency components in the signal. The notation in equation 3.1 can be expressed in an exponential form to obtain a more practical application in phasor format, equation 3.2.

$$f(t) = \sum_{n=-\infty}^{\infty} d_n e^{jn\omega t} \quad \text{where} \quad d_n = \frac{1}{T}\int_{\frac{-T}{2}}^{\frac{T}{2}} f(t)e^{-jn\omega t}dt \tag{3.2}$$

For digitally sampled signals a Discrete Fourier Transform, DFT, is used where the integral in the d_n coefficients in equation 3.2 for an analog signal becomes a summation over one period of the discrete sampled signal:

$$d_n = \frac{1}{T}\sum_{n=0}^{N-1} x(nT)e^{-jkn\omega T} \tag{3.3}$$

Ideally, signals in a power system have a single frequency component of 60 or 50 hertz depending on the operating frequency of the system. In practice, transformers, loads, and other system elements, as well as system disturbances introduce non-fundamental frequency components into the voltage and current signals. For phasor measurement a DFT is applied to extract the fundamental 60 or 50 hertz component of the sampled signal filtering out any other frequency component present in the signal. The Fourier coefficient for the fundamental component of a discrete sampled signal is given by Equation 3.4.

$$d_1 = \frac{1}{N}\sum_{n=0}^{N-1} x\left(\frac{n\omega}{N}\right)e^{-j\frac{n\omega}{N}} = \frac{1}{N}\sum_{n=0}^{N-1} x\left(\frac{n\omega}{N}\right)\left(\cos\left(\frac{n\omega}{N}\right) - j\sin\left(\frac{n\omega}{N}\right)\right) = Xe^{j\phi} \tag{3.4}$$

Where N is the number of samples per period T of the sampled signal. According to the sampling theorem to describe a signal completely it must be sampled at a rate at least twice the frequency of the component of interest. This required that a 60 hertz signal

be sampled at least at 120 hertz. With a higher sampling rate more information is extracted from a signal at the expense of a higher computational burden. For phasor computations the sampling frequency is determined by the ease of computation of the sine and cosine of the nω/N terms in equation 3.4. Based on this criterion a 720 hertz sampling rate is preferred for 60 hertz signals and a 500 hertz sampling rate for 50 hertz signals. This sampling rate produces sine and cosine factors of ±0.5, ±1.0, and ±0.86602 which, except for the last one, require minimum computational time 38]. Using the notation of equation 3.4 a sinusoidal voltage signal at a valid sampling rate produces the voltage phasor defined in Equation 3.5.

$$v(t) = V_{\max} \cos(\omega\tau + \theta) \Leftrightarrow V = \frac{V_{\max}}{\sqrt{2}} e^{j\theta} \tag{3.5}$$

Equation 3.5 can be applied to every phase of a three phase signal and by incorporating a positive sequence computation with the phasor representation of each phase a positive sequence phasor representation is obtained, Equation 3.6..

$$_1 = \frac{1}{3\sqrt{2}} \left(V_{a,\max} + V_{b,\max} e^{j\frac{2\pi}{3}} + V_{c,\max} e^{-j\frac{2\pi}{3}} \right) e^{j\phi} \tag{3.6}$$

In a similar manner negative sequence or zero sequence phasors can be computed for any three phase signal, but for many relaying operations the positive sequence phasor is of more practical use. Statistical or numerical techniques can also be applied to the phase angle obtained from equation 3.6 to estimate the frequency and frequency deviation

of the sampled signal. This frequency is the local frequency of the system which when averaged over longer periods reflects the behavior of the system frequency [10].

3.3.2 GPS Time Synchronization

To allow for the computation of the angle difference between two signals they must be sampled at the same time and the DFT factors must be applied in the same order. Samples taken at the same site are easily synchronized by using sample and hold techniques or a common sampling pulse. Samples taken at different locations require that a precise synchronizing pulse be available at each measurement site to guarantee synchronous sampling of the input signals [11].

For 60 hertz signals a one microsecond accuracy between synchronized sampling pulses is required to measure angle differences with less than 0.02 degree of error. Several timing system techniques can be used to obtain the required synchronization but the only system available worldwide with the desired precision is the Global Positioning System, GPS. The precise timing option in GPS receivers gives a one second synchronizing pulse with a less than 500 nanosecond error from which a sampling pulse can be derived with less than 1 microsecond error between sampling pulses, guaranteeing a 0.02 degree accuracy in the computation of any angle difference.

The GPS system was developed by the US Department of Defense, DOD, between 1974 and 1994. It consists of a constellation of 24 satellites distributed in three half-geo-stationary orbits, Figure 3.1.(a). These satellites are constantly monitored from Master

Control Stations, MCS, to guarantee the accuracy of the timing signals of each satellite. The distribution of the satellite orbits guarantees a world-wide coverage by a minimum of six satellites and a maximum of eleven at any place on the planet where a receiver has clear view of five degrees above the horizon [6], [7], [22].

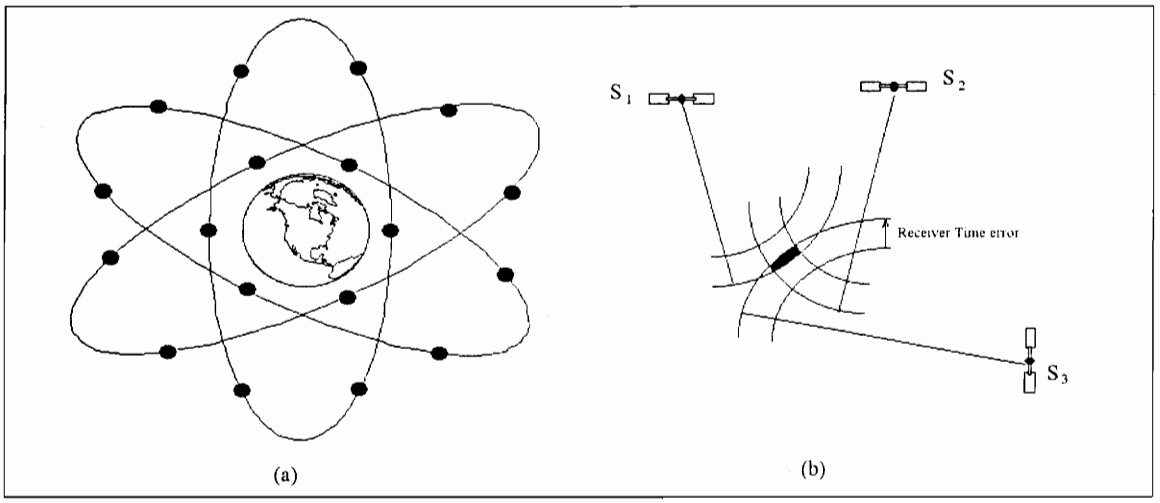

Figure 3.2. (a) GPS System Configuration. (b) Position Concept in 2 Dimensions.

The main purpose of the GPS system is to provide precise three dimensional positioning and velocity for vehicles anywhere in world. In a oversimplified explanation GPS receivers multiply the time delay of the signals received from the satellites by the speed of light to determine the distance between the receiver and the satellites. To allow the receiver to correct for delays in the satellite signals due to ionospheric disturbances each satellite transmits two L-band frequencies at 1227 and 1575 Megahertz. Almanac information received from the satellite allows the relay to determine the exact position of

any four satellites and use the distance to the satellites to establish its exact position [8]. Three satellite signals are used to estimate the receiver position, Figure 3.2.b, and the fourth signal is used to correct for position errors due to the low precision in the receiver time reference. The use of the fourth satellite to correct for errors in the time signal of the receiver eliminates the need for a precise and expensive time signal for each receiver. The time signal transmitted by the satellites is derived from two Cesium and two Rubidium atomic clocks on board each satellite which guarantee a very precise timing signal [7].

When the position of a site is known and fixed the precise time signal of a single satellite can be used to obtain a one second pulse in the receiver with a precision of 100 to 200 nanoseconds. Due to the military applications of the GPS system, a Selectable Availability, SA, option can be used by the military at any time [15]. The common access, CA, is a graded option with a reduced precision of ±500 nanoseconds. Even with this reduced precision the GPS receivers with CA capability are accurate enough to allow measurement of angle differences of 0.02 degrees [16].

For phasor measurement applications GPS receivers are set to determine their precise locations after initial installation. Once the location is known it is saved by the receiver and it is used to allow time synchronization with a single satellite signal. The signal obtained from the receiver is a one second pulse with its corresponding time tag in UTC format. In addition to the GPS receiver, additional circuitry is required to derive the sampling pulses from the one second pulse of the GPS receiver. Since the higher

frequency sampling pulses are derived from the receiver's one second pulse, their time is lower than that of the GPS one second pulse. This reduces the synchronization to a level slightly lower than that of the GPS receiver.

3.3.3 Virginia Tech PMU Development

The first PMUs were implemented at Virginia Tech by graduate students under the supervision of Dr. A.G. Phadke. The first PMU systems were put together from commercially available hardware and consisted of three separate systems: a data processing unit, a GPS clock, and a signal conditioning unit, Figure 3.3 [11], [14].

Each data processing unit, Figure 3.4, consisted of:

- A Motorola MVME133A microprocessor board with a Motorola 68020 microprocessor running at 12Mhz, a Motorola 68881 math co-processor and four megabytes of RAM.
- A Data Translation DT1402-F-16SE A/D board with 16 input channels with a single 12 bit, 4 microseconds A/D converter.
- A Mizar MZ8300 quad serial port board used for local and remote data communication.
- A Prototek 19 inch rack mounted cabinet with power supply and a VME Back plane.

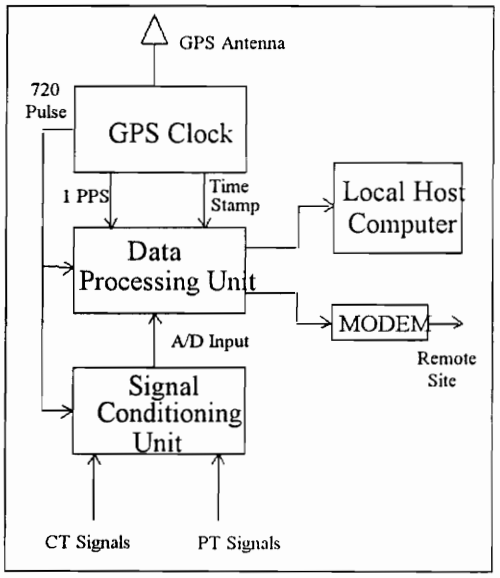

Figure 3.3. *Virginia Tech PMU.*

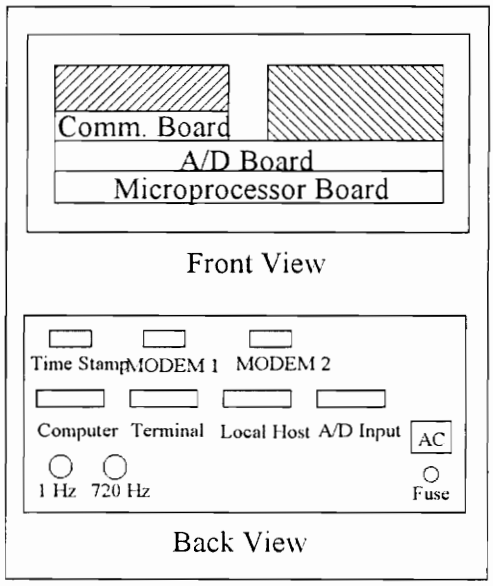

Figure 3.4. *Data Processing Unit.*

The signal conditioner unit consisted of isolation and filtering boards designed at American Electric Power, AEP, and implemented at Virginia Tech. The signal conditioner was developed to guarantee proper isolation and filtering with the required precision for phase angle measurement. It receives a 720 Hz sample and holds the signal from the GPS receiver used to sample the input signals. A parallel connection allows extraction of the held data by the A/D board in the data processing unit.

Two types of GPS clocks were used during the initial development of the PMU: a KODE Model 325 SatSync GPS clock and a Kinemetric Model GPS-DC clock. The manufacturers of both GPS clocks provided special output boards for the 720 hertz signal required for PMU applications. During the early implementation of the PMUs the GPS

system was not complete and satellites were not visible for periods of up to six hours. To avoid the problems caused by the lack of satellite signals the clocks were equipped with a Rubidium crystal oscillator that guaranteed pulse synchronization when the satellite signals were not available.

The Virginia Tech PMUs compute five phasors for fifteen input channels and save the computed data in a one second table every 720th sample and a three minute table every five cycles. A total of 8 tables can be stored in each unit. Data table collection is triggered by preset values for voltage magnitude, frequency , df/dt, angle difference and a linear combination of magnitude, frequency and df/dt. The serial ports allow transmission of a reference phasor consisting of a sample number and a voltage phasor every five cycles. A local host computer is used for automatic table retrieval and for on-line phasor display. Data retrieval is also possible from a remote location by the use of a MODEM.

The first three PMUs were installed on the west coast in the Boneville Power Administration, BPA, system and are functioning as research units at the present time. The second set of five units was delivered to AEP in 1988 and three of them were installed in the field and are still being used by AEP [12]. The algorithms running in the data processing unit have been modified by AEP engineers. The last set of three units was delivered to New York Power Authority in 1990 and two of those units are presently used to monitor the 750kV line between Marcy and Massena [13].

3.3.4 Commercial PMU

The PMUs developed at Virginia Tech are a good research tool but they lack the reliability and quality standards required for protection applications. In 1990 a transient recorder manufacturer, Macrodyne Inc, started the development of a commercial PMU with greater computational power, reliability, and flexibility than the research units developed at Virginia Tech.

The Macrodyne Model 1692 PMU can have up to 30 input channels to measure a maximum of 10 three phase input signals. Each input channel has its own 16 bit over sampling A/D with optical isolation for protection from the substations' transients. The A/Ds sample the input signals at 2880 Hz using a synchronized pulse derived from the 1 pulse per second, PPS, of the internal GPS receiver. The GPS one second pulse has an accuracy of 100 nanoseconds and the derived 2880 pulses have an accuracy of 500 nanoseconds.

The 2880 Hz sampled input data is digitally filtered with a low-pass Finite Impulse Response, FIR, filter with a cutoff frequency of 360 Hz to allow data decimation to 720 Hz. The PMU performs DFT and positive sequence transformation on each group of three phase sampled signals to obtain a positive sequence phasor of the fundamental frequency. The first three input channels of the PMU are reserved for the substation voltage whose phase angle is used to compute the local frequency and df/dt at the

substation. The steps of the DFT algorithm are synchronized to the one second pulse to eliminate angle shifts when angles are compared between different PMUs.

Figure 3.5 shows the block diagram of the Phasor Measurement Unit developed by Macrodyne Inc. As can be seen all the components are incorporated in a single unit. In addition to providing the internal synchronizing signals, the GPS receiver is used to generate synchronizing signals for use by other equipment in the substation. An incorporated LCD display and keypad eliminate the use of a local computer to communicate with the unit. A universal AC/DC power supply allows the unit to operate with input power from almost any AC or DC source including the substation batteries.

The GPS receiver inside the PMU determines its position from the set of four satellites with better distribution. Once the position is determined to a pre-selected accuracy the site coordinates are locked and saved as the fixed location of the unit. A precise 1 PPS is then available with only one satellite signal. GPS synchronization of the sampling pulses allows accuracy of 0.02 degrees in the angle differences measured by PMUs at different sites. Along with the 1 PPS, the GPS receiver sends a time tag every second that contains the day of the year (1-365), hour (0-23), minute (0-59) and second (0-59). This tag is received and stored by the PMU to time tag the 1 PPS signal while a sample number is used to time tag the 720 Hz input data.

The PMU has 16 digital channels used to monitor the status of the substation's switches, breakers and any other switching operation. Each digital channel can be enabled separately for triggering, provided its normal state (open or close) is defined. In the out-of-step relay implementation the digital channels of the PMU are used to monitor the status of the phase 'a' breaker of the critical transmission lines between the two measurement sites.

The 1692 PMU has two serial communication ports both of which are used in the current application. Port 1 is connected directly to the local relay unit and runs at 38,400 Baud with CTS/RTS handshaking used for data control. Through this serial port a complete time tag, sample number, PMU status, digital channel status, a voltage phasor and two current phasors are passed to the relay unit. The second PMU serial port runs at 9600 baud and is used for host communication to collect data tables, monitor the status of the PMU and change its operational parameters.

A DFT algorithm is used to compute the fundamental frequency component of each three phase input signal using a full data window (12 samples). The software combines a positive sequence transform with the DFT algorithm to obtain a positive sequence phasor from each set of three phase inputs. Phasor data from the DFT is stored in four groups of circular tables that are saved when a trigger (explained later) is detected by the PMU's trigger subroutine.

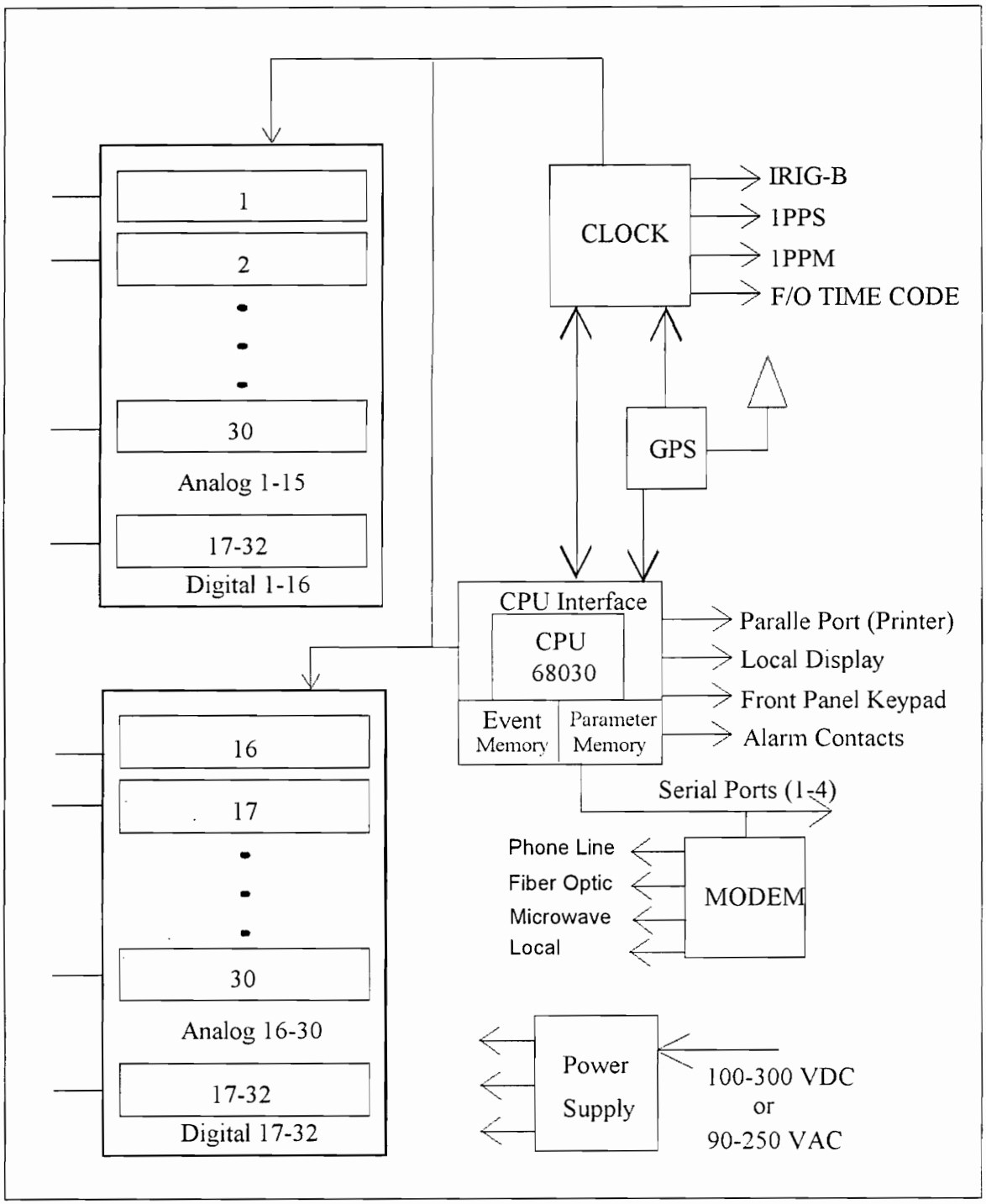

Figure 3.5. *Block Diagram of Macrodyne's 1692 Phasor Measurement Unit.*

Each group of tables consists of a trigger information table, a one second phasor table, a one second input table, and an extended data table. The information table contains the time of the trigger, status of the PMU, and parameter settings at the time of the trigger.

The two one-second tables store 720 lines of data taken every sample and give a close look at the system transients for a whole second. The extended table stores 16,560 lines with a variable time length of 9.2, 23, or 46 minutes depending on the selected output rate of 2, 5, or 10 cycles. The amount of pre-trigger data of both tables is selected separately for each type of table and varies from zero to the maximum number of lines in the table. For the out-of-step relay project the PMUs are set for a 100 line pre-trigger in the one second table and 200 lines in the extended table with an output rate of 2 cycles (9.2 minutes length on the extended table).

Due to limitations of the communication channels, on-line data output is not possible at the 720 Hz effective sampling rate of the DFT algorithm. For this reason, the PMU's on-line data is averaged and output at user selected rates of 2, 5 or 10 cycles (every 24, 60, or 120 samples). The on-line data from the PMU is divided into fixed on-line data that is always available, and user selected data that is set by the user through one of the serial ports or the front panel keypad. The fixed part of the on-line data consists of voltage phasor, frequency, df/dt, sample number, and status flag . To these the user can add a complete time tag, any combination of the sampled phasors, an additional status

flag, and the status of the digital channels. The on-line data is preceded by a leading flag and followed by a checksum that is computed by or-ing all the bytes of the on-line data string. For the out-of-step relay system the PMU is set by the relay unit to average phasors every 2 cycles (24 times per second) and to send on-line data consisting of voltage phasor, 2 current phasors, digital channel status, sample number, complete time tag and status flag. The frequency and df/dt are sent as part of the on-line data but are not used by the relay unit.

Seven different triggers are available in the PMU to determine for which events the data tables should be saved:

a. Voltage Maximum: This trigger compares the per unit magnitude of the substation voltage phasor to a user selected voltage maximum and produces a trigger when this value is exceeded.

b. Voltage Minimum: Voltage phasor magnitude is compared to a user selected minimum; when the voltage magnitude drops below this value a trigger occurs.

c. Angle: This trigger is only valid when a reference phasor is being received by the PMU. A trigger occurs when the absolute value of the referenced angle changes from the previous value by an amount greater than the trigger limit.

d. Frequency: The absolute value of the difference in frequency from 60 Hz is compared to the frequency trigger limit and if exceeded a trigger occurs.

e. df/dt: This is similar to the frequency trigger but in this case the df/dt value is used.

f. Digital Channels: Change of status from normal to alternate status on a digital channel causes a table trigger when the specific digital channel is enabled for trigger.

g. Linear Combination: A linear combination of frequency, df/dt, and voltage magnitude larger than a selected value will produce a table trigger.

h. User trigger: Table triggers in the PMU can be forced by the user through the host computer.

Any trigger requires that table space be available, triggers be enabled, and GPS signal be valid at the time of the trigger. In addition, digital channels also require that the particular channel be enabled for a trigger to occur. A user requested trigger is valid any time as long as table space is available in the PMU memory. Upon initialization of the out-of-step relay system the relay units set the trigger parameters, output rate, and on-line data of the local PMUs. Saved, or frozen tables from the PMUs are recovered by a host computer with the option of freeing the space used by a table or leaving the table in the PMU memory. Tables collected from the PMUs of the out-of-step relay system were used to analyze and evaluate the operation of the out-of-step relay algorithms and models. The triggers in the PMUs were set to save tables when a disturbance occured in the voltage phasor magnitude or when one of the digital channels monitoring the circuit breakers of critical transmission lines changed status.

3.3.5 PMU Testing

On June 25 and 26, 1992 a series of line switching operations were performed on 500kV lines at Plant Scherer in the Georgia Power Co. system. With the cooperation of Georgia Power Company, Tennessee Valley Authority, Florida Power and Light, and Macrodyne Inc, PMUs were installed in six locations in three states, Figure 3.6, to test the detection of angle swings by the PMUs and to revalidate simulation models of the Southern Company [30].

The test consisted of the opening and closing of the circuit breakers of the Scherer-Klondike and Scherer-Bonnaire 500kV lines. The recorded swings were later compared to system simulations of the same events. The tests showed that the PMUs were capable of recording system wide swings and that the model used by Southern Company was good in comparison with actual system measurements. Figure 3.7 shows the angle swings obtained from the PMUs and from the simulation. All angles are referenced to the angle at Plant Scherer. The simulation is more accurate for the area surrounding the Scherer test area, where better simulation results were expected, and less accurate for the Florida and Tennessee locations where equivalents were used to represent the systems external to the Southern Company [30].

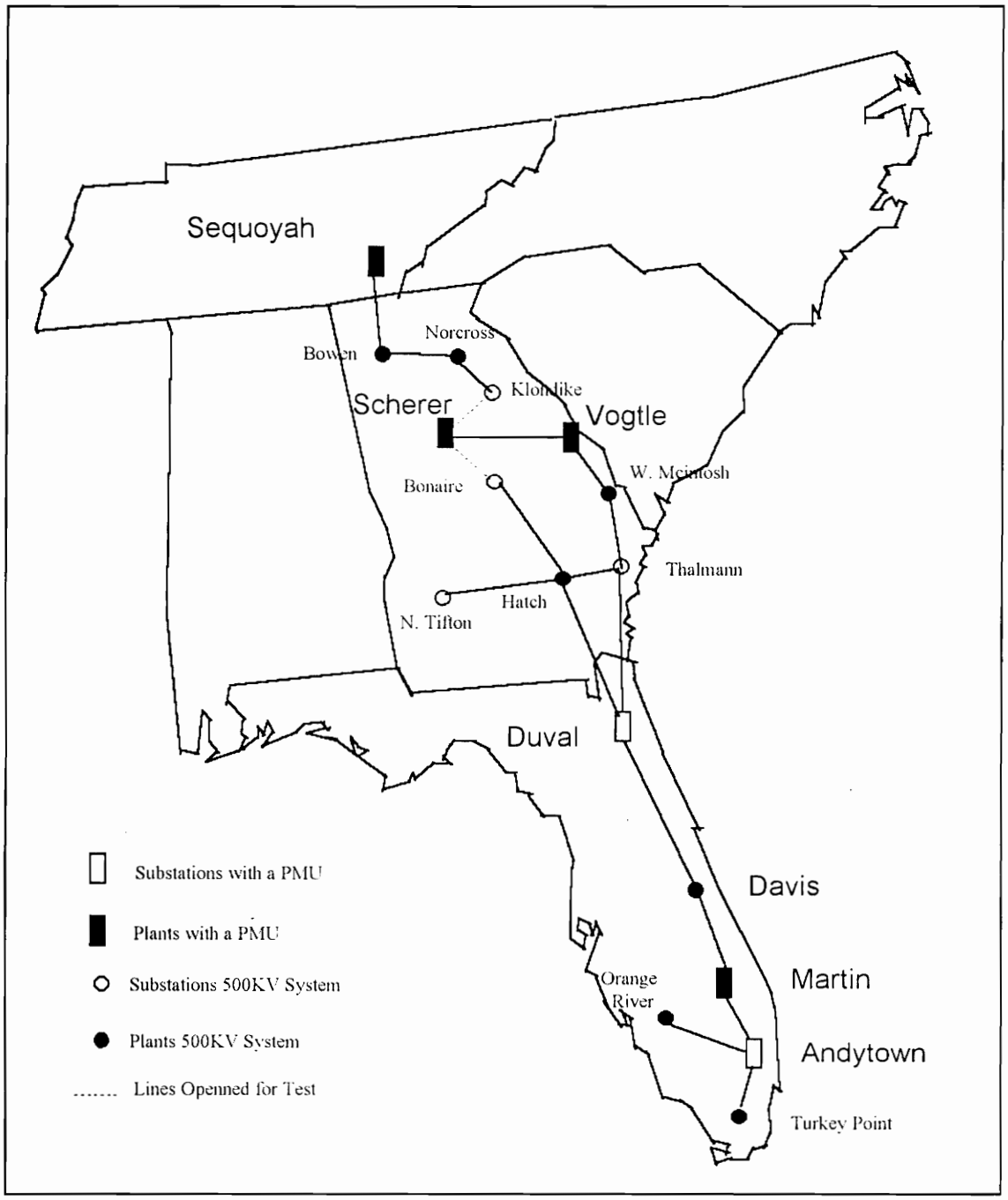

Figure 3.6. *PMU distribution for 1992 Disturbance Test.*

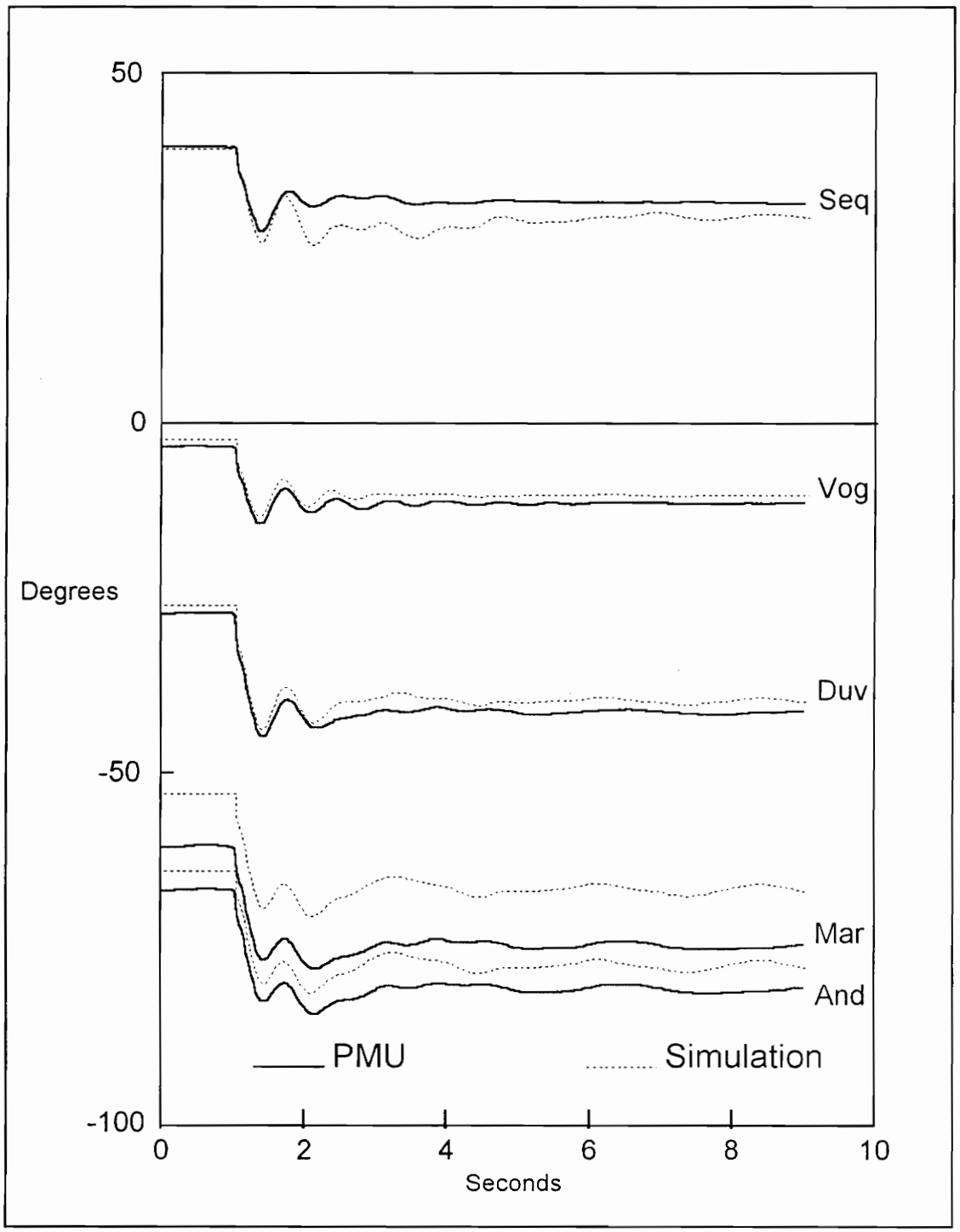

Figure 3.7. Angle Plots for 1992 disturbance test, Plant Scherer Angle as Reference.

4

THE SWING EQUATION AND THE EQUAL AREA CRITERION

4.1 Introduction

The development of the out-of-step relay system requires that assumptions be made for the development of a system model. Once a model is established the key concepts can be applied for the development of the relaying algorithms. In this chapter section 4.2 lists the major assumptions made for the development of the out-of-step relay. In section 4.3 the swing equation is derived and applied to a two machine system. Section 4.4 presents the derivation of the equal area criterion for a finite machine against an infinite bus. Section 4.5 expands the equal area criterion for two finite machines. In section 4.6 the equal area criterion is applied to a fault case and in section 4.7 it is applied to a loss of generation case.

4.2 Model Assumptions

Modeling the Florida systems as a single machine connected to second machine modeling the rest of the country is the major assumption made for the derivation of the out-of-step relaying algorithms. By using a two machine model it is assumed that all major generation in Florida swings coherently against the eastern United States. Studies and

simulation have shown that a two machine model is valid for most of the power swings seen in the Florida peninsula, specially for those that affect the stability of the 500kV interconnection at Duval. Simulations have also shown that a three or four machine model for the Florida systems will be better for the detection of modes of oscillations inside Florida [108]. But before the three or four machine model could be applied, the case of the simpler two machine model must be solved and tested to establish its true limitations. Besides the two machine model the following assumptions, which include the assumptions of classical stability, are used in the derivation of the models and algorithms used by the out-of-step relay system [91], [98], [100]:

a. The mechanical input power of the generators remains constant for the period of the swing. In a two machine system stability is determined by the first swing whose period of oscillation is of the order of one or two seconds. This period is too short for the governors of the prime movers to take any action that affects the angle swing. And even if any action was taken it will only enhance the stability of the system.

b. Florida and the Eastern United States can be modeled by an equivalent generator represented by a direct axis transient reactance in series with a voltage. Based on the concept of constant flux linkage the classical representation of generators for transient stability is that of an emf behind a transient reactance.

c. The mechanical angle of each equivalent generator coincides with its electrical angle. This assumption is not true for absolute angles, but it is valid for the angle difference.

All angles measured by the PMUs are electric angles but for the algorithms the angle difference and not the individual angles are used.

d. Load for both equivalents can be represented as a constant shunt admittance at the terminals of the equivalent generators. This assumption is made for convenience in the derivation of the swing equation. When load is represented as a constant admittance it can be included in the system impedance matrix reducing the amount of required computations. Several studies have shown that loads have their own dynamic behavior and can vary depending upon seasons and systems. The adaptive nature of the load model used by the relay helps to correct for errors in the constant admittance load model.

e. Damping is negligible. For the first swing of the system the oscillation produced assuming no damping is larger than the actual oscillation giving a more conservative result. This assumption reduces the complexity of the swing equation and allows the application of the equal area criterion.

f. Three phase clearing of faulted lines. This assumption is based on the facts that a three phase faults are more severe for stability studies than asymmetric faults. The protection of lines in the Florida system is set to open the three lines five cycles after any line fault, and a five cycle period is too small compared to the duration of the swing and can be ignored.

g. Angle swings at the Florida-Georgia interconnection are caused by loss of generation in Florida or by a fault in one of the 500kV lines connecting substation Duval in northern Florida to the 500kV system in Georgia.

4.3 The Swing Equation

When a fault or a loss of generation occurs in a power system it creates a sudden loss of equilibrium between the generated power and the power demanded by the system load. Given the assumption of constant input power the only energy reserve in the system is the kinetic energy stored in the rotating masses of the generators. During a disturbance this stored energy is used to deliver additional power to the system in an attempt to reach the new equilibrium power. Depending on the nature and location of the disturbance this rate of change in the kinetic energy changes the electric torque applied to generators' shaft. In the case of a two machine system, Figure 4.1, the angular difference between generators will change resulting in a power swing between the two units.

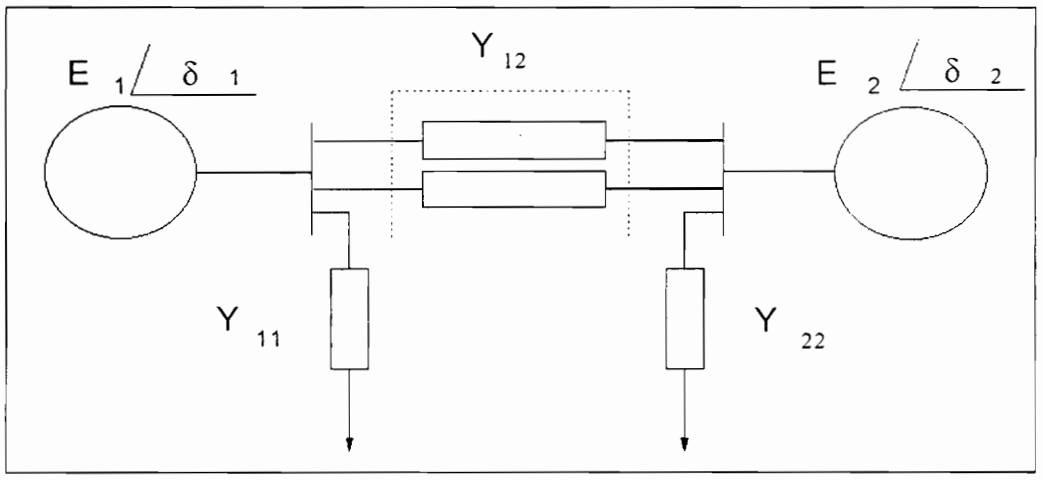

Figure 4.1. Two Machine System.

According to Newton's Second Law any change in the torque applied to the generators will cause an acceleration in the machines' rotor angle, equation (4.1)

$$T = J\alpha^{2} \tag{4.1}$$

Where

T is the sum of all the torques applied to the shaft in N-m.
J is the total moment of inertia of the generator and the prime mover in kg-m.
α is the acceleration produced by the applied torque in mechanical-radians/s^2.

The torque applied to the shaft is divided into a mechanical torque which includes the torque applied by the prime mover less the mechanical losses, and electrical torque which consists of the electric output torque and the electrical losses. There is also a damping torque created by the load, the machine damper windings, and the controllers of the prime mover but it is not considered in this derivation based on the assumption of no damping which reduces the complexity of the swing equation.

The angular acceleration of the generator's shaft in equation 4.1 can be expressed as a function of the mechanical angle of the rotor, equation 4.2.

$$\alpha = \frac{d^{2}\theta_{m}}{dt^{2}} \tag{4.2}$$

where θ_m is the mechanical angle of the rotor in radians.

Substituting equation 4.2 in equation 4.1 and dividing the torque into its electrical and mechanical components gives the well known expression for the swing equation.

$$T_m - T_e = J\frac{d^2\theta_m}{dt^2} \tag{4.3}$$

Assuming that the angular velocity of the rotor, ω_m, is constant for the length of the transient, equation 4.3 can be expressed in terms of mechanical and electric powers.

$$P_m - P_e = J\omega_m \frac{d^2\theta_m}{dt^2} \tag{4.4}$$

where ω_m is in mechanical-radians/s.

Dividing equation 4.4 by the machine rating an expression is obtained for the swing equation in terms of per unit power, equation 4.5.

$$\frac{P_m - P_e}{S_{machine}} = \frac{J\omega_m}{S_{machine}} \frac{d^2\theta_m}{dt^2} \tag{4.5}$$

The moment of inertia information provided by the generator manufacturers comes in the form of the H constant which is defined as the stored kinetic energy in megajules divided by the machine rating in MVA[1], equation 4.6.

$$H = \frac{\frac{1}{2}J\omega_m^2}{S_{machine}} \tag{4.6}$$

Substituting for the moment of inertia from equation 4.6 in equation 4.5 gives equation 4.7.

[1] W.D. Stevensons Jr., "Elements of Power System Analysis", fourth edition, 1982, McGraw Hill, p. 378.

$$P_{m,pu} - P_{e,pu} = \frac{2H}{\omega_m} \frac{d^2\theta_m}{dt^2} \tag{4.7}$$

Since the rotor angles are in continuously increasing the mechanical angle, θ_m , can be expressed in terms of synchronously rotating reference, equation 4.8.

$$\theta_m = \omega_{m,s} t + \delta_m \tag{4.8}$$

Where $\omega_{m,s}$ is the synchronous speed in mechanical radians and δ_m is the rotor angular displacement from the synchronous reference in mechanical radians.

The second derivative of equation 4.8 shows the equivalence between the rotor angle and the angular displacement from the synchronous reference, equation 4.9.

$$\frac{d^2\theta_m}{dt^2} = \frac{d^2\delta_m}{dt^2} \tag{4.9}$$

Equation 4.7 can be expressed in terms of the rotor displacement from the synchronous frame as:

$$P_{m,pu} - P_{e,pu} = \frac{2H}{\omega_{m,s}} \frac{d^2\delta_m}{dt^2} \tag{4.10}$$

Based on the assumption of equality between electrical and mechanical angles equation 4.10 can be expressed in terms of the electrical degrees, δ_e

$$P_{m,pu} - P_{e,pu} = \frac{2H}{\omega_s} \frac{d^2\delta_e}{dt^2} \tag{4.11}$$

where ω_s is the synchronous speed in degrees per second.

To simplify the expression in equation 4.8 the inertia constant, M, is introduced in equation 4.12.

$$P_{m,pu} - P_{e,pu} = M\frac{d^2\delta_e}{dt^2} \quad \text{where} \quad M = \frac{2H}{\omega_s} \tag{4.12}$$

The notation in equation 4.12 is the swing equation used in the development of the out-of-step relay algorithms. Degrees are used instead of radians to obtain better accuracy in the computations of the angle difference with integer notation.

For a two machine system the swing equations for the generators are given by equation 4.13.

$$\frac{P_{1m,pu} - P_{1e,pu}}{M_1} = \frac{d^2\delta_1}{dt^2} \quad \text{and} \quad \frac{P_{2m,pu} - P_{2e,pu}}{M_2} = \frac{d^2\delta_2}{dt^2} \tag{4.13}$$

Letting

$$\delta = \delta_1 - \delta_2 \tag{4.14}$$

the swing equation for a two finite machine system can be expressed as:

$$\frac{P_{1m,pu} - P_{1e,pu}}{M_1} - \frac{P_{2m,pu} - P_{2e,pu}}{M_2} = \frac{d^2\delta_1}{dt^2} - \frac{d^2\delta_2}{dt^{21}} = \frac{d^2\delta}{dt^2} \tag{4.15}$$

Defining the equivalent inertia constant as:

$$M_{eqv} = \frac{M_1 M_2}{M_1 + M_2} \tag{4.16}$$

Multiplying equation 4.15 by equation 4.16 and grouping the mechanical and electric powers, an equation is obtained for the angle swing between two machines in terms of their angle difference, equation 4.17.

$$P_{m,eqv} - P_{e,eqv} = P_{a,eqv} = M_{eqv}\frac{d^2\delta}{dt^2} \tag{4.17}$$

where $P_{m,eqv} = \dfrac{M_2 P_{1m,pu} - M_1 P_{2m,pu}}{M_1 + M_2}$, and $P_{e,eqv} = \dfrac{M_2 P_{1e,pu} - M_1 P_{2e,pu}}{M_1 + M_2}$

Given a reduced network between the two generators, Figure 4.1, the electric power delivered from machine one to machine two is given by equation 4.12.

$$P_e = \mathrm{Re}al[E_1{}^*(E_1 Y_{11})^* + E_1(E_2 Y_{12})^*]) \tag{4.18}$$

$$= |E_1|^2 G_{11} + |E_1||E_2||Y_{12}|\cos(\delta_1 - \delta_2 - \theta_{12})$$

According to the model assumptions the mechanical input power remains constant for the length of the transient while the electric power changes as a result of the angle acceleration between the two machines. By replacing equation 4.18 in the equivalent electric power term in equation 4.17, an expression is obtained for the equivalent electric power which is used in the implementation of the relaying algorithms.

$$P_{e,eqv} = P_c + P_{\max}\frac{M_2\cos(\delta - \theta_{12}) - M_1\cos(\delta + \theta_{12})}{M_1 + M_2} \tag{4.19}$$

where $P_c = \dfrac{M_2|E_1|^2 G_{11} - M_1|E_2|^2 G_{22}}{M_1 + M_2}$ and $P_{\max} = |E_1||E_2||Y_{12}|$

The out-of-step relay algorithms use equation 4.17 and the equal area criterion to determine the stability of angle swings caused by loss of generation in the Florida system or by a fault in one of the interconnecting 500kV transmission lines.

4.4 The Equal Area Criterion

The equal area criterion is a graphical representation of a power angle oscillation of a single machine against an infinite bus. For this discussion an infinite bus, Figure 4.2, is an energy source with constant phase angle, magnitude and frequency. For a generator oscillating against an infinite bus the swing equation is of the form:

$$M\frac{d^2\delta}{dt^2} = P_m - P_e = P_a \tag{4.20}$$

where Pm = Mechanical input power of the single machine and Pe = Electrical output power of the single machine.

The electric power in equation 4.20 has the form:

$$P_e = |E|^2 G_{11} + |E||Y_{12}|\sin(\delta - \phi_{12}) \tag{4.21}$$

Where $\phi = \theta_{12} - 90^0$

Multiplying both sides of equation 4.20 by $\frac{2}{M}\frac{d\delta}{dt}$ equation 4.22 is obtained:

$$2\frac{d^2\delta}{dt^2}\frac{d\delta}{dt} = \frac{2P_a}{M}\frac{d\delta}{dt} \tag{4.22}$$

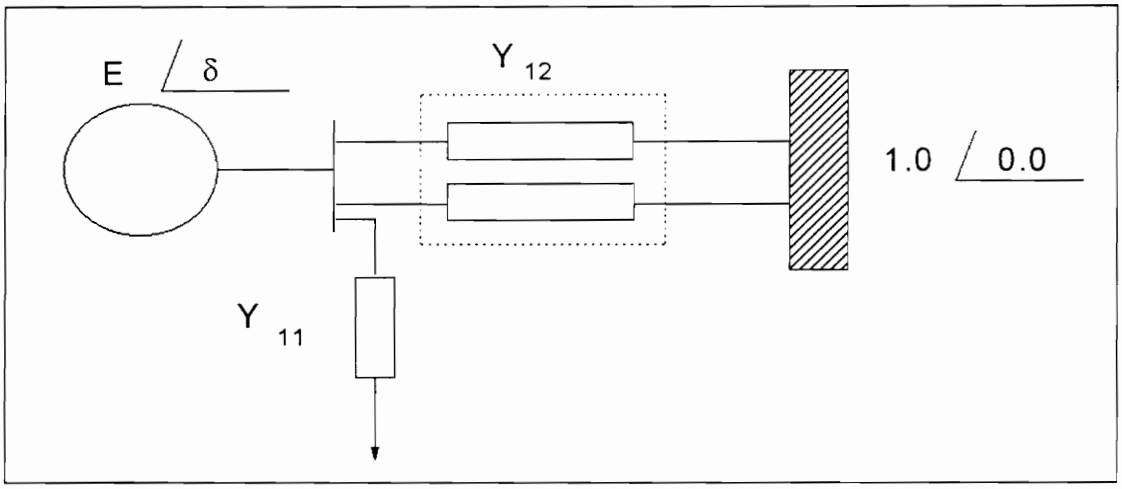

Figure 4.2. *One machine Connected to and Infinite Bus*

The left side of equation 4.22 is the time derivative of $\left(\frac{d\delta}{dt}\right)^2$ and can be expressed as:

$$\frac{d}{dt}\left[\left(\frac{d\delta}{dt}\right)^2\right]=\left(\frac{2P_a}{M}\right)\frac{d\delta}{dt} \tag{4.23}$$

By multiplying equation 4.23 by dt a differential is obtained instead of a derivative

$$d\left[\left(\frac{d\delta}{dt}\right)^2\right]=\left(\frac{2P_a}{M}\right)d\delta \tag{4.24}$$

Integration of equation 4.24 from the equilibrium angle, δ_0, to any angle, δ, gives

$$\left[\frac{d\delta}{dt}\right]^2=\frac{2}{M}\int_{\delta_0}^{\delta}P_a d\delta \tag{4.25}$$

In terms of the angular velocity equation 4.25 can be represented as

$$\frac{d\delta}{dt}=\omega-\omega_0=\sqrt{\frac{2}{M}\int_{\delta_0}^{\delta}P_a d\delta} \tag{4.26}$$

The angular velocity in equation 4.26 will be zero if the machine reaches a new stable equilibrium point which requires that

$$\int_{\delta_0}^{\delta} P_a d\delta = 0 = \frac{1}{\omega_s}\int_{\delta_0}^{\delta} T_a d\delta = \frac{1}{\omega_s} W \tag{4.27}$$

where W is the kinetic energy

Figure 4.3 shows a power angle curve, equation 4.20, with a graphical representation of the kinetic energy in equation 4.27. If a perturbation is applied to system by temporarily reducing the required electric power, a positive acceleration is produced in the single machine, equation 4.20. This accelerating power tends to bring the machine angle back to its equilibrium point by storing the sudden excess in input power as kinetic energy in the generator rotor. When the equilibrium point is reached the angle acceleration becomes zero but the machine is not at synchronous speed and the angle velocity is still positive. This non-zero velocity carries the angle past its operating point causing a negative accelerating power in equation 4.20. The negative acceleration reduces the angle velocity of the rotor by returning to the system some of the stored kinetic energy. If the perturbation is small the velocity is reduced until it becomes zero and the angle starts to return to its operating point. If damping is not considered the machine will continuously oscillate around its operating point. When damping is considered the angular oscillations dies down and the angle settles at the operating point.

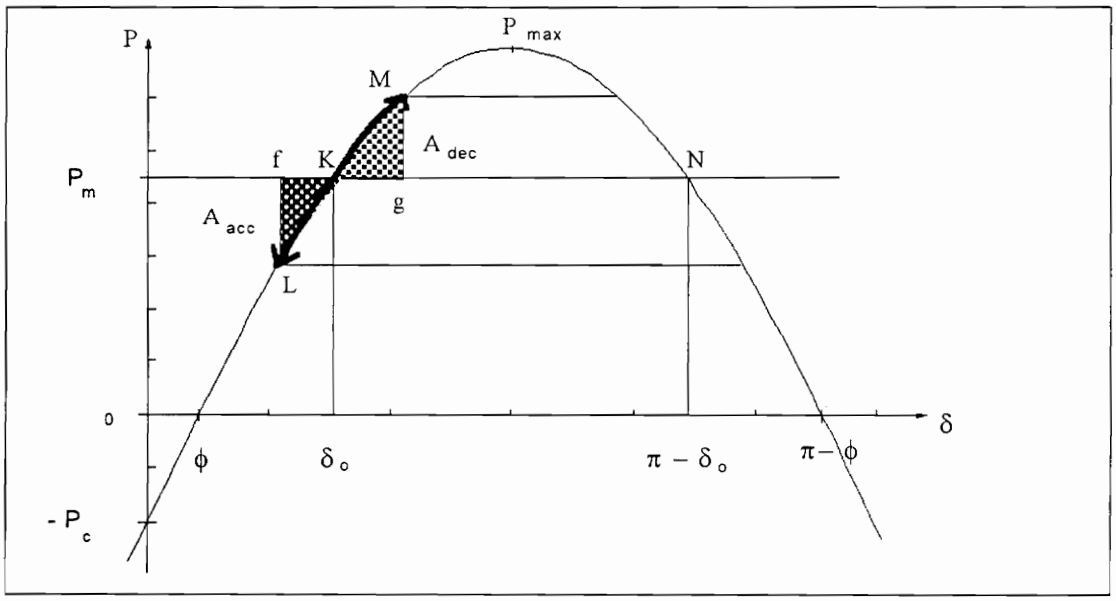

Figure 4.3. *Graphical Representation of Equal Area Criterion.*

In figure 4.3 the area between points K, f, and L is proportional to the accelerating energy produced by the disturbance, while the area between points K, g, and M is proportional to the decelerating energy that tends to bring the system back to its operating point. It can be seen in figure 4.3 that the largest available decelerating area is determined by the unstable equilibrium point, N. If the machine angle reaches this point with a positive velocity then both the acceleration and velocity will be positive causing the machine angle to go out-of-step with respect to the infinite bus resulting in an unstable swing.

From the proportionality between the areas in Figure 4.3 and the kinetic energy changes in the machine it can be concluded that as long as the maximum decelerating area is larger than the accelerating area the machine will be capable of storing enough kinetic

energy to bring the system back to its operating point before it goes out-of-step with the infinite machine.

The traditional application equation 4.27 is known as the equal area criterion because it is used to determine the angle at which the decelerating area **equals** the accelerating area. This angle is called the critical clearing angle and is used to obtain the critical clearing time that determines the fault clearing time to maintain stability in the case of a faulted line. In the out-of-step relay application it is proposed that equation 4.27 be used to determine the accelerating and decelerating areas of the power curves and that the ratio of these areas be used to determine the degree of system stability for a given system swing. Area ratios with values of unity or greater represent an unstable swing.

4.5 Equal Area for a Two Machine System

The equal area criterion can be applied to a two machine system if the equivalent electric power for a two machine model, equation 4.19, can be expressed in terms of the electric power of a single machine against an infinite bus, equation 4.21. This will result in a power angle curve similar to Figure 4.3 for a two machine system. This requires that the angle dependent part of the electric power in equation 4.19 be expressed in terms of a sine curve. In equation 4.19 the varying part of the electric power is of the form:

$$P_{\max}\frac{M_2\cos(\delta-\theta_{12})-M_1\cos(\delta+\theta_{12})}{M_1+M_2} \tag{4.28}$$

It has been shown by Kimbark[1] that Equation 4.28 can be expressed in terms of the sine of the angle difference by equation 4.29. Kimbark's graphical derivation of equation 4.29 is presented in appendix A.

$$\frac{P_{max}}{M_1+M_2}\sqrt{M_1^2+M_2^2-2M_1M_2\cos 2\theta_{12}}\,\sin(\delta-\gamma) \qquad (4.29)$$

where $\gamma = -\arctan\left(\frac{M_1+M_2}{M_1-M_2}\tan\theta_{12}\right) - 90°$

Equation 4.29 proves that the electric power in equation 4.21 is a power curve similar to that shown in Figure 4.3. Equation 4.29 allows the use of the equal area criterion for a two machine system by assuming that the angle difference between the machines behaves like the angle of a single machine against an infinite bus. For the out-of-step relay application, due to its simplicity, equation 4.19 is used for the calculation of the electric power instead of 4.29.

4.6 Equal Area for a Fault Case

By assuming a one machine infinite bus, OMIB, behavior in the case of a fault on two machine system, the electric power transmitted by one generator is reduced and its kinetic energy increases due to the sudden excess in input mechanical power, Figure 4.4. In this case it is assumed that the breakers of the transmission line clear the fault instantaneously by opening the transmission line.

[1] E.W. Kimbark, "Power System Stability", Volume I, John Wiley and Sons, Inc., New York, 1948, p.p.132-135.

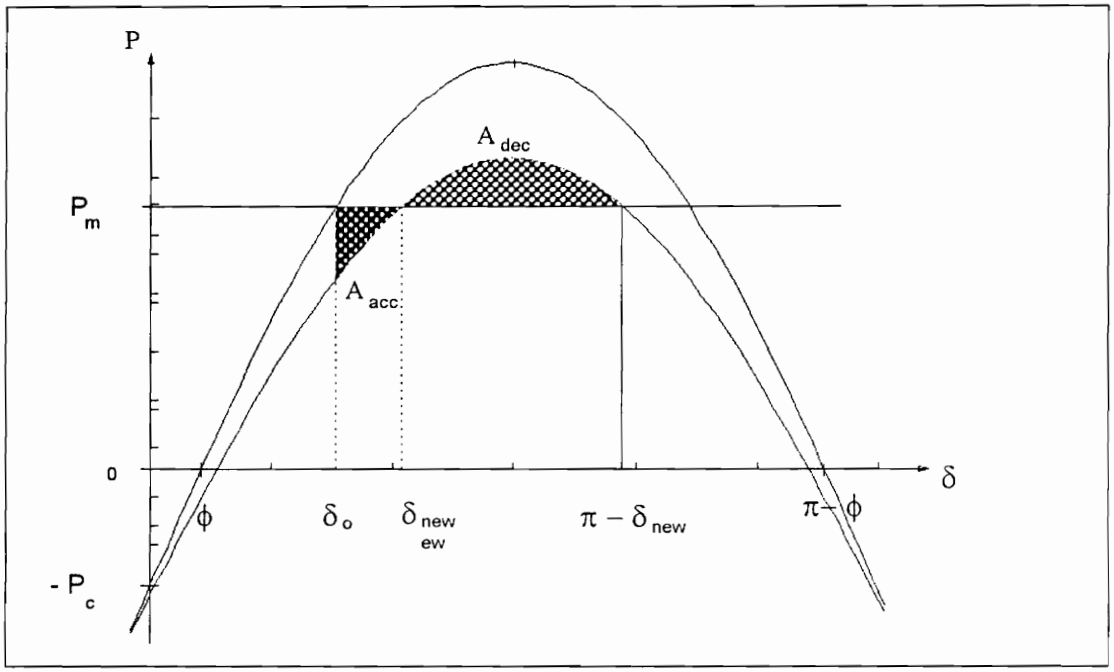

Figure 4.4. *Equal Area Criterion, Fault Case.*

The kinetic energy stored in the machine increases the speed of the rotor increasing the angle difference between the two machines. This increase in angle difference enhances the power transfer between the two units, reducing the rate of change in the kinetic energy until a new equilibrium point is reached. The accelerating area is proportional to the kinetic energy stored in the generators and the maximum decelerating area is proportional to the maximum kinetic energy that the generators can store before the angle different becomes so large that the generators go out-of-step.

The new operating point for a fault case is determined by the amount of power that can be transmitted through the remaining impedance between the generators. If the new value of Y_{12} is known the new operating point can be computed using equation 4.30.

$$\delta_{new} = \arcsin\left(\frac{P_m - P_c}{P_{\max,new}}\right) - \theta_{12,new} \tag{4.30}$$

where $P_{\max,new} = |E_1||E_2||Y_{12,new}|$

Once the new operating point is known the accelerating and decelerating angles can be computed to determine if the swing is stable or unstable, equation 4.31.

$$A_{acc} = \int_{\delta_0}^{\delta_{new}} [P_i - P_c - P_{\max}\sin(\delta + \theta_{12})d\delta$$

$$= (\delta_{new} - \delta_0)(P_m - P_c) + P_{\max}(\cos(\delta_{new} + \theta_{12}) - \cos(\delta_0 - \theta_{12})) \tag{4.31}$$

$$A_{dac} = \int_{\delta_{new}}^{(\pi - \delta_{new})} [P_i - P_c - P_{\max}\sin(\delta + \theta_{12})]d\delta$$

$$= (\pi - 2\delta_{new})(P_i - P_c) - 2\cos(\delta_{new} + \theta_{12})$$

If the values for the accelerating area in equation 4.31 are greater than the decelerating area the swing is unstable, otherwise it is stable. For the case of a stable swing the area ratios give a measure of the degree of stability of the swing.

4.7 Equal Area for a Loss of Generation Case

If the amount of power delivered by one of the generators suddenly decrease the other machine will release some of its kinetic energy to supply the sudden demand in electric power. The resulting increase in the angle difference increases the power delivered between the units until a new operating point is reached, Figure 4.5. In this case the accelerating area represents the kinetic energy delivered by the generators to reach the new operating point and the decelerating area is the maximum kinetic energy that can be delivered before the units go out-of-step.

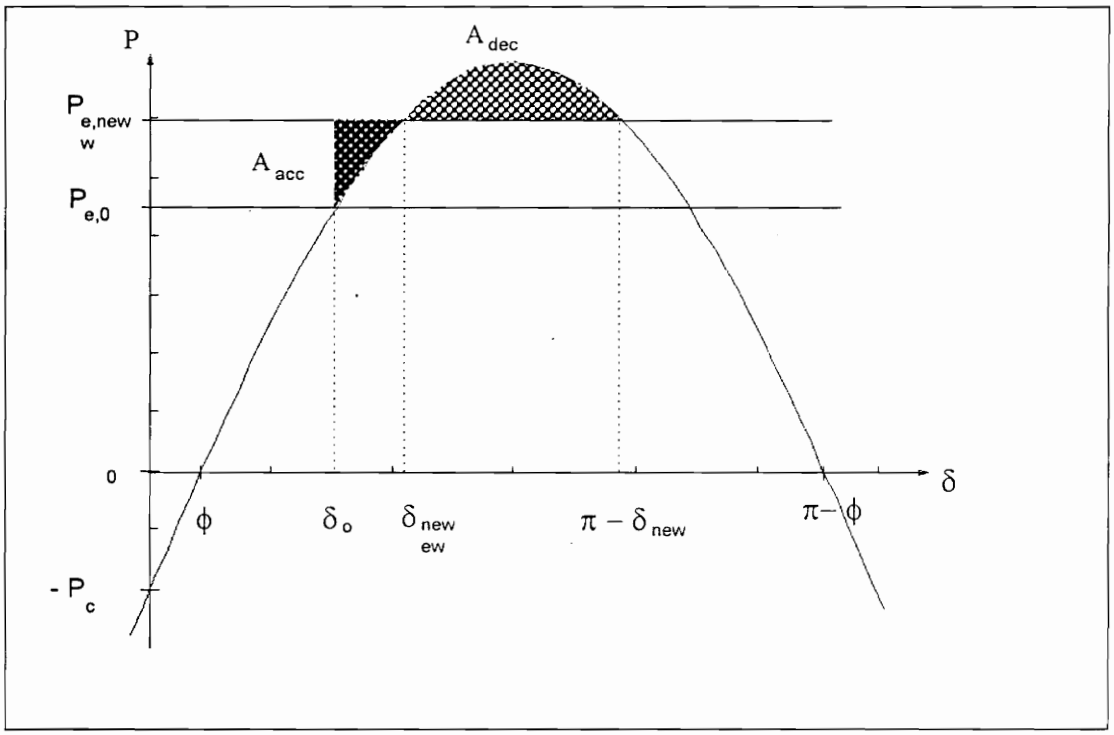

Figure 4.5. *Equal Area Criterion, Loss of Generation Case.*

Determination of the new operating point is not as simple as with the fault case. Although the swing curve remains constant the amount of generation loss is unknown and needs to be estimated to determine the new operating point. The step by step solution method can be applied to equation 4.20 to obtain an estimate of the new operating power. Least square can be applied to the obtained result from several samples to obtain a least square solution to the new operating point.

The step by step solution method is based on assuming that the measured angle velocity is constant through the measurement interval and that the accelerating power computed from the measured angle difference is constant from the middle of the previous interval to the middle of the present sample period. With these assumptions equation 4.20 can be rewritten as:

$$\frac{d^2\delta_n}{dt^2} = \frac{\omega_{n-1/2} - \omega_{n-3/2}}{\Delta t} = \frac{P_{a.n-1}}{M} \tag{4.32}$$

The change in angle in terms of the velocity is given by equation 4.33.

$$\Delta\delta_n = \delta_n - \delta_{n-1} = \Delta t\omega_{n-1/2} \tag{4.33}$$

therefore

$$\Delta\delta_n - \Delta\delta_{n-1} = \Delta t(\omega_{n-1/2} - \omega_{n-3/2}) = (\Delta t)^2 \frac{P_{a.n-1}}{M} \tag{4.34}$$

equation 4.34 can be rewritten as:

$$\Delta\delta_n = \Delta\delta_{n-1} + (\Delta t)^2 \frac{P_{a.n-1}}{M} \tag{4.35}$$

A prediction of the next angle can be obtained using equation 4.36.

$$\delta_{n+1} = \delta_n + \Delta\delta_n = \delta_n + \Delta\delta_{n-1} + (\Delta t)^2 \frac{(P'_m - P'_e)}{M} \tag{4.36}$$

where $P'_m = P_m - |E|^2 G_{11}$, $P'_e = P_{\max} \sin(\delta - \phi)$

and $P_{\max} = |E||Y_{12}|$ and $\phi = \theta_{12} - 90°$.

According to the step by step algorithm the change in angle due to the accelerating power is given by equation 4.37

$$\delta_n = \delta_{n-1} + \Delta\delta_{n-1} \tag{4.37}$$

where $\Delta\delta_n = \Delta\delta_{n-1} + \frac{180f}{H}(\Delta t)^2 (P'_m - P'_{e,n-1})$

and δ is in electrical degrees and P'_m and P'_e in per unit.

In terms of the initial equilibrium point, δ_0, equation 4.37 becomes:

$$\delta_n = \delta_0 + \frac{(\Delta t)^2}{2M}\left[n(P'_m - P'_{e,1}) + \sum_{k=1}^{n-1} (2k-1)(P'_m - P'_{e,n+1-k}) \right] \tag{4.38}$$

Since P'_m is constant Equation 4.38 can be written in the form:

$$\delta_n = \delta_0 + \frac{(\Delta t)^2}{2M}\left[aP'_m - nP'_{e,1} - \sum_{k=1}^{n-1} (2k-1) P'_{e,n+1-k} \right] \tag{4.39}$$

where $a = n + \sum_{k=1}^{n-1} (2k-1)$

Since the new operating power, $P_{m,}$, is unknown equation 4.39 can be solved for P'_m from which P_m can be determined, equation 4.40.

$$P'_m = \frac{2M}{a(\Delta t)^2}[\delta_n - \delta_0] + \frac{1}{a}\left[nP'_{e,1} + \sum_{k=1}^{n-1}(2k-1)P'_{e,n+1-k} \right] \tag{4.40}$$

By computing the values for P'_e and using the measured angle for several samples, a least squares solution technique can be applied to equation 4.40 to estimate the new operating point. Once the new operating point is known the equal area criterion can be applied to determine stability for a loss of generation case.

5

RELAY IMPLEMENTATION

5.1 Introduction

Three digital relay units were designed and implemented to perform the swing and fault detection, stability determination, and data storing required by the out-of-step relay system. Two units were developed for field installation and a third one was designed for laboratory use in the development, updating, and testing of the relay hardware and algorithms. The hardware is the same for the three units and the software of the two field units differs only in the interpretation of local and remote phasor data. The software of the laboratory unit varies depending on the tests or updates performed on the original algorithms. In this chapter section 5.2 describes the hardware components used to implement the relay units. Section 5.3 describes the software developed for the field implementation of the different algorithms used in the operation of the out-of-step relay system. Section 5.4 describes the laboratory tests performed in the out-of-step relay system prior to its field installation.

5.2 Relay Unit Hardware

Each relay unit consists of a mother board, intelligent communications board, DC power supply, isolated output board, ROM disk emulator board, and a properly isolated

enclosure, Figure 5.1. In addition the laboratory unit has a hard disk, a monitor and a keyboard for a better user interface.

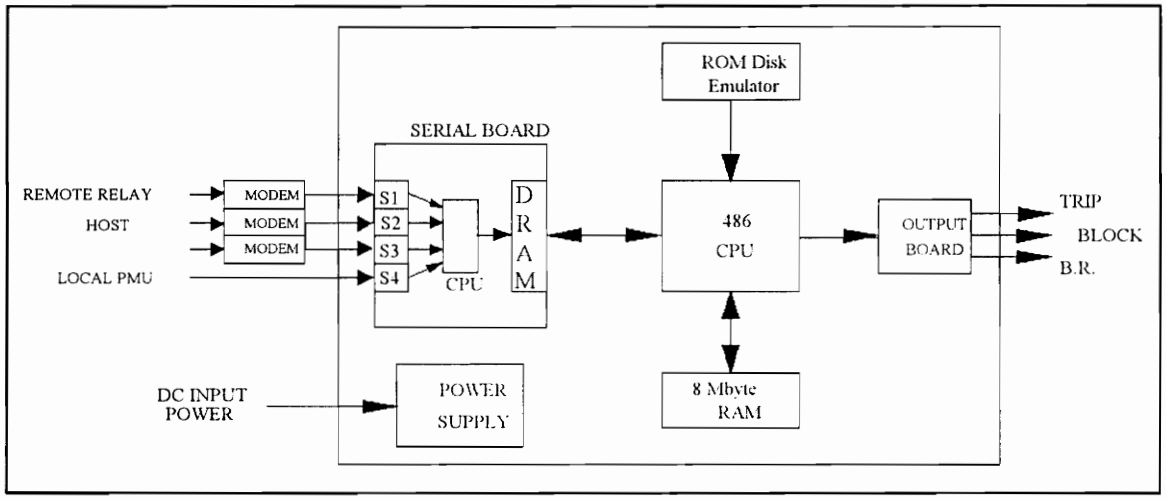

Figure 5.1 *Relay unit, hardware block diagram*

The relay's mother board has a 30 MHz 80486 microprocessor, 8 megabytes of RAM, 256 bytes of cache memory and is capable of performing 2.6 MIPS under ideal running conditions. These characteristics easily satisfy the requirements of the relay unit to perform all the required calculations in one 30th of a second keeping the PMU accuracy of 0.02 degrees in the measured angles. Future operation of the relay may involve a more complex computer model and additional input data from a third PMU which will push the microprocessor closer to its limits. The only time constraint experienced in the present application is the delay of the data communication from the remote relay unit, whose data is required before any calculation can be performed.

Data communication is handled by an intelligent communications board with its own microprocessor that controls 8 communication channels. During initialization the mother board of the relay unit sets the operating parameters for the communication board but for normal operation, data transmission, reception, and port handshaking are performed by the communication board independently of the mother board. Two kilobytes of Dual ported RAM (DRAM) on the communication board are used to transfer data to and from the mother board. At this stage of the implementation only three of the eight available ports are used in the out-of-step relay application and the other five ports are reserved for future expansion. Port one is hardwired to the local PMU and runs at 38400 Baud. Port two is connected to a four-wire modem for communication with the remote relay unit on a leased telephone line at 9600 Baud. The third port runs at 38400 Baud and is connected to a two-wire modem that can be called by a host computer through the switching unit.

A ROM disk emulator is used to store data, software, and automatically boot the system when a reset or power failure occurs. On power up the disk emulator board initializes the mother board and the communication board copies the software to RAM and starts the execution of the program. A watch-dog timer is attached to the ROM board and is activated when the software fails to write and read from specific memory locations for more than 30 seconds. When this occurs the watchdog timer resets the unit forcing a

re-boot of the operating system and relay software. Table data is lost whenever a re-boot occurs.

Table 5.1 Digital relay Output Signals

DB37 Pin	Relay Signal
Pin 1	Block
Pin 2	Trip
Pin 3	Block-if-Re-close (Pin must be set)
Pin 9	Local PMU Communications error
Pin 10	Local PMU GPS error
Pin 11	Local PMU loss of Synch.
Pin 13	Remote PMU Communications error
Pin 14	Remote PMU GPS error
Pin 15	Remote PMU Loss of Synch

5.2.1 Communication Hardware

The output board sends the trip, block, or block-if-re-close output signals along with the relay status signals. This board is optically isolated to avoid damage to the relay from substation transients. A female DB37 connector in the output of the unit is used to send the status and relay signals as listed in Table 5.1.

The power supply accepts a variable 80 to 130 volts DC input to allow operation from the substation batteries and permits the unit to operate when the AC power of the substation fails. The relay power supply also provides connections to supply power to the host modems. Figure 5.2 shows the back-plane connections of the relay unit.

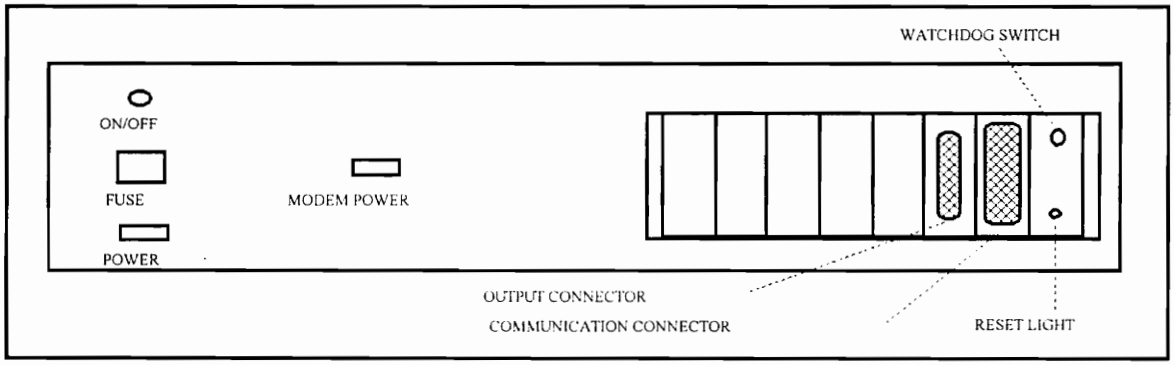

Figure 5.2 *Relay Unit back Plane*

Two Qblazer modems are used to communicate between the PMU, the relay unit and the host computers. These modems run at terminal interfaces of 38400 Baud with 9600 Baud modulation and data compression algorithms. Both modems are set to auto-answer after 4 rings for the modem of the relay unit and 6 rings for the PMU modem. Both host modems are connected to a Trailblazer eight channel switching unit. The same phone number is called for both units but an additional digit is used to connect to the PMU or the Relay Unit. At Hatch substation the relay is connected to channel 3 and the PMU to channel 4 of the telephone switching unit. In Duval the relay is connected to channel 3 and the PMU to channel 2 of the switching unit.

Two four-wire CODEX modems are used to establish continuous communication between the two relay units. These modems run at 9600 Baud on a leased telephone line and perform CTS/RTS handshaking with the relay units. The Codex modems do not have DC power supply and any failure in the substation AC power will stop the relay operation. For a permanent installation a DC powered modem would be required. All modem communications in the PMUs and the relay units are performed with 8 bit data and no parity.

5.3 Relay Software

During normal operation the program receives data from the local PMU at 38,400 Baud every two cycles. The PMU data includes a complete time tag, sample number, status flags, phasor data, breaker status, and additional default data. The phasor data, sample number, and status flags received from the local PMU are copied to an output buffer for re-transmission to the remote relay unit at 9600 baud. The time tag from the local PMU is stored and later used to update the load value from the three stored load curves, and to time tag the samples and tables when a trigger occurs. When the data from the remote relay unit is received it is synchronized to the local PMU data before any operation is performed. After data reception the program checks the digital channel status flags from both PMUs to determine if changes have occurred in any of the key transmission lines monitored by the PMUs. If a line switching has occurred, the impedance matrix of the system model is changed to reflect the changes in the system lines.

At every sample the system angular difference and real power flow between the equivalents are computed using the latest system model and the measured voltage phasors. The computed values for electric power and angle difference are stored in stacks six samples deep where the sixth sample can be used as pre-fault value when a disturbance is detected. The angle differences of the last four samples are used to determine if an angle swing is in progress. If a swing is detected the new operating point is computed using a least-squares solution of the swing equation solving for the new input mechanical power, equation 4.38. The new input power for an angle swing is computed from the stored values of the angle difference and the electric power of the last four samples. In the case of a fault (breaker opening) the new operating point is computed based on the new system impedance matrix, angle difference, and power flow in the system prior to the fault.

Once the new operating point is known for either type of disturbance the equal area criterion is applied to determine the stability of the equivalent system. Before a final decision is made by the relay unit the angle difference between the two equivalents is predicted for the next thirty samples using the latest system model, electric power flow, and voltage phasors. The predicted angle difference is compared to the measured angle difference for four consecutive samples and only when the four predicted values are within a preset error limit, the output signal is considered valid and is sent to the output board. When the errors in the predicted values are not between the allowed limits the system model is considered to be in error and the output signal is not valid. The limit used

to determine the validity of the predicted angles is variable and can be changed through the host computer.

Three output signals are set by the relay unit: Block for a stable swing, Trip for unstable swings, and Trip-if-Re-Close for unstable swings that will become stable if the transmission line breakers re-close successfully after 30 cycles (only for the case of a fault in one of the critical lines). In addition to the output signal, status signals are sent to the output port every two cycles. The input phasors, computed data, and flags of the relay unit are stored in circular tables where they are saved when a trigger is detected.

5.3.1 Subroutine Descriptions

The relay unit software consists of 11 major subroutines, 7 support subroutines, and 4 macros that are used to perform all the required functions. The following paragraphs describe the main subroutines used by the relay program and how they work together to obtain the desired results.

5.3.2 Main Subroutine

The main Subroutine is divided in two sections: initialization and main loop. During initialization the relay unit resets all the required variables, disables the time delay in all the used ports of the communications board, flushes all the communications buffers, resets the watch dog timer, and initializes the host modem connected to the host output port. The communications board is set by default to wait for the confirmation of the

instruction's execution before returning control to the main program. This feature is disabled in the relay implementation to allow independent operation of the communication board once the data has been passed to the communication buffers. The parameters used by each communication channel are set by a configuration file during power up. This configuration file is set to initialize all channels for CTS-RTS handshaking, 8 bits, no parity, and one stop bit. The baud rates are set to 38400 for the local PMU and host, ports 1 and 3, and 9600 for the remote relay, port 2. After initialization of the communication channels a call to subroutine H_MODEM sets the host modem to auto answer after four rings. During normal operation the modem initialization is repeated every ten minutes if the modem is not connected to the telephone line as determined by the carrier detect signal on the host serial port.

After initialization the program loops through a set of instructions through which data is collected, angle difference and power flow are computed, angle swings and line faults are monitored , and data is stored in circular tables. The first subroutine called by the main loop is the GET_DATA subroutine that polls for data from the local PMU, remote relay unit, and host computer. When there is data at both the local PMU and the remote relay the program resets the watch dog timer flags and continues with the execution of the main loop. If the watch dog flags are not reset within a period of 30 seconds a hardware re-boot will be issued by the watch dog board. All data stored in circular tables is lost when a re-boot occurs.

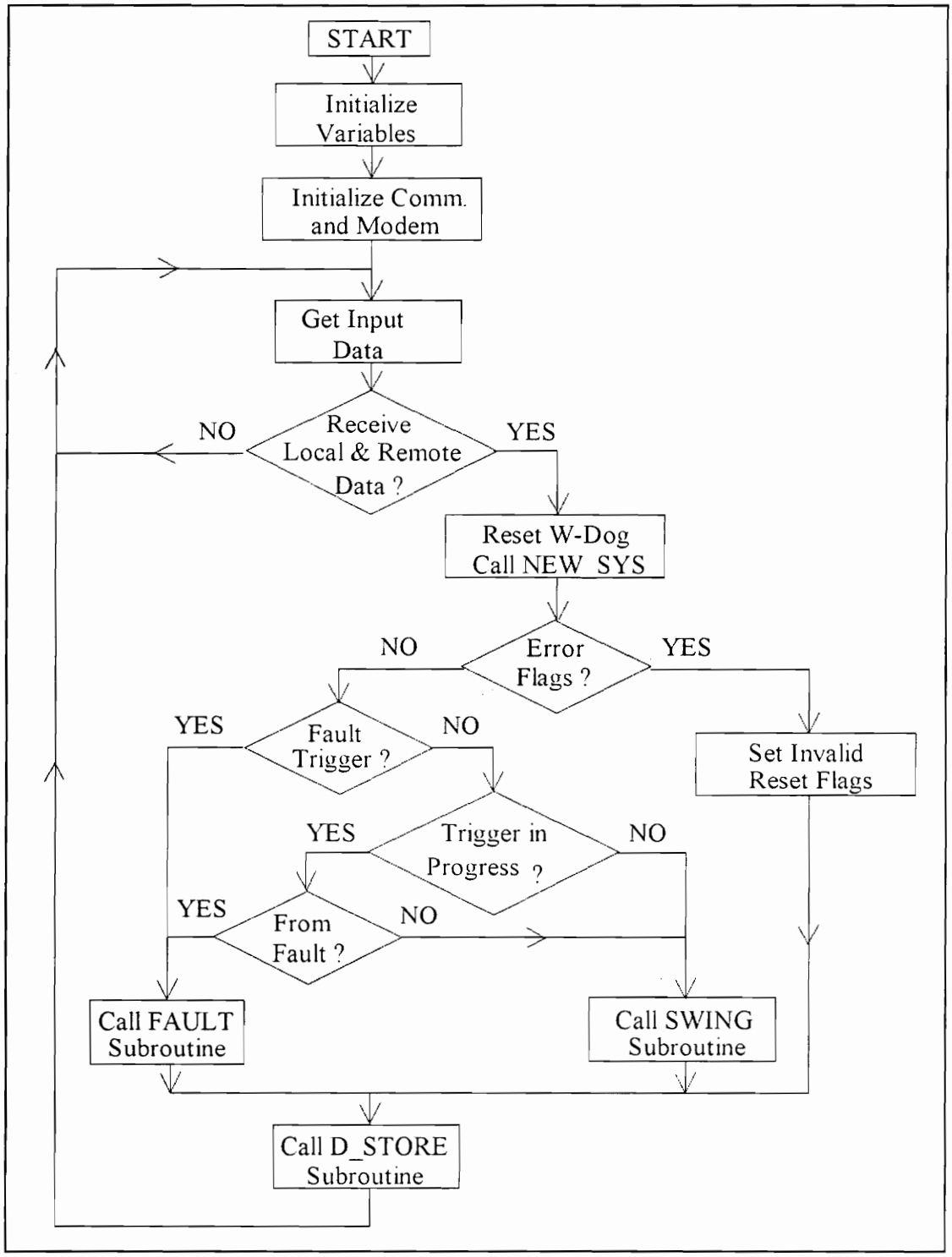

Figure 5.3 *Main Subroutine Flow Chart*

After data reception the main loop executes the NEW_SYS subroutine to determine if changes have occurred in the system model. The CALC_PE subroutine is then called to compute the angle difference and the power flow between the two equivalents. The trigger flags are checked next to determine if a fault has occurred in one of the critical lines. If no faults are detected the program checks the trigger-in-progress flags and calls the SWING or FAULT subroutines if one of the trigger-in-progress flags has been set. If there is no trigger in progress, the S_ANGLE subroutine is executed to detect any swings in the equivalent's angle during the last four samples. If a swing is detected the SWING subroutine is executed to determine the stability of the detected swing. A trigger in progress flag will cause a return to the subroutine that set the flag and it is used to perform the predicted angle test used to validate the decision taken by the SWING or FAULT subroutine. At the end of the main loop the received and computed data are saved by the calling the D_STORE subroutine. After data storage the program returns to the beginning of the main loop to poll for data from the local PMU and remote relay. When an error in the received data is detected or an invalid trigger is determined the main loop disables the trigger for 10 samples but allows tables to be frozen so that the data can be studied to correct any problems with the relay algorithms.

5.3.3 GET_DATA Subroutine

The intelligent communication board uses two independent 300 byte buffers to store the data received from the local PMU and remote relay unit, in addition to a 100 byte buffer used to send data to the remote relay. The GET_DATA subroutine polls for data reception from any of the three input buffers and retrieves any completed data lines. The lengths of the data lines from the remote relay and local PMU are fixed at 19 and 29 bytes respectively, and are preceded by a leading flag. The GET_DATA subroutine polls for the length of the received data following the leading flags and uses this byte count to determine when a complete line has been received by any of the buffers. Data received from the local PMU consists of a status flag, complete time tag, sample number, voltage phasor, two current phasors, frequency, df/dt, digital channels, and a checksum as shown in Figure 5.4

Upon reception of a complete data string the subroutine re-computes the checksum of the received data and sets a communication error flag when the received and computed checksums do not match. Data received with communication errors is stored in the circular tables but is ignored in the determination of angle swings or line faults. Relay triggering is suspended for 10 samples when a communication error is detected in the local PMU or remote relay data buffers to flush the bad data from the data stacks used to save the pre-fault state of the system.

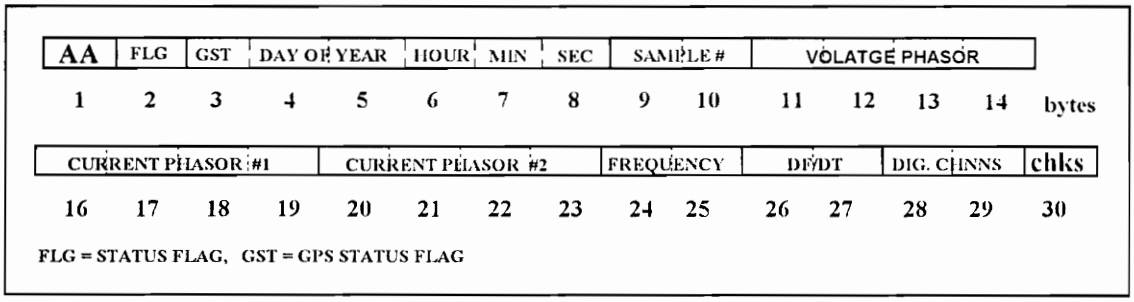

Figure 5.4 *On-line Data From PMU.*

Part of the data received from the local PMU is moved to an output buffer that is sent to the remote relay unit. Data in this buffer consists of the sample number, voltage phasor, current phasors, digital channel status, PMU status flag, and a status flag added by the relay unit. The relay unit status flag is used to indicate to the remote unit if a communication or GPS error has occurred in the local system. The same type of data sent to the remote relay will also be received from the remote unit and together with the local PMU data will be sorted by calling the DATA_SORT subroutine.

Data received from the host computer is divided into commands, which are 4 bytes long and are preceded by an AA leading flag, and parameters, which are 6 bytes long and are preceded by an AB leading flag. All data sent by the host includes a checksum byte at the end of the data string. The commands and parameters accepted by the relay unit are listed in Table 5.2.

Table 5.2 Host Command Format

Leading Flag	Data bytes	Command
AA	00 01	Send Table Data Line
AA	00 02	Send Table Information
AA	00 03	Defrost Table
AA	00 04	Send Table Status
AA	00 05	Send Relay Parameters
AA	00 06	External Freeze
AA	xx 07	Table Select
AB	01 xx xx	Day Flag
AB	02 xx xx	Min. Angle Jump Limit
AB	03 xx xx	Prediction Error Fault Case
AB	04 xx xx	Prediction Error Gen. Drop

Except for the table defrost and table select commands, all commands from the host computer request data from the relay unit. When a command is received the relay unit moves the requested data to the output buffer and enables the communication channels to interrupt at low priority to send the data. A pending output buffer is available to ensure that all requested data is sent to the host computer. The table select command uses the

high byte of the command word to choose one of the eight tables in the relay unit. A table has to be frozen before it can be selected or the command will be ignored by the relay unit. Once a table is selected the data lines from the table can be requested by the host computer or the table can be defrosted to free the memory space used by the table.

The parameter data received from the host computer is used to update one of the four user selected parameters in the relay unit. The first byte of the three-byte data has a value from 1 to 4 and indicates which parameter is to be updated. The Day parameter uses a value of 1 to 7 to indicate which of the first seven days of the year corresponds to a Saturday. This information is needed to adapt the Saturday and Sunday system load data tables for any year. The Angle Limit parameter is used to determine the minimum angle jump in the equivalent's angle difference that will be considered for an angle swing determination. The Angle Prediction parameter determines how close the predicted angle should be to the measured angle for the relay output signal to be valid when a swing occurs. Since the new operating point for the fault and generation drop cases is computed differently a separate prediction flag is used for each type of angle swing.

5.3.4 DATA_SORT Subroutine

Data received from the local PMU and remote relay unit needs to be sorted and synchronized before it can be used by the other relay subroutines. The local PMU data is received with no delay and is stored in data buffer five samples deep. The remote relay

data line is received with a delay of one or two samples and needs to be synchronized to the data from the local PMU. When the remote unit data line is received its sample number is compared to the sample numbers in the buffer of the local PMU data and if it matches one of the PMU sample numbers the corresponding data line of the local PMU buffer is moved, together with the remote unit data, to the data buffers used by the different relay subroutines. If the remote data sample number does not match any of the sample numbers of the local data buffer the latest local data line is moved to the data buffers and a flag is set to indicate lack of synchronism in the received data. A lack of synchronism flag is also set when the sample numbers from the local PMU or remote relay are not continuous. This flag disables the trigger for the next ten samples but allows changes in the system model.

5.3.5 CALC_PE Subroutine

Using a reduced four-bus impedance matrix of the system model (Figure 5.5), the CALC_PE subroutine computes the voltage and current phasors at the terminals of the two equivalents using the measured voltage phasor at Hatch and Duval. The four bus impedance matrix is a reduced form of the six bus model which contains the Hatch-Thalmann and Duval-Thalmann lines. For ease of computation the four bus impedance matrix is pre-computed for all the possible faults in the three interconnecting lines. These pre-computed matrices are stored in the relay memory and are used when the system configuration changes. The four bus matrix is updated with the latest impedance load,

from the load curves of the Florida system, before the current calculation is performed. Once these voltage and current phasors are computed the transient reactance of the two equivalents are used to compute the phasor voltages at the equivalent generators (voltage behind the transient reactance). The difference in angle of these computed phasors is stored as the system angle difference.

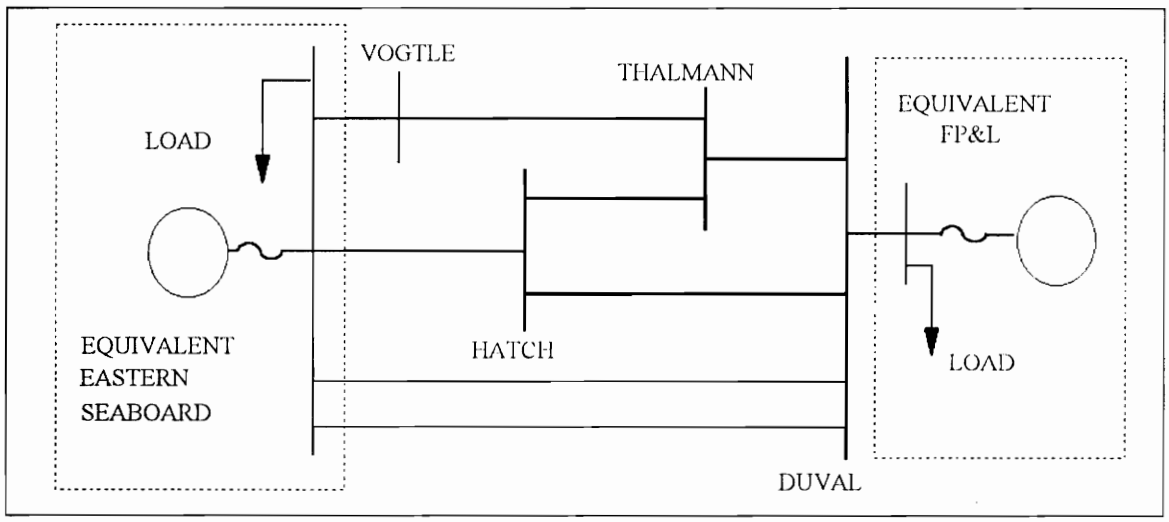

Figure 5.5 *Six Bus Reduced System*

The CALC_PE subroutine computes electric power flowing between the two equivalents using the voltage phasor of the two equivalents and a reduced two-bus impedance matrix determined by the present system conditions. From the swing equation for a two machine system, equation 4.17, the electric power is computed. The CALC_PE subroutine stores the computed electric power in a data buffer six samples deep where the oldest sample is used as the steady state value of the mechanical input power when a disturbance occurs in the system. This is based on the classical stability assumption that

during steady state the electric power equals the mechanical input power to the generators (zero acceleration).

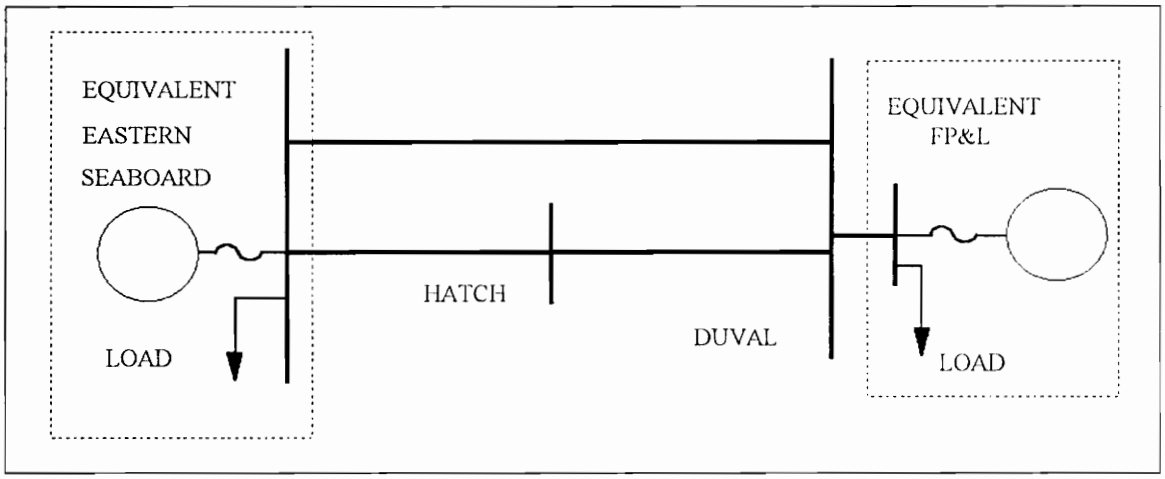

Figure 5.6. *Four Bus Reduced System*

When a fault occurs the distance relays of the transmission line open the faulted line 5 cycles after the occurrence of the fault. During the fault period the data provided by the DFT of the PMU will be in error for at least 2 samples, due to the effect of the transient in the DFT algorithm. To avoid these data errors the relay unit discards the five samples prior to the detection of the open breaker and keeps data stacks six samples deep to ensure that values corresponding to the steady state of the system are kept in memory and are not mixed with the erroneous DFT data.

5.3.6 FAULT Subroutine

When a breaker opens due to a fault in one of the key transmission lines, the impedance matrix of the four-bus reduced model changes. The FAULT subroutine uses

the pre-fault values of electric power, the voltage phasor of the equivalent generators, and the new system configuration to determine the new operating point using equation 4.30. The electric power P_e is computed using the new impedance matrix and the steady state values of the voltage phasors.

Once the new operation point is determined the EQUAL_AREA subroutine determines the stability of the angle swing produced by the fault. If the computed decelerating area is larger than the accelerating one the swing is stable and a block signal is moved to the output buffer. Before sending the output signal the CALC_PE subroutine calls P_ANGLE to predict the angle difference for the next 30 cycles, and sets the trigger in progress flag to compare the predicted angle to the measured angle for the next 4 cycles before validating and sending the output signal.

When the accelerating area is greater than the decelerating one, the swing is unstable and P_ANGLE is called to predict the system angle difference for the next 30 cycles. CALC_PE uses the angle predicted for cycle number 30 to call the subroutine B_CLOSE which computes the equal area criterion assuming a successful re-close after 30 cycles. If after this second equal area computation the system is determined to be unstable a trip signal is moved to the output buffer and the angle predictions are checked for the next 4 samples. If the new equal area prediction finds the system to be stable when a successful re-close occurs, the block-if-re-close signal is moved to the output buffer and

the FAULT subroutine sets the trigger in progress flag to wait for a breaker re-close for the next 30 cycles. If a successful re-close occurs the output signal is changed to block, otherwise the output signal is set to trip.

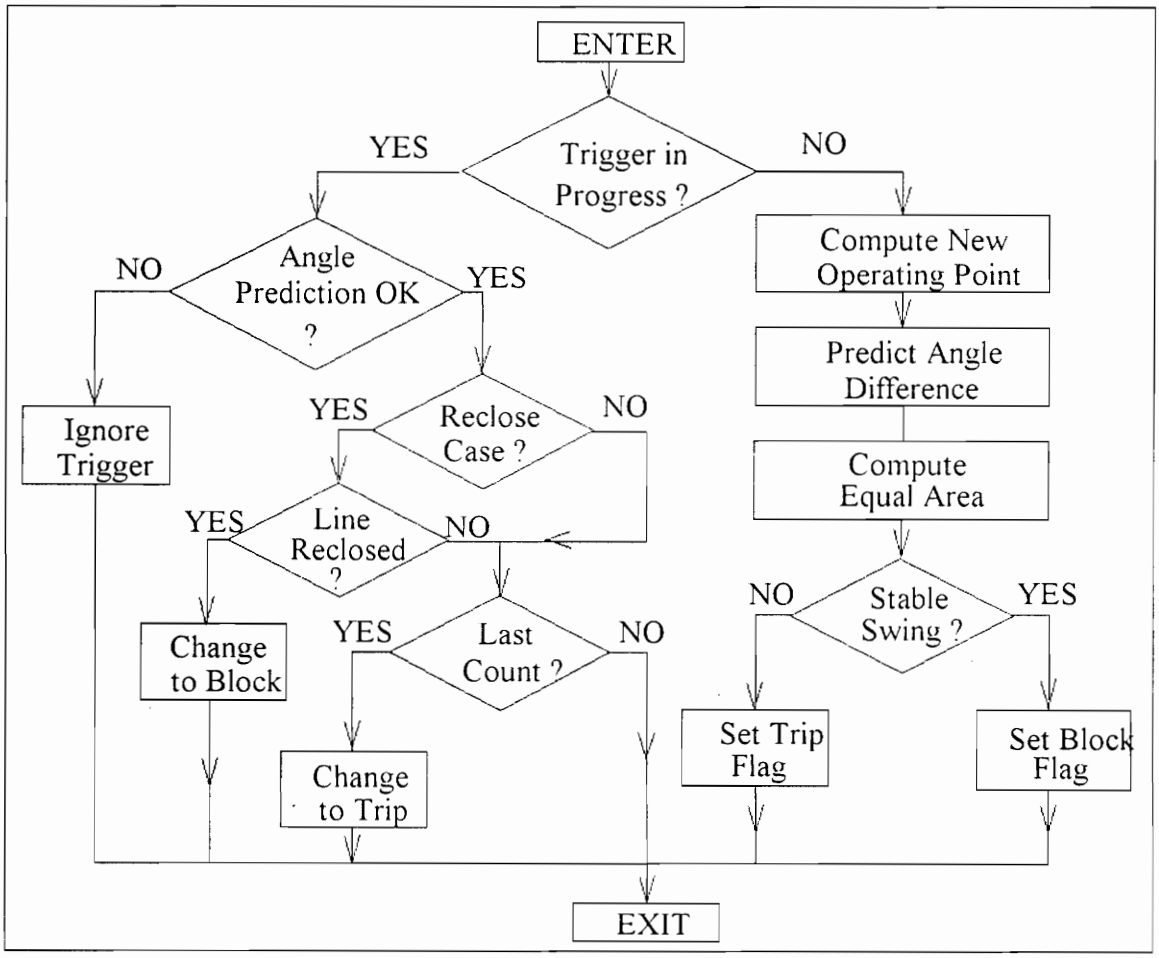

Figure 5.7. *FAULT Subroutine Flow Chart*

The output signals are not sent to the output board unless they are validated by comparing the predicted and measured angle differences for four consecutive samples, this applies also to the block-if-re-close signal. Signal validation occurs only if the error in the

predicted angle for the four consecutive samples is below a pre-determined limit which can be changed from the host computer.

5.3.7 SWING Subroutine

This subroutine uses equation 4.39 to determine the new operating point for a loss of generation in the Florida system. Equation 4.40 is used with six samples for the least squares solution of the swing equation solved for the input power.

Once the new operating point is known the SWING subroutine calls P_ANGLE to predict the system angle difference for the next 30 cycles. The new operating point is then passed to the EQUAL_AREA subroutine to determine the stability of the angle swing. Subroutine SWING moves a 'Block' signal to the output buffer for a stable swing and a 'Trip' signal if the swing is unstable. The trigger in progress flag is then set to test the predicted angle for the next 4 samples.

In the execution of the main loop the trigger in progress flag from the SWING subroutine is overwritten when a fault trigger occurs. This is done to avoid possible errors due to the delay in the opening of the circuit breaker which may cause the relay to trigger for an angle swing before the breaker opens to clear the fault. If the swing trigger is executed in a fault case it will send the wrong output signal since all computations are performed with the pre-fault system impedance matrix.

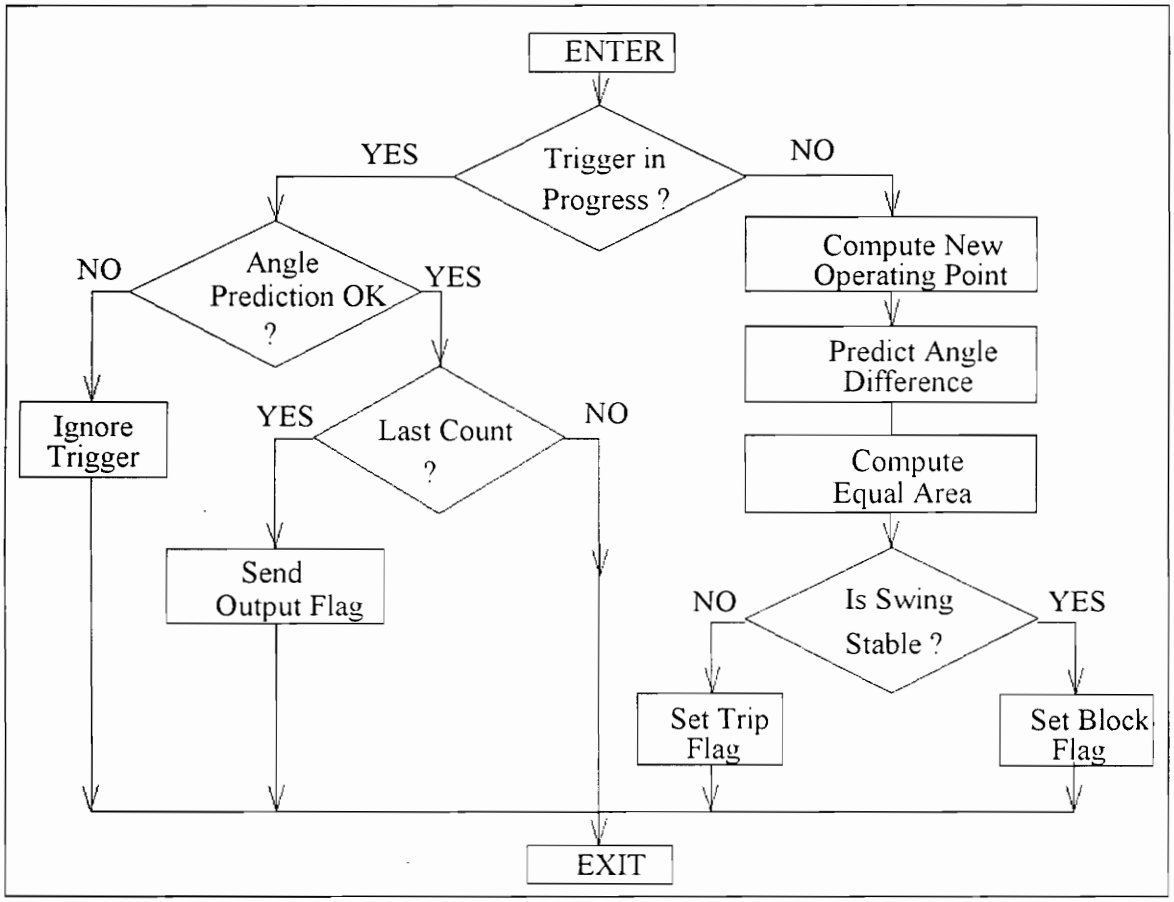

Figure 5.8. *SWING Subroutine Flow chart*

5.3.8 P_ANGLE Subroutine

This subroutine uses equation 4.36 to predict the system angles for the next 15 samples (30 cycles) using the steady state angle difference and the latest system impedance matrix. The angles computed with equation 4.36 are stored in a data buffer where they are used by the FAULT, SWING and D_STORE subroutines.

5.3.9 S_ANGLE Subroutine

The S_ANGLE subroutine uses parameters set from the host computer to determine if an angle swing has occurred over the last four samples (8 cycles). S_ANGLE assumes that when a swing occurs the angle difference will increase or decrease for four consecutive samples due to the system swing. To avoid triggers due to line switching operations it is required that the changes in the angle should have a positive or negative slope allowing for only one change of direction in the slope , equation 5.1.

$$|\delta(k) - \delta(k-1)| > LIMIT \tag{5.1}$$

for k = 0 to 4 with only one change in SIGN[$(k) - \delta(k-1)$]

5.3.10 EQUAL_AREA Subroutine

This subroutine uses equation 4.31 to compute the equal area criterion given the steady state angle and the new operating point of the system. The angle determined by the computed electric and mechanical input power can not always be computed using equation 4.31. When this occurs the new operating point can not be reached by the system. In these cases the equal area computation is not possible, the accelerating area is set equal to 1 and the decelerating area is set equal to zero to indicate an unreachable operating point and an unstable swing.

5.3.11 NEW_SYS Subroutine

The digital channel status flags received from the local PMU and the remote relay unit give the status of the phase 'a' breakers for Duval-Hatch, Hatch-Thalmann and Duval Thalmann transmission lines. In the Hatch PMU, digital channel one monitors the Hatch-Duval line and channel two monitors the Hatch-Thalmann line. The relay units assume that the Duval PMU digital channel one monitors the Duval-Hatch line and channel two the Duval Thalmann line, but as of now the connections at Duval to the phase 'a' breaker of the two lines have not been made.

The NEW_SYS subroutine checks for changes in the digital channel status. When a change is detected the current magnitude of the corresponding line is computed and compared to its previous value. If the current magnitude has changed by more than 50% from its previous value the change is considered valid. For a breaker opening the current magnitude is expected to drop and for breaker closing the magnitude of the current should increase. Once the breaker change has been validated the NEW_SYS subroutine determines which impedance matrix of the set stored in the relay memory corresponds to the new system configuration and changes the impedance buffer to the new values. The M_UPDATE subroutine is then called to compute the new two-bus reduced model using the latest load from the load curves and the new impedance matrix.

When the detected change is a breaker opening a special flag is set to trigger the relay for a line fault. If the breaker re-closes, a flag is set to store the transient data in one of the tables but no trigger flag is generated. Before this subroutine is exited the magnitude of the line currents are computed and stored so that they can be used to compare the current magnitudes to their previous value when a change occurs.

5.3.12 L_CURVE Subroutine

This subroutine updates the impedance value used to represent the load in the Florida system. The subroutine is executed every hour as determined by the time tag received from the local PMU. The load value used by the subroutine is determined by the day of the year flag and the hour and day data from the local time tag. The day of the year from the time tag is divided by seven and if the remainder is equal to the day flag the Saturday load curve is used. If the remainder is one higher than the day flag the Sunday load curve is used. When the remainder is other than the two set numbers the weekday load curve is used. The hour of the day is then copied and shifted left by two bits (multiply by four) to determine the offset from the beginning of the curve where the load data is located. The load curves used by the relay unit are shown in Figure 5.9.

5.3.13 D_STORE Subroutine

This subroutine uses circular tables to store the received and computed data of the relay unit as well as the status and output flags. The data tables have 40 lines of data (80

cycles) of which 10 lines are used as pre-trigger. When a trigger occurs the subroutine collects data for the next 30 samples and jumps to the next block of memory where the next table will be stored. If no space is available for the next table, the trigger will be ignored and no table will be saved until table space is freed by the host computer. The data saved in the circular tables consists of local and remote voltage phasors, local current phasors, angle difference, electric power, predicted angle difference and status flags. In addition to the circular table data lines, an information block is saved for every table when a trigger occurs. The information block contains the trigger cause, complete time tag, the equal area results, and some partial results of the equal area subroutine. This additional information is used to study the relay operation and to time tag the event.

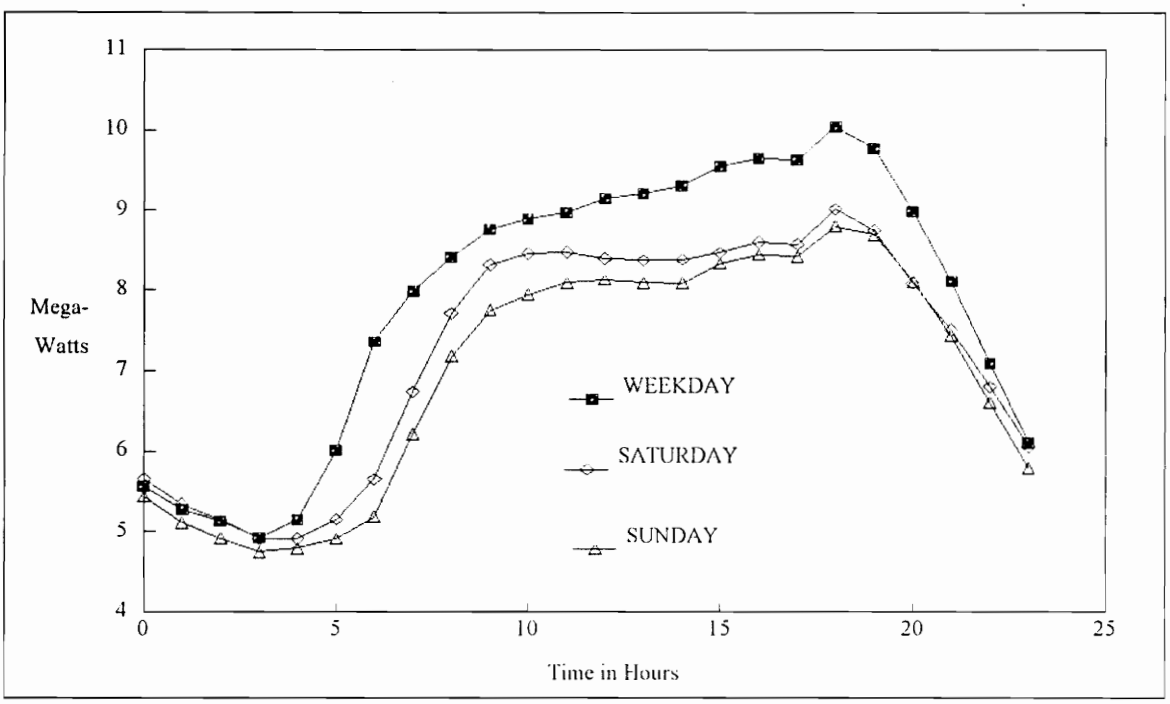

Figure 5.9. *Load curves for Florida system*

5.4 Hardware Testing

Before the system was installed in the field it was tested for proper operation for a period of two weeks. During the first week of testing the individual components were tested to meet the system requirements. The most important hardware tests involved the recovery of the individual units from a power or communication failure. Power failure and restoration were simulated by temporarily cutting the power supply to the PMUs, Relay Units, and system modems; all units recovered as expected from power failure tests.

In addition to power and communication failure the relay unit was tested for memory corruption error. A subroutine was developed to test for RAM corruption error. This subroutine purposely corrupted the RAM forcing the relay unit to re-boot the program from the ROM disk emulator. The relay unit performed as expected by re-booting the relay software and re-initiating the program every time a memory error occurred.

Communication tests consisted on purposely removing and restoring the different communication links and observing the operation of the receiving and sending units. All units recovered from the simulated communication faults. To test for possible timing problems with the communication channels they were run at higher and lower Baud rates and with longer data strings at normal baud rate. All tests results indicated compliance with the relay operation. The communication tests did not include the switching unit used

for host communication of the relay and PMU. The switching units were tested later by themselves for proper operation. The lack of a four wire telephone line limited the testing of the four wire modems, for the system test the modems were substituted by a hard-wired connection.

During the second week of testing the complete relay system, with the exception of the four wire modems and the telephone switching units, was run continuously for a week. During this week of operation failure and restoration of the different units were performed at several times and proper system restoration was observed. The operation of the different components was closely monitored for possible errors and simulations were run to test the operation of the relay algorithms. After a week of error free operation the hardware was considered ready for field installation and was sent to the two utilities for field installation.

5.5 Software Testing

Software testing consisted of real time simulations of stable and unstable swings with the system model used by the relay unit. To perform the software testing a real time playback unit was developed to produce real time sinusoidal signals of power swing cases from the EMTP [107]. A GPS clock was used to synchronize the output signals of the playback unit and obtain the frequency stability required to test the precision of the relay algorithms.

The data from the EMTP simulations was formatted and converted to hexadecimal tables used by the playback unit. A base simulation was run to create a steady state signal prior to the angle swings. In addition to playing back the EMTP data the playback unit send a signal at the time of the fault to trigger a digital channels of the PMU used to signal the opening of a transmission line. Loss of generation cases were also simulated by using a three generator model in the EMTP and removing a generator to cause a stable or unstable swing [65], [107].

Table 5.3 shows the load values for the Florida equivalent for the different EMTP simulations used to test the relay algorithms. The load value for the Eastern equivalent was fixed at 95000+j25000 Megawatts [108]. Figures 5.10 to 5.19 show the angle difference measured by the relay and the equal area results for the different cases. All relay outputs agree with the simulation data.

Table 5.3 Load Data and Power Transfer used for the EMTP Simulations[1]

Swing Case	Florida Equivalent Load	Power Transfer
Low Load Stable	7800+2275	2000
Low Load Unstable	7800+j2275	4000
Low Load Marginally Stable	7800+j2275	3700
High Load Stable	11700+j3412	2000
High Load Unstable	11700+j3412	4500
High Load Marginally Stable	11700+j3412	4000

All values in Megawatts.

[1] S.L. Anderson. "Reduced Order Power System Models". Master's Thesis. Virginia Tech. Blacksburg. VA, December 1993. p. 33.

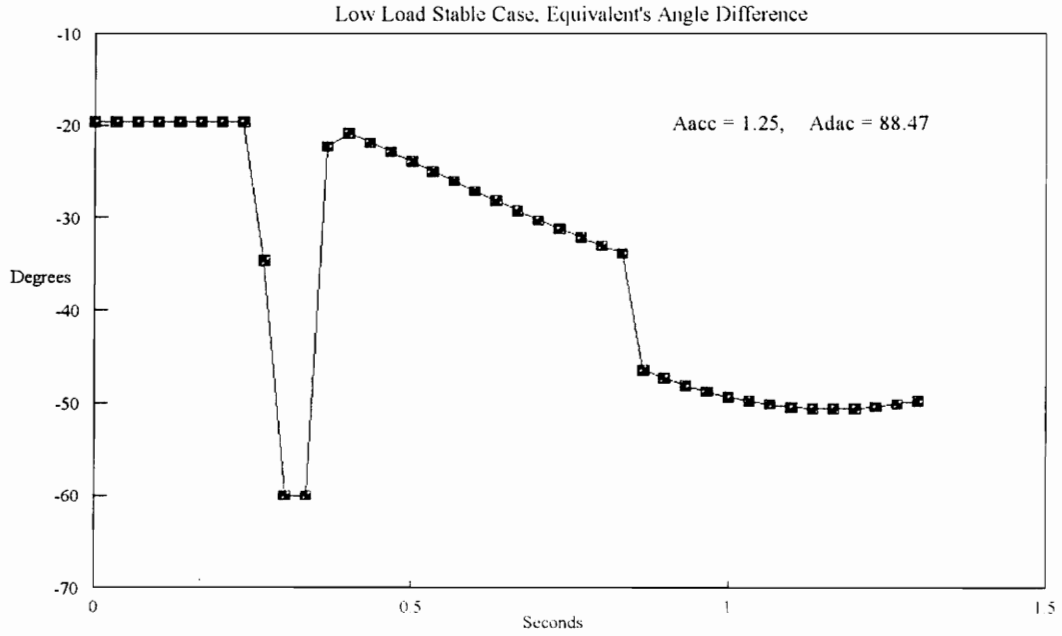

***Figure 5.10**. Low Load Stable Case from EMTP Simulation*

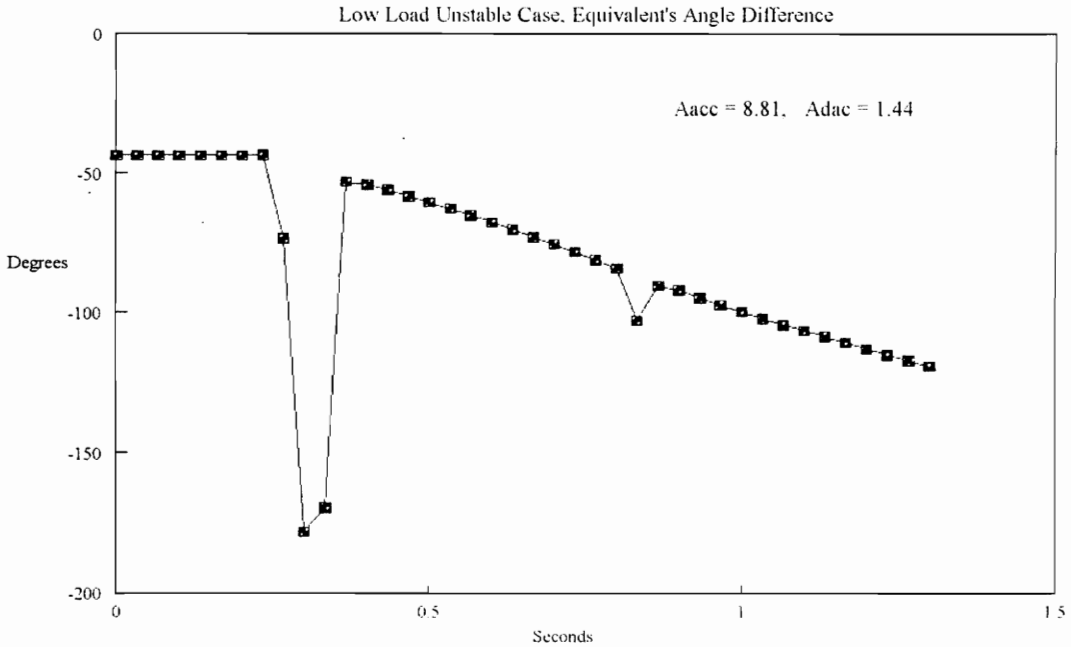

***Figure 5.11** Low Load Unstable Swing from EMTP Simulation.*

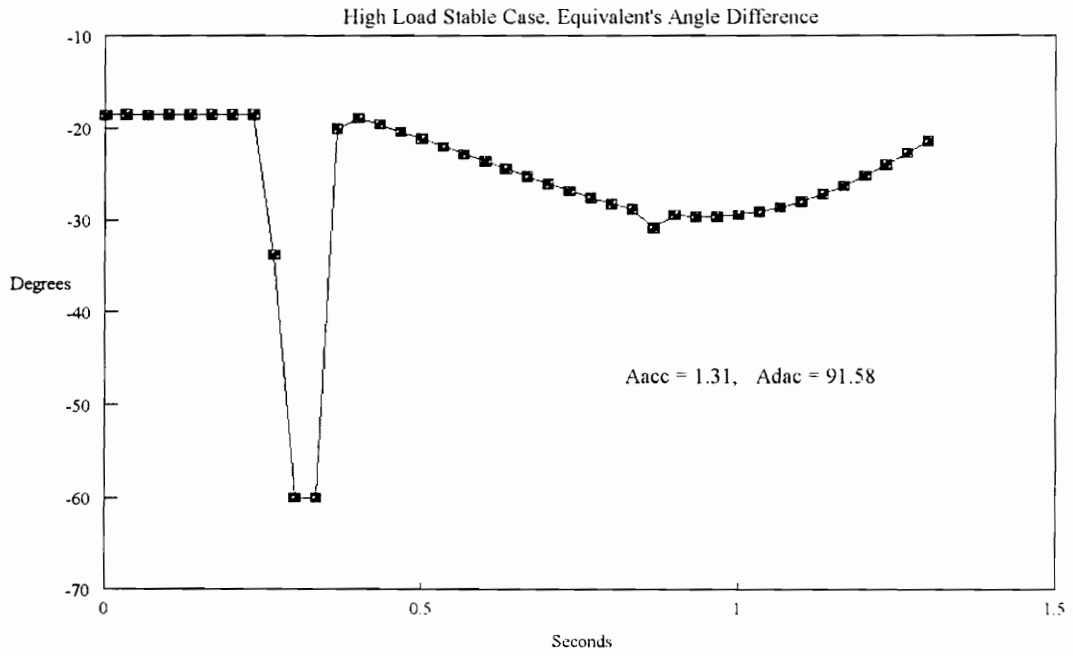

***Figure 5.12**. High Load Stable Swing from EMTP Simulations*

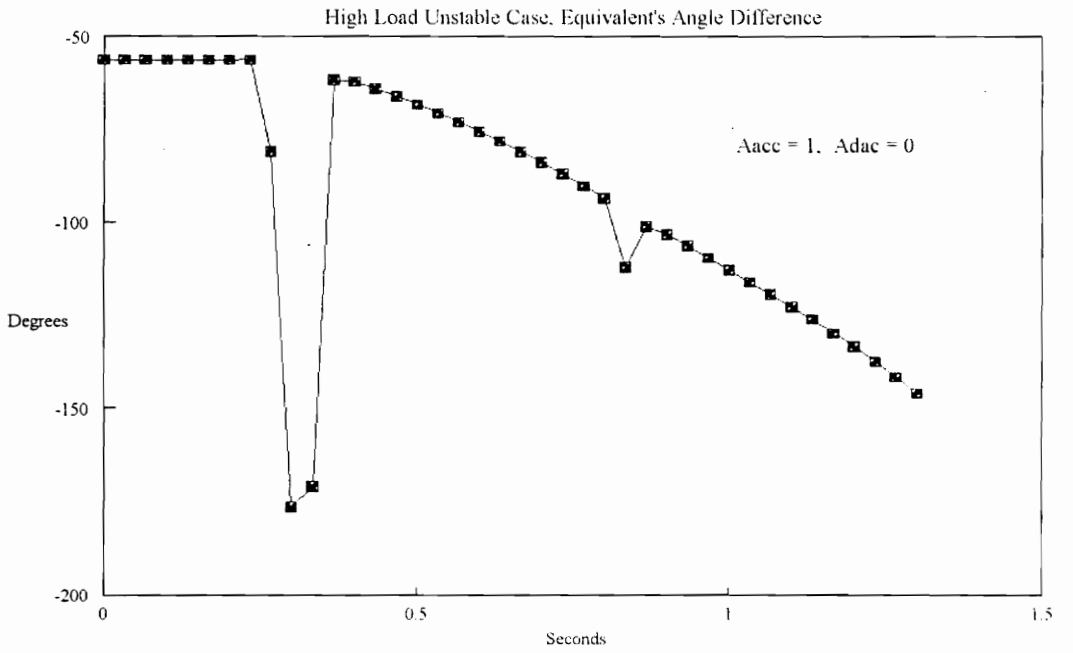

***Figure 5.13**. High Load Unstable Swing from EMTP Simulation.*

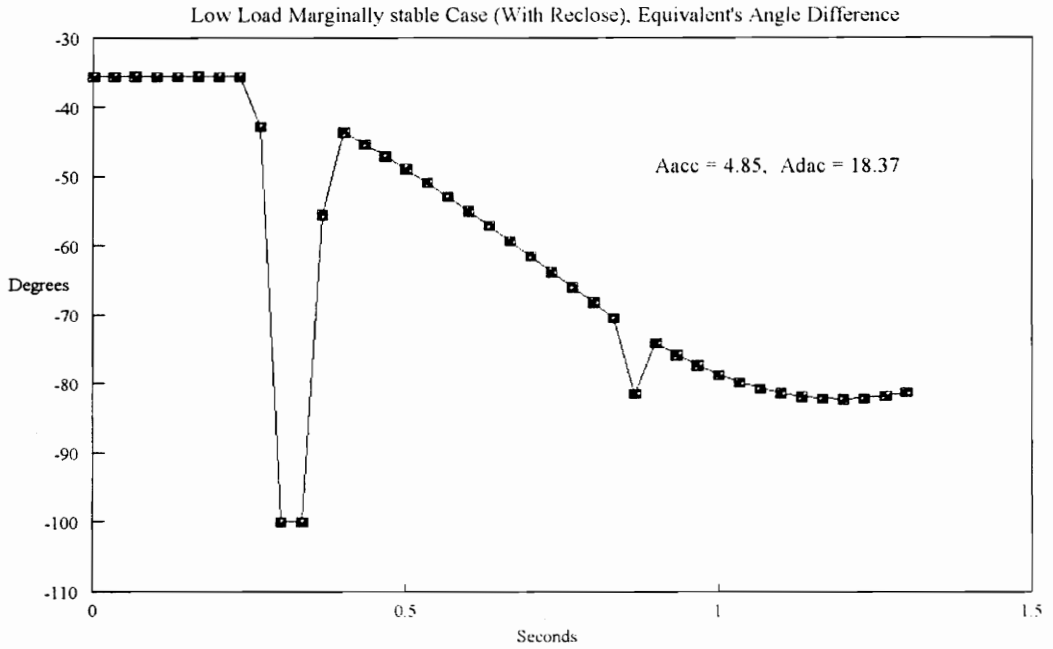

Figure 5.14 *Low Load Marginally Stable with Re-Close, from EMTP Simulation.*

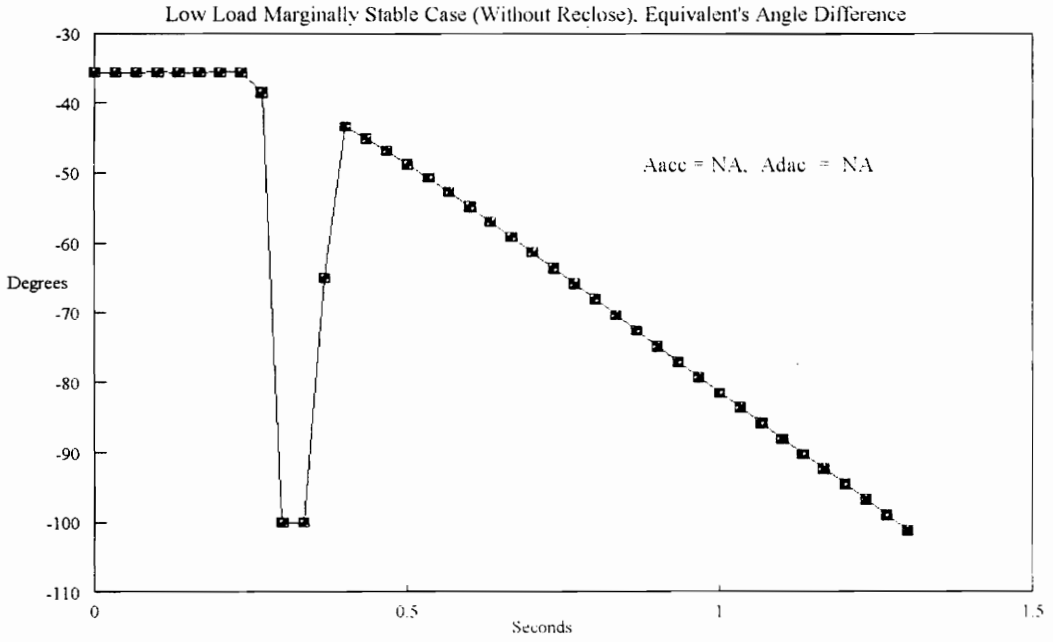

Figure 5.15*. Low Load Marginally Stable Without Re-Close, from EMTP Simulation.*

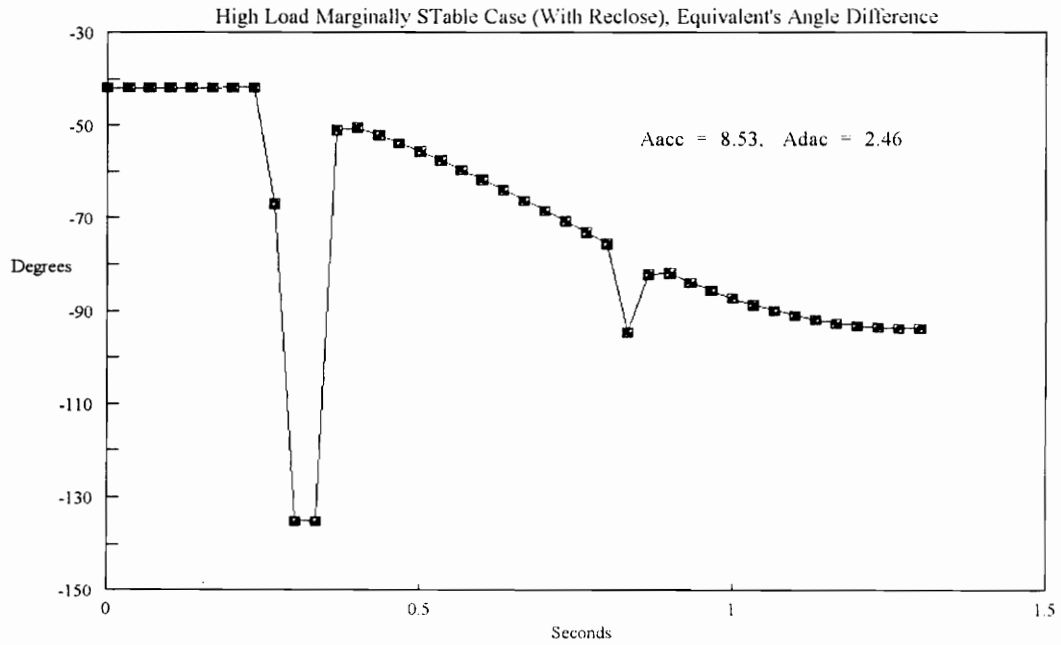

Figure 5.16 *High Load Marginally Stable with Re-Close from EMTP Simulation.*

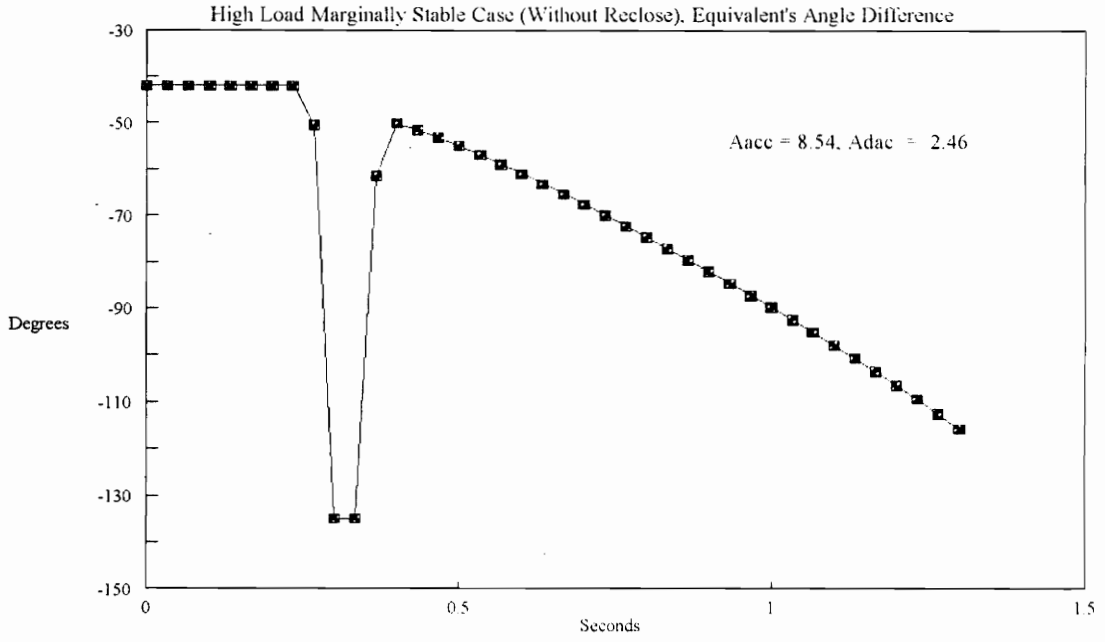

Figure 5.17. *High Load Marginally Stable Case, No Re-Close, from EMTP Simulation.*

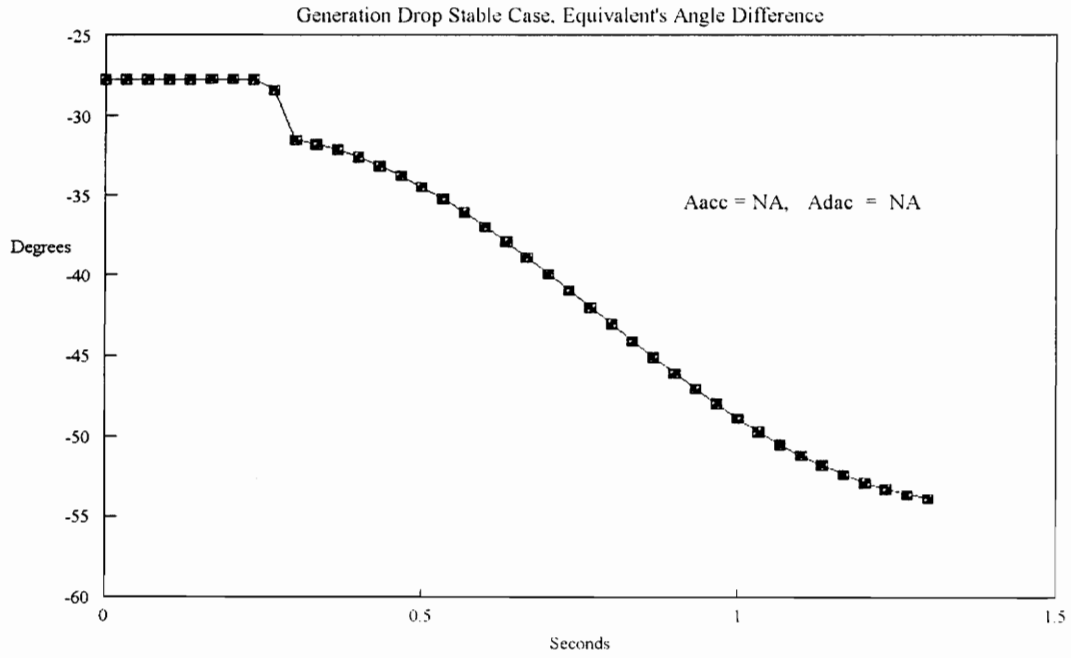

Figure 5.18. *Loss of Generation Stable Case from EMTP Simulation.*

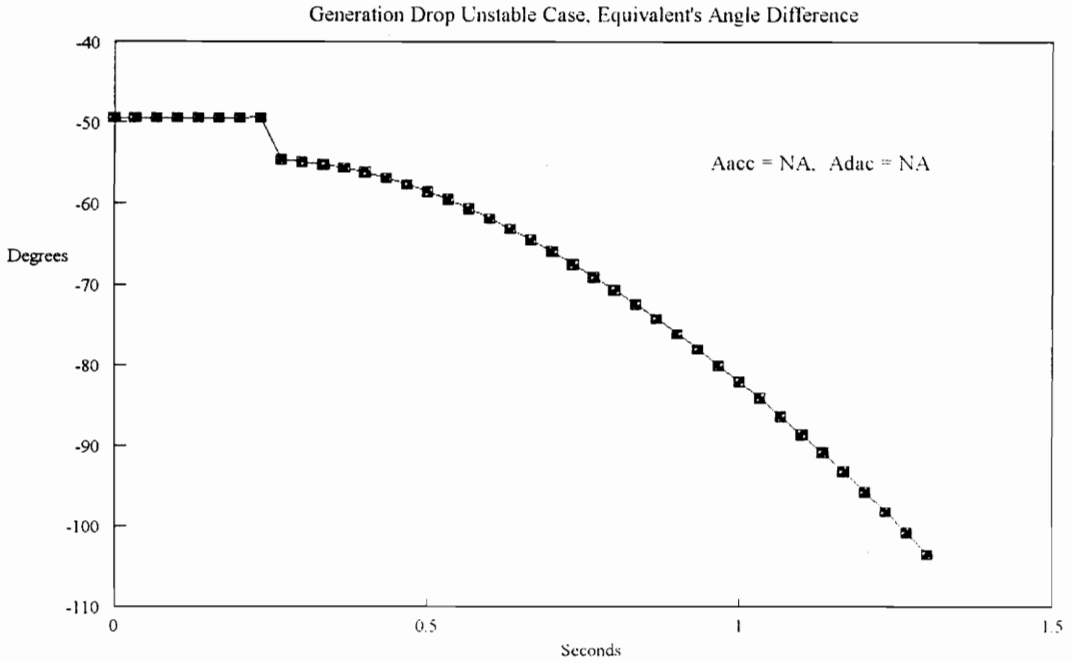

Figure 5.19. *Loss of Generation Unstable Case from EMTP Simulation.*

6

FIELD INSTALLATION AND RESULTS

6.1 Introduction

The adaptive out-of-step relay system implemented in the Florida-Georgia interface consists of two Phasor Measurement Units (PMUs), two digital relays, and a dedicated leased telephone line, Figure 6.1. In addition, a telephone line and a telephone switching unit were used at each site to communicate with the relay and the PMU with a remote host computer. In this chapter section 6.2 describes the system connections to the two PMUs. Section 6.3 describes the field installation and problems encountered. Section 6.4 describes the twelve most significant events detected by the relay system and results of the relay for each of the detected cases.

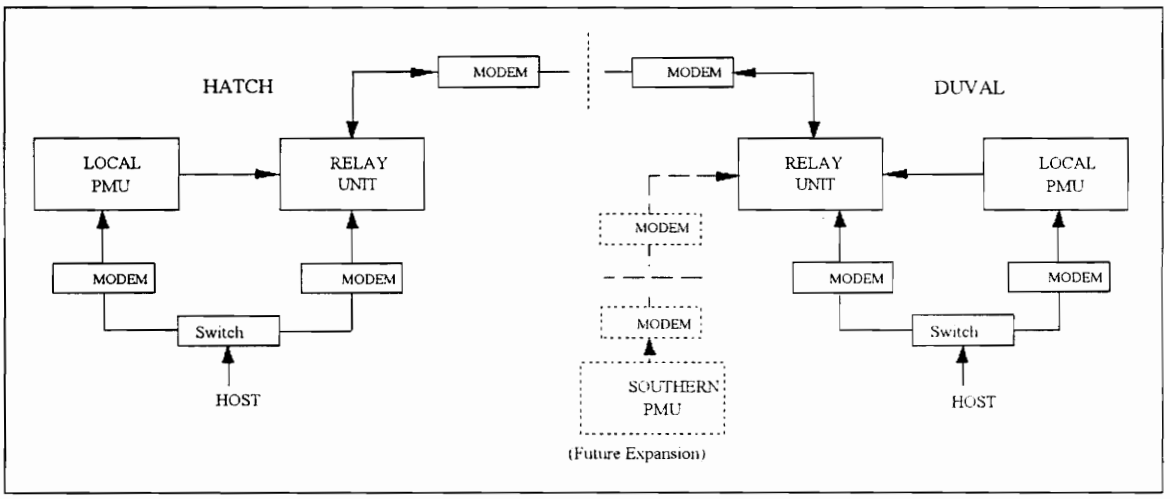

Figure 6.1. *Relay System Block Diagram*

6.2 PMU Connections

The two PMUs installed at substations Duval of FP&L and Hatch of GAPCo, measure the synchronized voltage and current phasors needed for the implementation of the out-of-step relay algorithms. Most of the voltage and current phasors measured by the PMUs are not used in the relay algorithms but are stored in the PMUs' data tables and used for post-disturbance studies. In addition to phasor measurement the PMUs provide information on the status of the breakers of the Duval-Hatch and Duval Thalmann lines.

6.2.1 Duval Connections

The PMU at Duval monitors seven positive sequence phasors consisting of one voltage and six currents. Figure 5.1 shows the one line diagram for the 500/230kV substation with the points monitored by the PMUs marked. The voltage monitored at Duval is that of the 500kV West Bus and is a phase to phase input to the PMU. Shunts of 0.12 ohms are used for all the currents. Table 6.2 lists all the signals connected to the Duval PMU with the corresponding PT and CT ratios.

A breaker and one half configuration is used for both the Thalmann and Hatch lines. This configuration requires that digital channels 1 and 4 detect an opening in order for the Hatch line to be considered open. Digital channels 2 and 3 detect the opening of the Thalmann line. Figure 6.2 shows the breaker points monitored by the digital channels of the PMU.

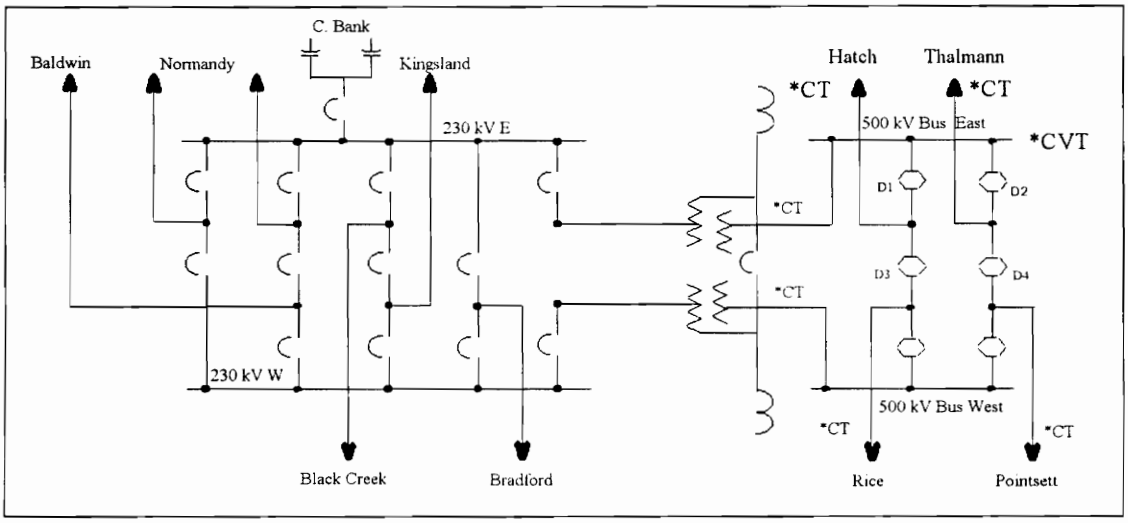

Figure 6.2. Duval PMU connections.

Table 6.1 Duval PMU Channels Connection

PMU Input	Location	Signal Type	PT/CT Ratio
Phasor 1	Hatch 500kV Line	Voltage	4350/1 Ph.-Ph.
Phasor 2	Hatch 500kV Line	Current	2000/1
Phasor 3	Thalmann 500kV Line	Current	2000/1
Phasor 4	Poinsett 500kV Line	Current	2000/1
Phasor 5	Rice 500kV Line	Current	2000/1
Phasor 6	West Auto-Transformer	Current	2000/1
Phasor 7	East Auto-Transformer	Current	2000/1
Dig. Chan. 1	Hatch Line Breaker	Phase 'a' Pole	NA
Dig. Chan. 2	Thalmann Line Breaker	Phase 'a' Pole	NA
Dig. Chan. 3	Thalmann-Poinsett Breaker	Phase 'a' Pole	NA
Dig. Chan. 4	Hatch-Rice Breaker	Phase 'a' Pole	NA

6.2.2 Hatch Connections

The PMU at Hatch monitors ten positive sequence phasors consisting of four voltages and six currents, Table 6.2. All voltage connections to the PMU are line to neutral. Shunts of 0.10 ohms are used for all currents. Figure 6.3 shows the one-line diagram of the 500 and 230kV substations at Hatch. This figure also shows the four breakers monitored by the digital channels of the PMU. The breaker and one half configuration used in Hatch for the Duval and Thalmann lines disconnects the lines and the corresponding bus. For the Duval line to be considered open digital channels 1 and 2 must detect an opening; digital channels 3 and 4 detect the opening of the Thalmann line.

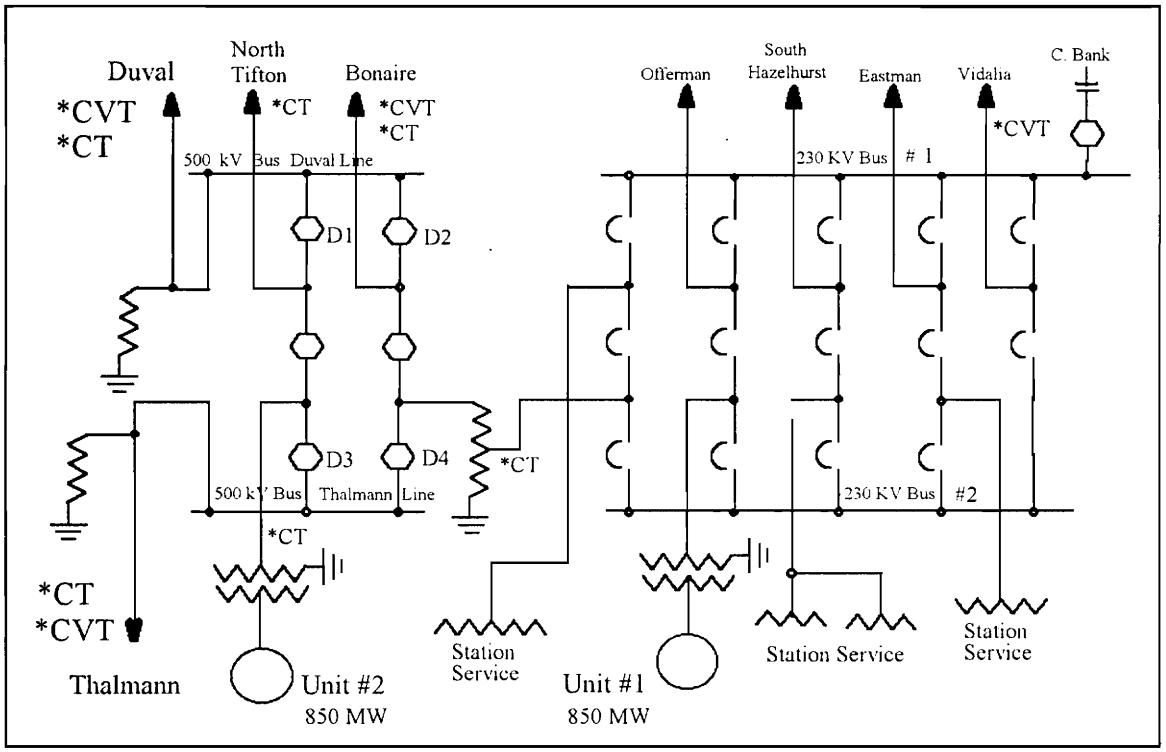

Figure 6.3. Hatch PMU Connection

Table 6.2 Hatch PMU Channels Connection

PMU Input	Input Quantity	Signal Type	PC/CT Ratio
Phasor 1	Duval 500kV Line	Voltage	4350
Phasor 2	Duval 500kV Line	Current	400
Phasor 3	Thalmann 500kV Line	Voltage	4350
Phasor 4	Thalmann 500kV Line	Current	400
Phasor 5	Bonaire 500kV Line	Voltage	4350
Phasor 6	Bonaire 500kV Line	Current	400
Phasor 7	N. Tifton 500kV Line	Current	400
Phasor 8	H.S. GSU BK #2	Current	600
Phasor 9	L.S. 500/230 BK 10	Current	800
Phasor 10	Vidalia 230kV Line	Voltage	1155
Digital Channel 1	Duval 500kV Line	Phase 3 Pole	NA
Digital Channel 2	Duval 500kV Line	Phase 3 Pole	NA
Digital Channel 3	Thalmann 500kV Line	Phase 3 Pole	NA
Digital Channel 4	Thalmann 500kV Line	Phase 3 Pole	NA

6.3 Relay Installation

The installation of the hardware of the relay system was completed on September 22-23, 1993 at the Hatch and Duval 500kV substations. Communication problems delayed the complete operation of the system until October 13, 1993. During the initial installation an error in the configuration file of the communication board prevented the relay units from receiving or sending data to the modem connected to the remote relay unit. During testing of the relay unit at Virginia Tech the remote relay communication channel was set to 38400 Baud to test for errors in data handling by the data reception subroutine. Unfortunately the configuration file was not changed back to the 9600 Baud used by the Codex Modems and the program was burned into the EEPROMs with the wrong baud rate. It was not possible to correct this error during field installation and a second trip was required to correct this problem. In addition, the voltage phasor measured by the PMU at Hatch substation gave the wrong magnitude. GAPCo personnel tried to solve the problem but no apparent cause was found. At that point it was decided to change input boards in case one of the input channels had failed.

During the second trip (Sept. 29 - Oct. 1) new EEPROMs were installed with the corrected software and communication was established between the two units. The GPS engine and GPS controller program of both PMUs were updated and the input board at the Hatch PMU was changed. The PMU at Hatch showed a zero magnitude for the first phasor (voltage phasor). A negative sequence test was performed (on the incorrect input

channel) and it led to the wrong conclusion that there was a problem with the interface board of the Hatch PMU. The interface board was removed and sent to Macrodyne for repair. The PMU and relay units at Duval were operational and the system was installed with a loop back connection at Hatch to allow testing of the relay unit at Duval. The unit at Duval was monitored from Virginia Tech to detect any possible problems with the software.

No problems were found with the interface board by Macrodyne and a problem was observed with the relay unit at Duval Substation. The unit re-booted randomly in periods no greater than 9 hours. Tests were run at Virginia Tech to try to detect the problem but it was not possible to recreate the error with the lab equipment. A third trip was required to solve the voltage phasor problem with the Hatch PMU and the re-boot problem with the relay unit's software.

During the third trip (Oct. 12-13, 1993) a second check in the sequence of the input channels of the PMU at Hatch revealed an incorrect wiring for the three phases of the first phasor which gave a negative sequence for the first phasor. The inputs for the first phasor from the disconnect switches were re-wired for positive sequence input. It was discovered that phase sequence 1,2 and 3 in Georgia does not correspond to phases a, b, and c in Florida. Only the first voltage phasor in Hatch was corrected for the 120 phase shift to obtain the correct angle difference. The negative sequence error in the wiring of the first phasor at Hatch was later corrected by Georgia Power personnel and the inputs to

the PMU from the disconnect switches were rewired keeping the 120 phase shift on the first phasor. Only the first phasor was rewired to keep the rest of PMU data in the sequence used by Georgia Power Co.

After correcting the sequence input to the first phasor the relay unit at Hatch was replaced by a PC running the relay software through a debugger to try to detect the reason for the random re-boots. During a two hour test the debugger found that the error was produced by an illegal instruction execution. The problem occurred exactly on the hour, which meant that it could be produced by the load update subroutine. The GPS time tag from the PMU was changed to emulate a change in the hour and the problem occurred again. A check on the load change subroutine detected an error in a divide instruction that used the wrong size operand. The errors were produced only when the magnitude in the register prior to the division was greater than a word size and that depended on the real part of one of the input phasors. The computer used during this trip was capable of burning new code in the EEPROMs and the problem was solved at the substation. After changing the code the unit at Hatch was left operating for 16 hours while the unit at Duval ran the original program. The unit at Duval re-booted at least twice during that period and the unit at Hatch did not re-boot. The code was changed at Duval and the units were left operating on October 13.

After the third trip the units worked with no problems for two days, and then the host communication was lost to the unit at substation Hatch. The problem was reported to

GAPCo. personnel and they confirmed a lack of response from other equipment connected to the same switch box. The problem was solved by GAPCo but no reason was given. The relay host modem at Duval failed four days after the last trip and it was replaced by FP&L personnel. The reason for the failure of the Duval modem is not known but the relay unit's power supply for the modem is suspected. The unit worked with the replacement modem and the problem did not occur again.

In January 1994 an eight channel telephone switching unit was installed at Duval and Hatch. These units allow collection of data from the PMUs as well as from the relays using the same telephone line. Several problems with the host communication were observed after the installation of the telephone switching units. Communications with the PMU had no problem but relay communication was not possible during some hours of the day especially at Duval. It was assumed that the error was in the relay communication board or communication software and both were tested for several weeks. Future testing done by FP&L personnel found the error to be caused by a small ground voltage in the input telephone line that triggered a protection in the telephone switching unit. The ground voltage was not always present and did not affect the PMU since it was set to answer after one ring and did not allow time for the switching unit protection to trip. The protection in the switching unit was disabled and the problem was eliminated.

PMU testing revealed that the digital inputs to the PMU at Duval were not present. The connections were added by FP&L personnel at Duval in early March

completing the full installation of the relay. The only part of the installation that was not accomplished was the DC power supply for the CODEX modem on the dedicated telephone line. These modems were connected to AC outlets at the substations and were not reliable in case of substation power failure. It is worth mentioning that these modems were not part of the planned installation.

6.4 Major Swings

During the 15 months of operation the out-of-step relay detected more than 200 events in the Duval-Hatch line; appendix C lists all the collected cases. The sensitivity of the relay parameters was set to detect any angle swing greater than 0.15 degree and any opening of phase 'a' of the interconnecting 500kV lines. The collected cases with the largest swings are presented in this section with the results obtained by the relay algorithm at the time of the swing and the corrected results with the improved relay algorithm. The changes used in the improved relay algorithm are explained in Chapter 7.

More than 95% of the collected cases were due to angle swings where loss of generation is suspected. The loss of generation cases are harder to predict since the amount of generation loss is unknown at the moment of the prediction and needs to be estimated from the system model, measured angle swing and power flow. The line fault cases are easily predicted by correctly changing the model of the system, but the use of incorrect load values added some error to these cases as well.

The following cases were due to loss of generation in one of the utilities in Florida. The angle and power swing measured by the relay are shown for every case. The predicted angle swing for the two machine model is also shown for the original and improved algorithms. Information is given in every case on the predicted new operating point and generation loss in the two machine model. The results of the equal area criterion are given as accelerating and decelerating areas for both the original and the improved algorithms. A larger decelerating area indicates a stable swing. All cases recorded by the relay were stable swings and were flagged as such by the original and improved algorithms.

It was observed from the collected data that some of the angle swings changed their original swing between 0.4 and 0.5 seconds after the beginning of the first swing. These are considered to be compound events and the relay predictions of the original algorithm are based on the first swing detected. The improved algorithm gives two triggers for compound swings.

Table 6.3 Table of Major Swings

Case Number	Measured Swings on Page	Relay Results (*) on Page	Comments on Page
21	6.12	6.13	6.14
87	6.15	6.16	6.17
127	6.18	6.19	6.20
150	6.21	6.22	6.23
157	6.24	6.25	6.26
166	6.27	6.28	6.29
180	6.30	6.31	6.32
251	6.33	6.34	6.35
266	6.36	6.37	6.38
276	6.39	6.40	6.41
299	6.42	6.43	6.44
334	6.45	6.46	6.47

(*) Results are shown for all cases for the improved and original algorithms. The improved algorithm is presented in Chapter 7.

Case 21:

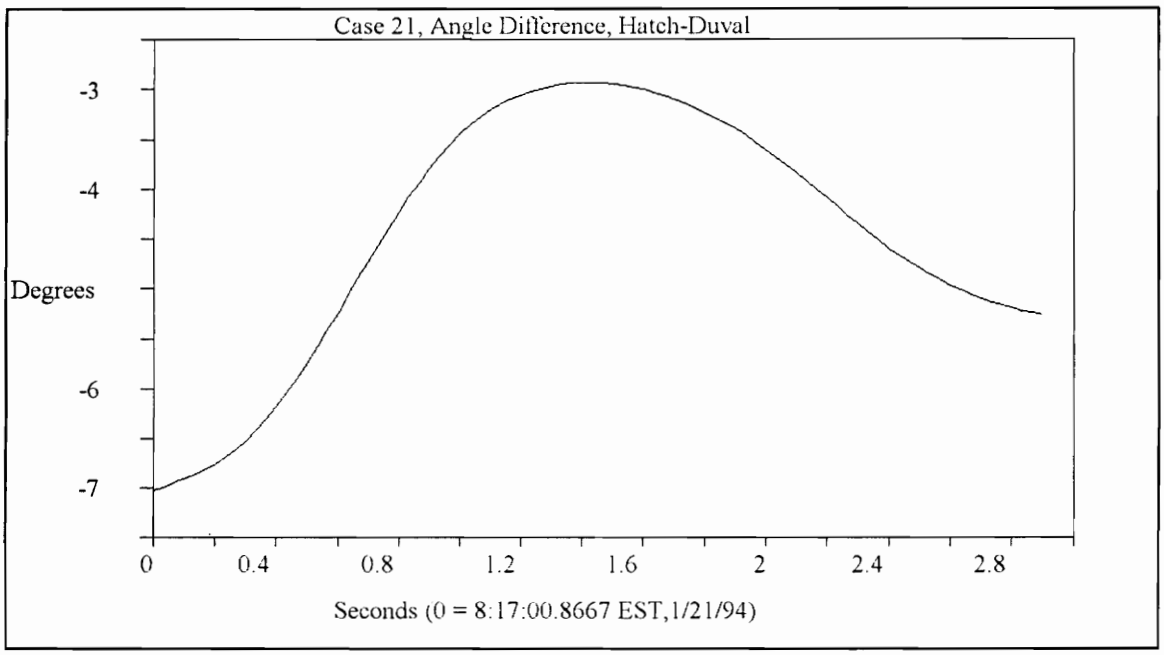

Figure 6.4. *Measured Angle Swing, January 21, 1994*

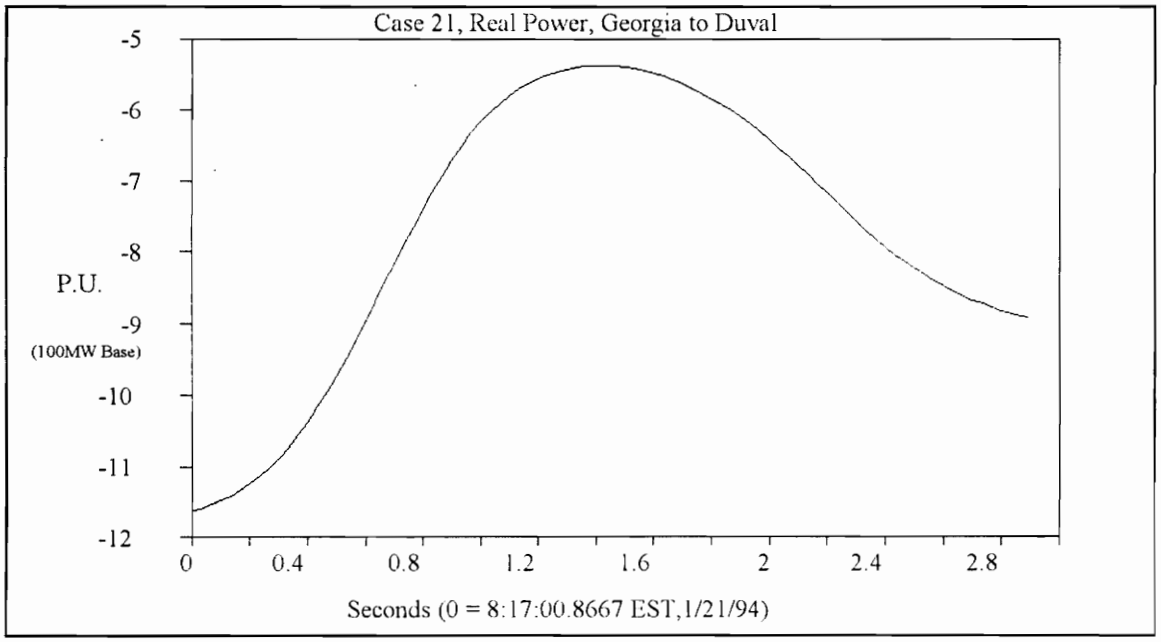

Figure 6.5. *Measured Real Power Swing, January 21, 1994*

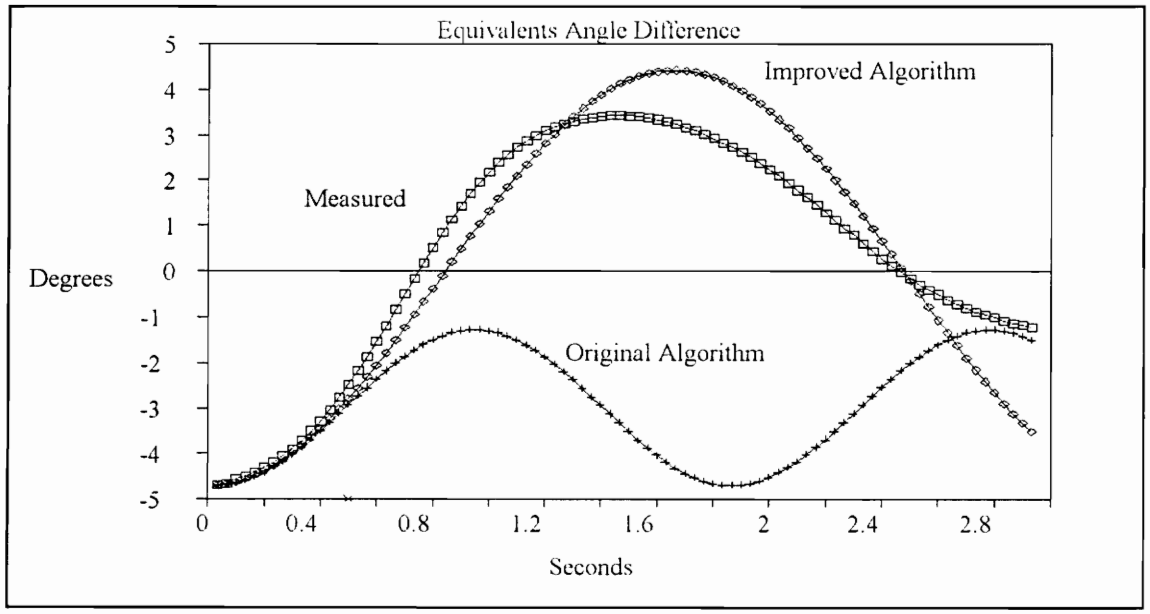

Figure 6.6. *Relay Predicted Angle Swing, January 21, 1994*

Table 6.4 Relay Outputs For Case 21:

	Original Algorithm	Improved Algorithm
Estimated Inertia Constant	NA	7563.64
Pre-fault Operating Power	7.8597	7.8597
Predicted New Power	9.5672	-3.8796
Pre-fault Operating Angle	4.6904	4.6904
Predicted New Angle	2.9817	-179.8595
Accelerating Area	0.3093	82.9764
Decelerating Area	125.3602	131.8614
Output	Stable	Stable

Comments:

For this swing power was flowing from Florida to Georgia. The improved relay algorithm (Chapter 7) assumes that power flows from Georgia to Florida all the time. The relay outputs listed in Table 6.4 show a very large estimate for the inertia constant of Florida due to this assumption. Figure 6.4 shows that the relay did not trigger at the beginning of the swing. The triggering limits for the relay were reduced after this event and the size of the pre-trigger was increased to allow storage of the complete events.

Figure 6.7 shows the computed velocity of the angle difference between Hatch and Duval. This is the expected behavior of the angle velocity except for the glitch at 0.1 seconds in the event time.

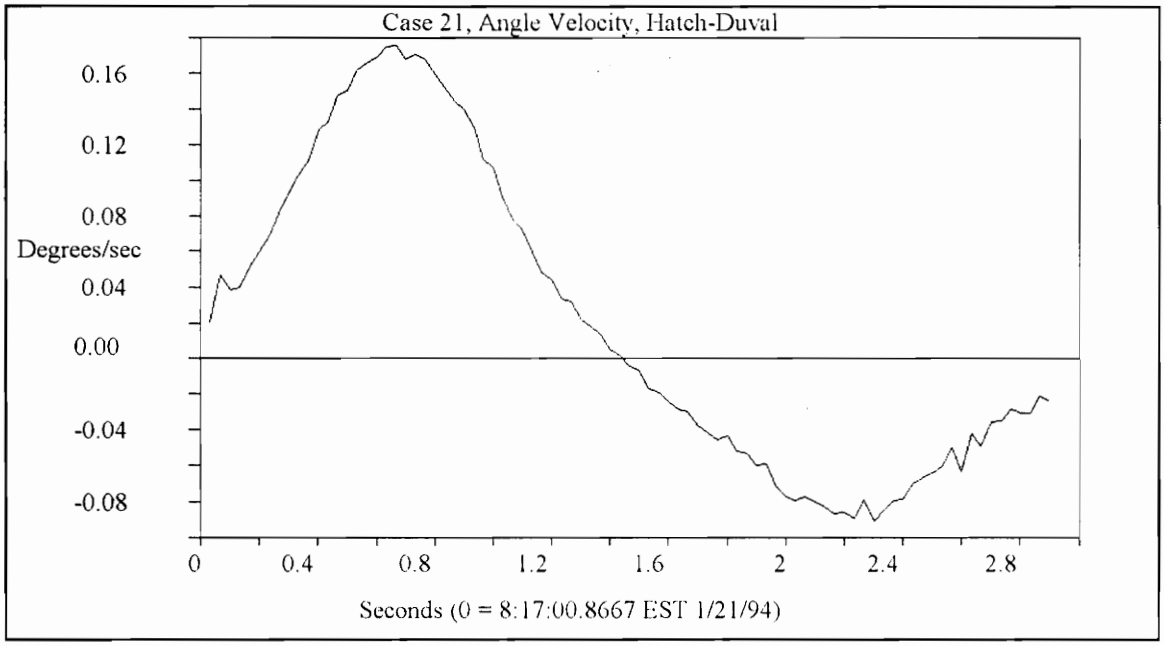

Figure 6.7. *Measured Angle Velocity, January 21, 1994*

Case 87:

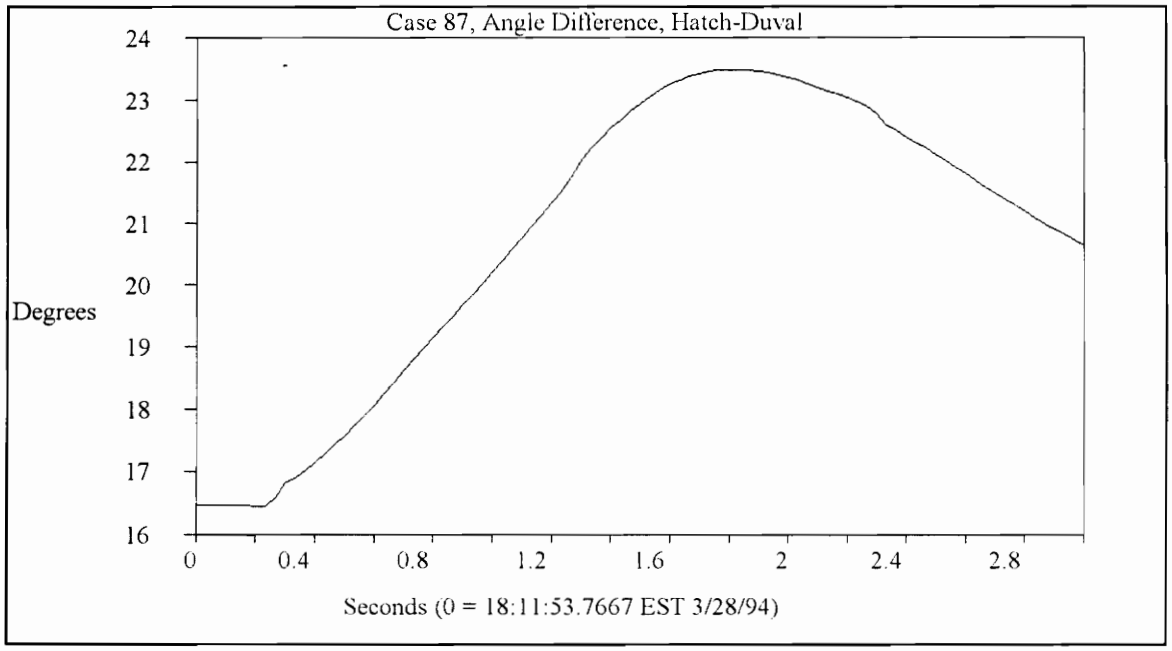

Figure 6.8. *Measured Angle Swing, March 28, 1994*

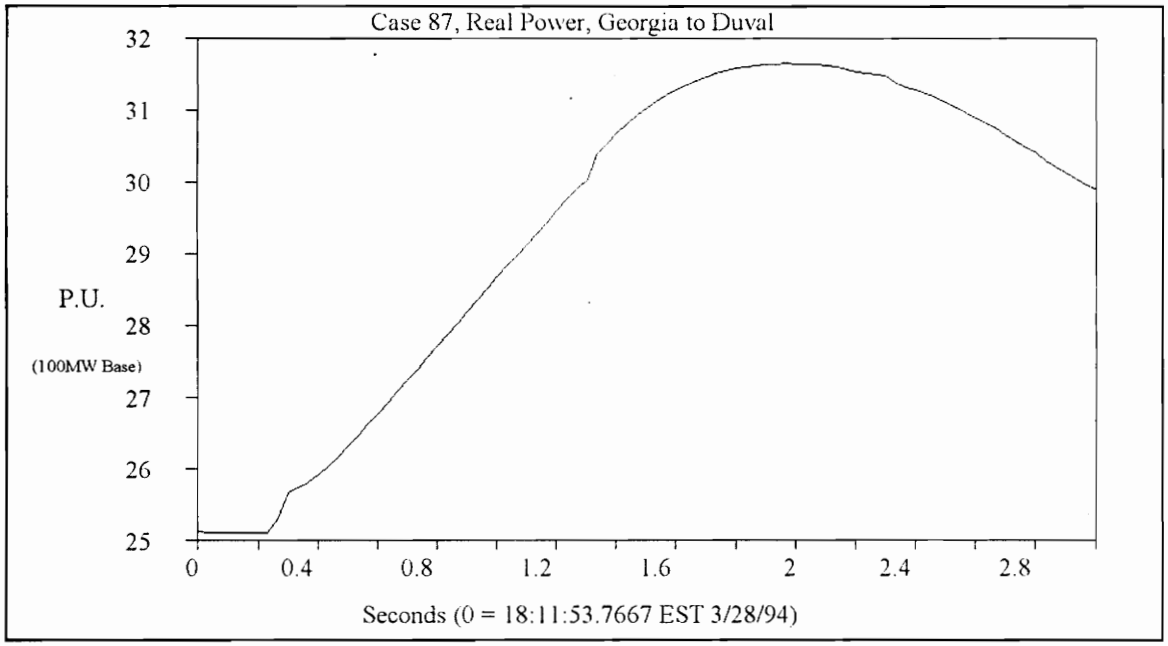

Figure 6.9. *Measured Power Swing Velocity, March 28, 1994*

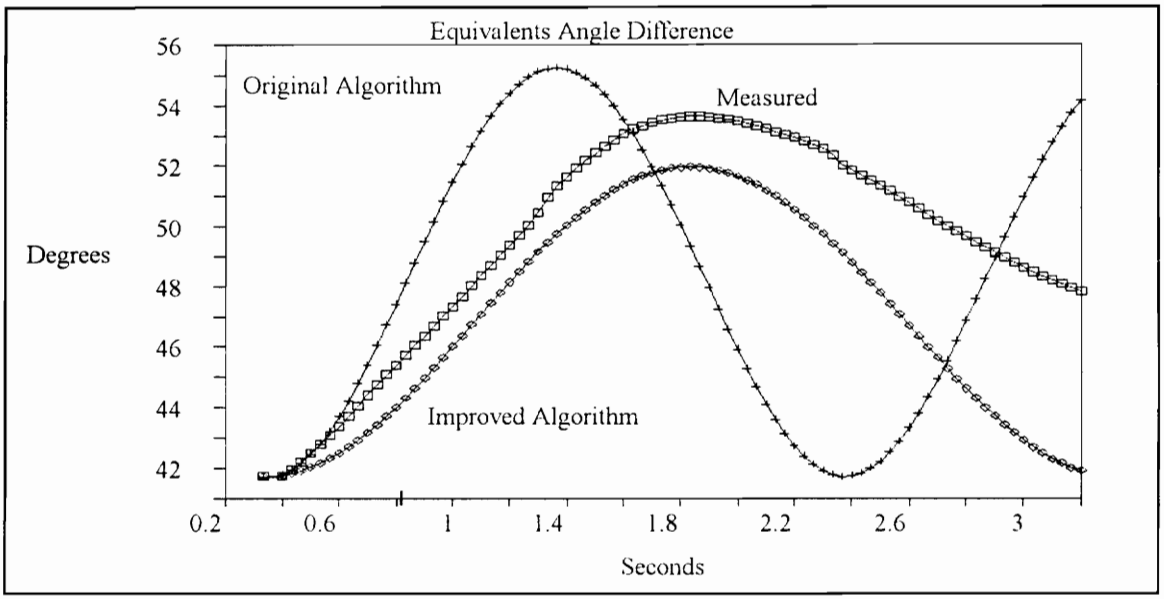

Figure 6.10. *Predicted Angle Swing, March 28, 1994*

Table 6.5 Relay Outputs For Case 87:

	Original Algorithm	Improved Algorithm
Estimated Inertia Constant	NA	2586.85
Pre-fault Operating Power	-29.9327	-29.9327
Predicted New Power	-32.4496	-34.8610
Pre-fault Operating Angle	-41.3719	-41.3719
Predicted New Angle	-48.3688	-46.7693
Accelerating Area	8.1101	6.4038
Decelerating Area	227.2859	238.2718
Output	Stable	Stable

Comments:

The angle velocity for this case, Figure 6.8, indicates that the acceleration changed twice during this swing at 0.4 and 1.3 seconds. This is also suggested by the shape of the swing curves in Figures 6.8 and 6.9 but it is not as clear. The prediction of the improved algorithm is very good considering all these changes.

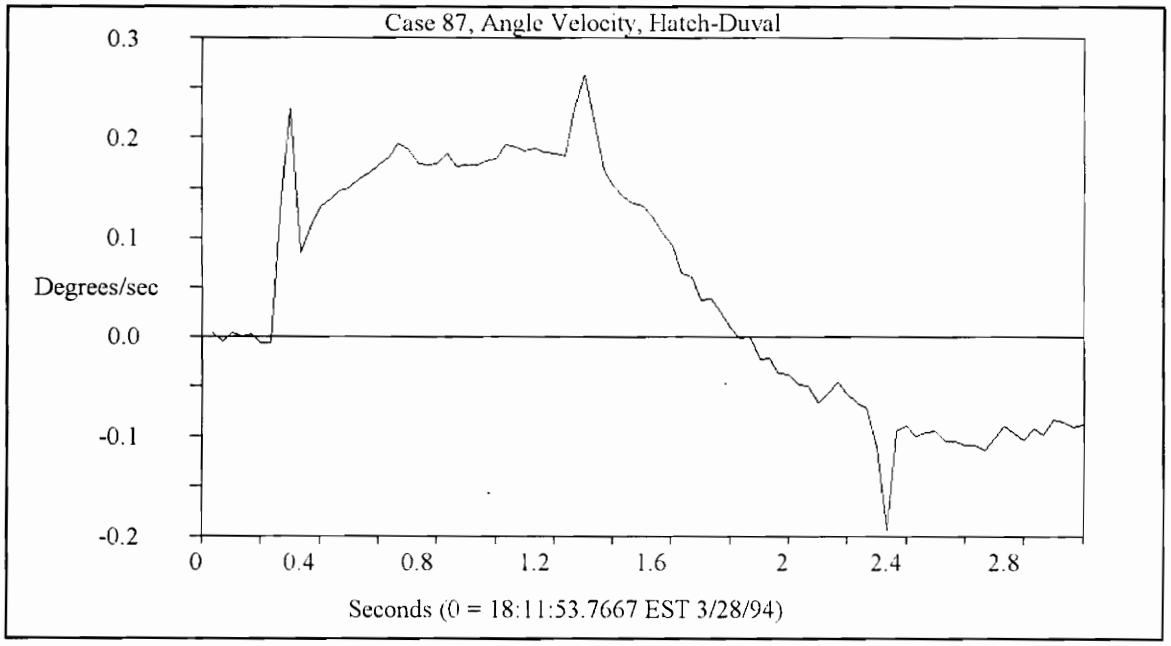

Figure 6.11. *Measured Angle Velocity, March 28, 1994*

Case 127:

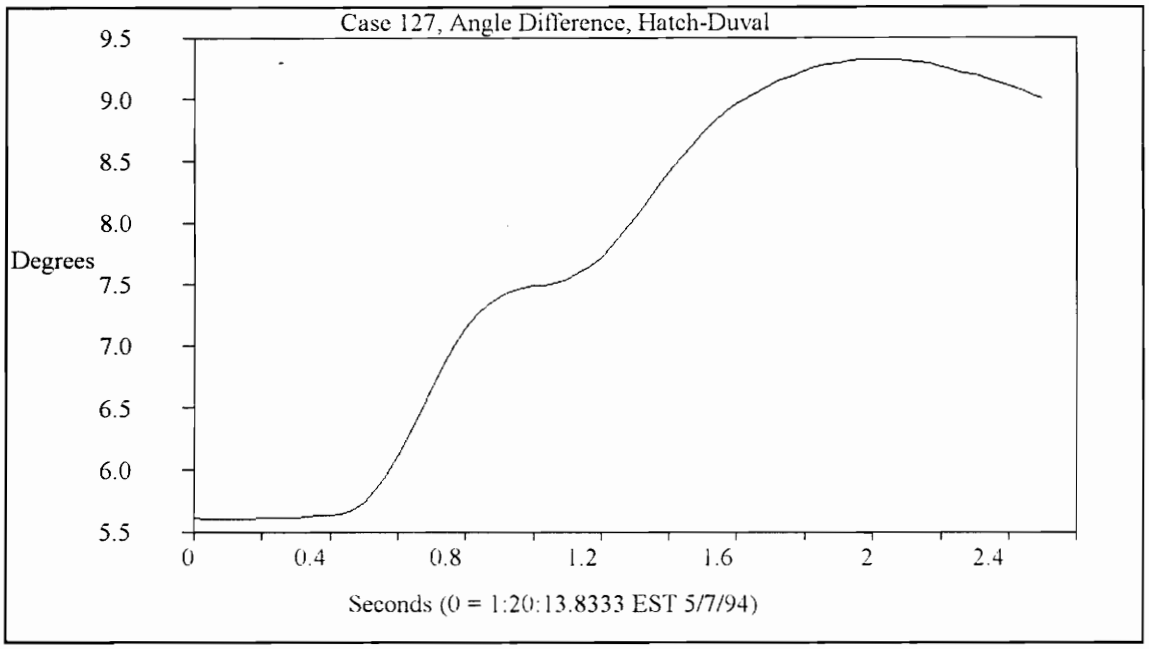

Figure 6.12. *Measured Angle Swing, May 7, 1994*

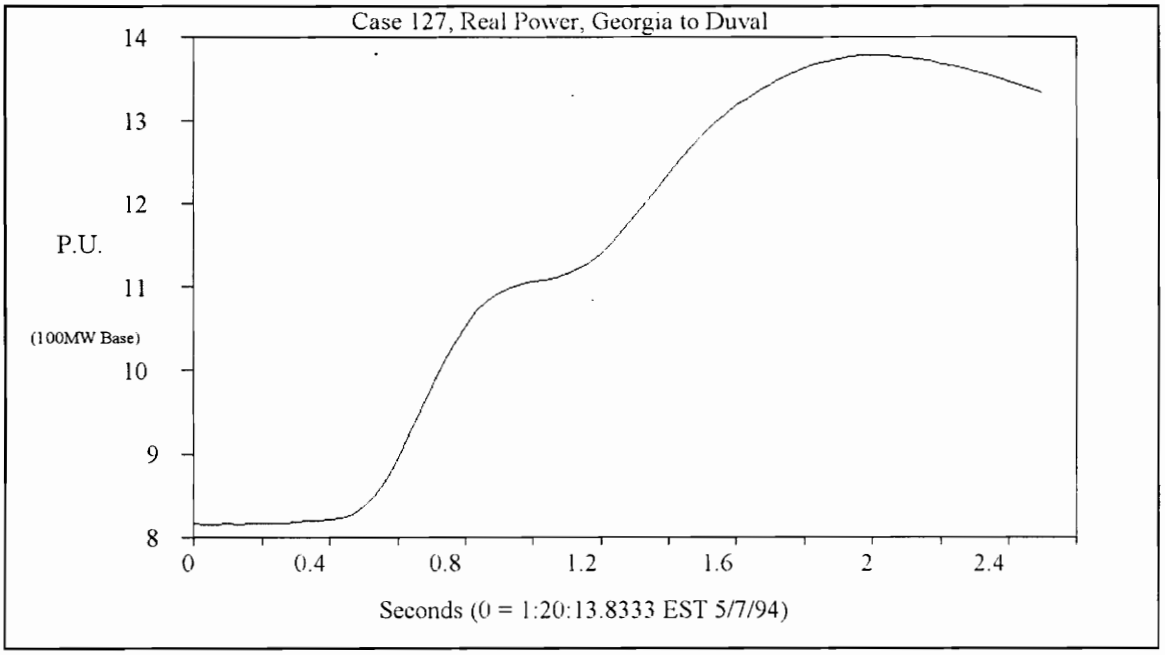

Figure 6.13. *Measured Power Swing, May 7, 1994*

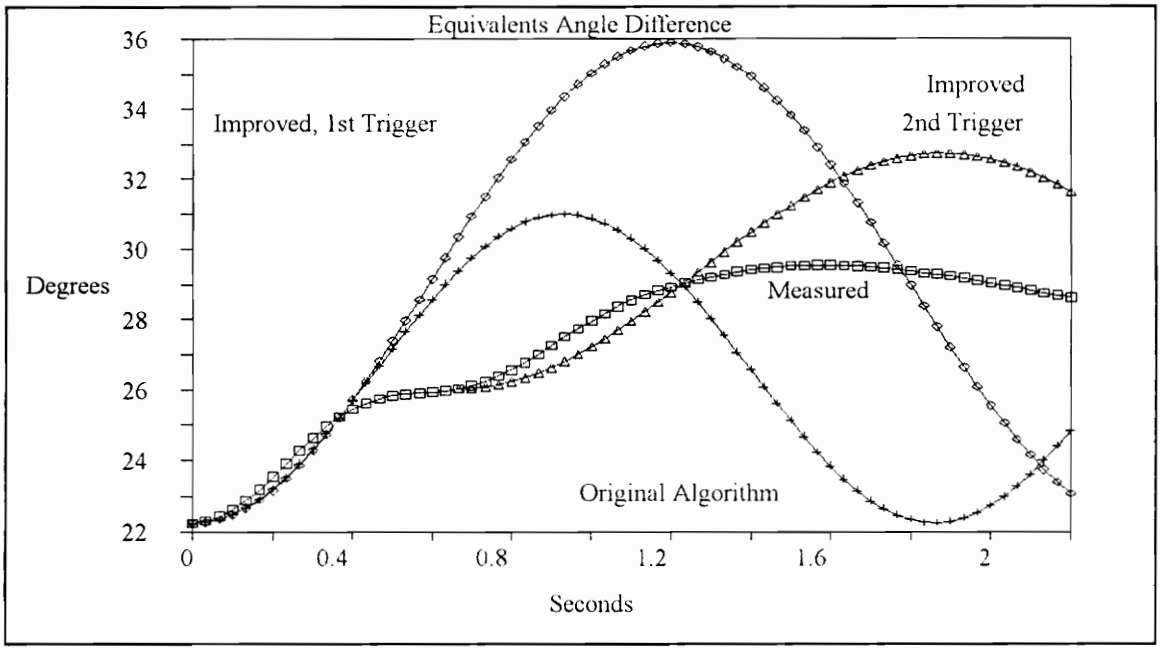

Figure 6.14. *Relay Predicted Angle Swing, May 7, 1994*

Table 6.6 Relay Outputs For Case 127:

Algorithm	Original	Improved 1st Trigger	Improved 2nd Trigger
Estimated Inertia Constant	NA	1750.82	1826.09
Pre-fault Operating Power	-14.8905	-14.8905	-17.9473
Predicted New Power	-15.8197	-19.9025	-20.4181
Pre-fault Operating Angle	-22.2451	-22.2451	-26.0356
Predicted New Angle	-26.6053	-29.0022	-29.3666
Accelerating Area	2.4532	4.3836	2.2993
Decelerating Area	154.3867	170.5904	172.8213
Output	Stable	Stable	Stable

Comments:

This is a compound swing case with a very good prediction for the first trigger in the original algorithm. The estimated inertia constants for the improved algorithm triggers are apparently too high, Figure 6.14. The behavior of the angle swing and angle velocity is not as expected for a normal swing. The velocity increases after one second when it should have become negative, Figure 6.15. This point indicates the beginning of a second swing. The behavior of the acceleration for the first swing is more homogeneous than for the second swing as shown by the angle velocity in Figure 6.15.

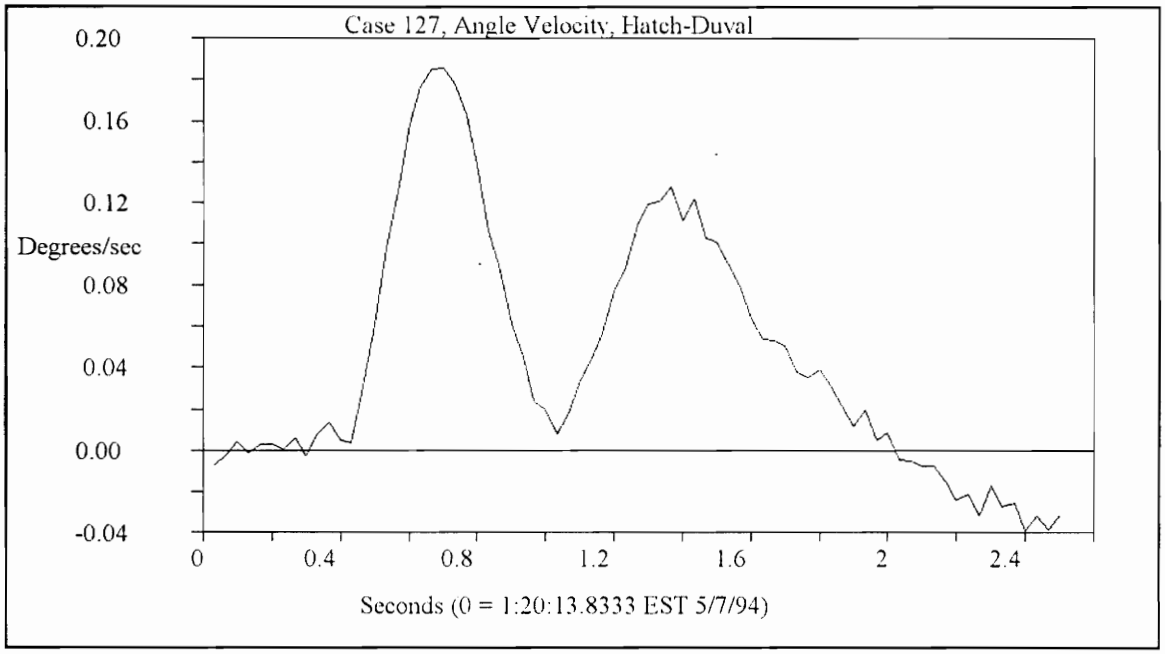

Figure 6.15. *Measured Angle Velocity, May 7, 1994*

Case 150:

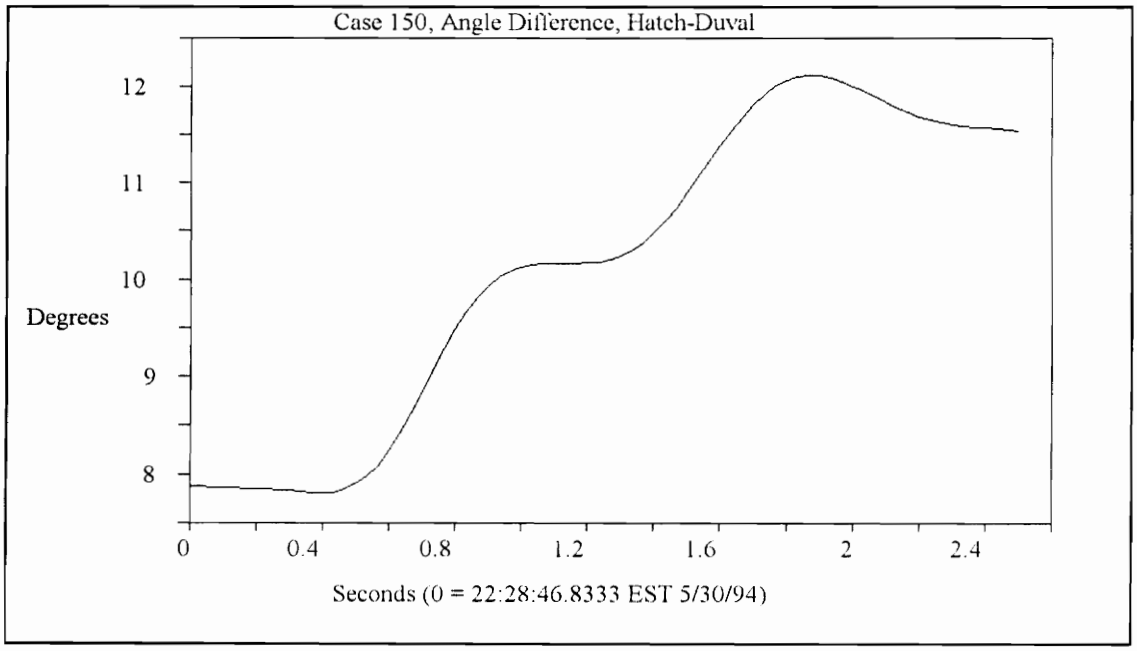

Figure 6.16. *Measured Angle Swing, May 30, 1994*

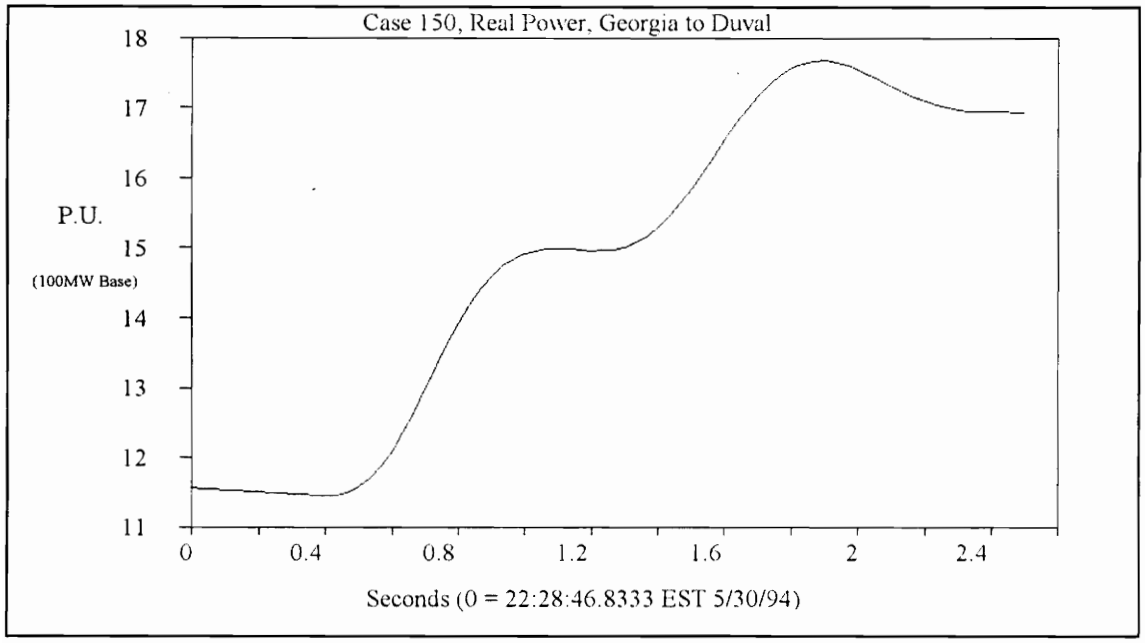

Figure 6.17. *Measured Power Swing, May 30, 1994*

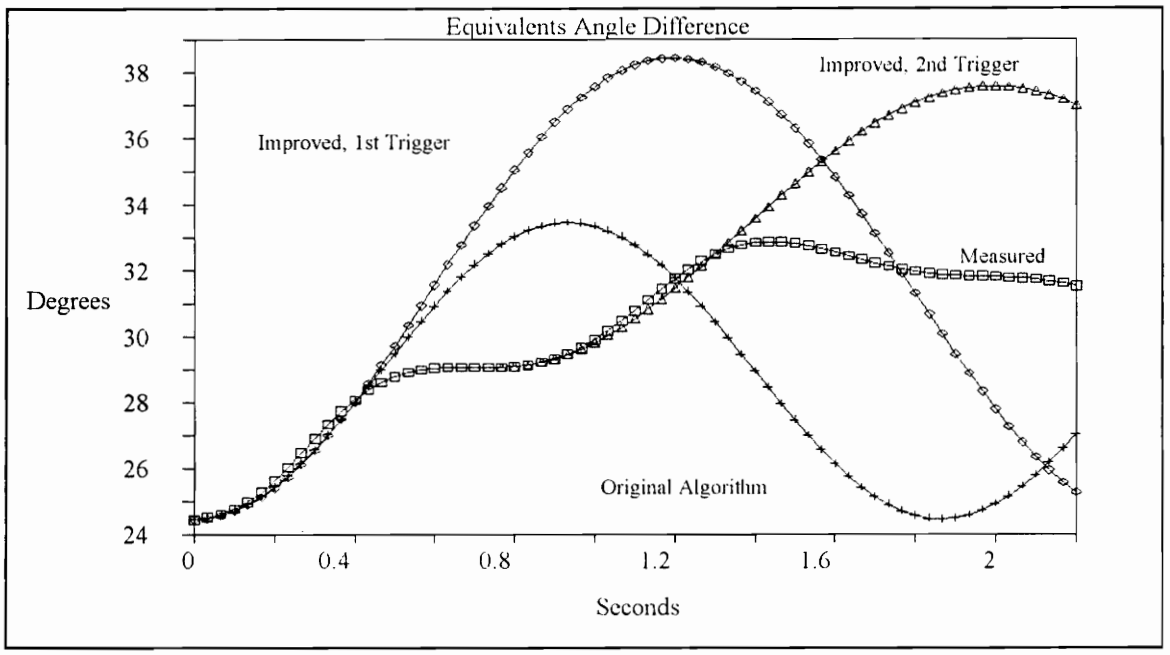

***Figure 6.18**. Relay Predicted Angle Swing, May 30, 1994*

Table 6.7 Relay Outputs For Case 150:

Algorithm	Original	Improved 1st Trigger	Improved 2nd Trigger
Estimated Inertia Constant	NA	1709.05	1804.14
Pre-fault Operating Power	-16.0719	-16.0719	-19.7231
Predicted New Power	-16.5778	-20.4792	-23.2013
Pre-fault Operating Angle	-24.4410	-24.4410	-29.0762
Predicted New Angle	-28.7570	-30.6785	-33.9258
Accelerating Area	2.5625	4.1960	2.2202
Decelerating Area	158.0475	173.6236	185.0708
Output	Stable	Stable	Stable

Comments:

This is a compound swing case with a very good prediction for the first trigger in the original algorithm. The estimated inertia constants for the improved algorithm triggers are apparently too high. The behavior of the acceleration for both swings is very homogeneous as shown by the angle velocity in Figure 6.16. For the compound swings the second swings seems to start when the velocity decreases near zero.

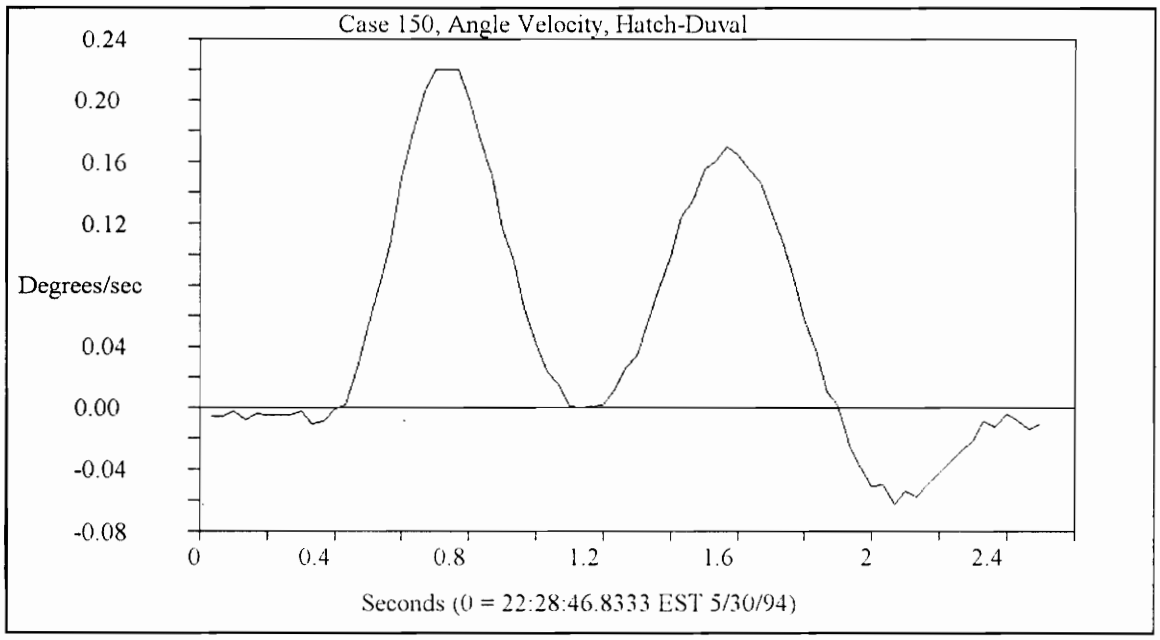

Figure 6.19. *Measured Angle Velocity, May 30, 1994*

Case 157:

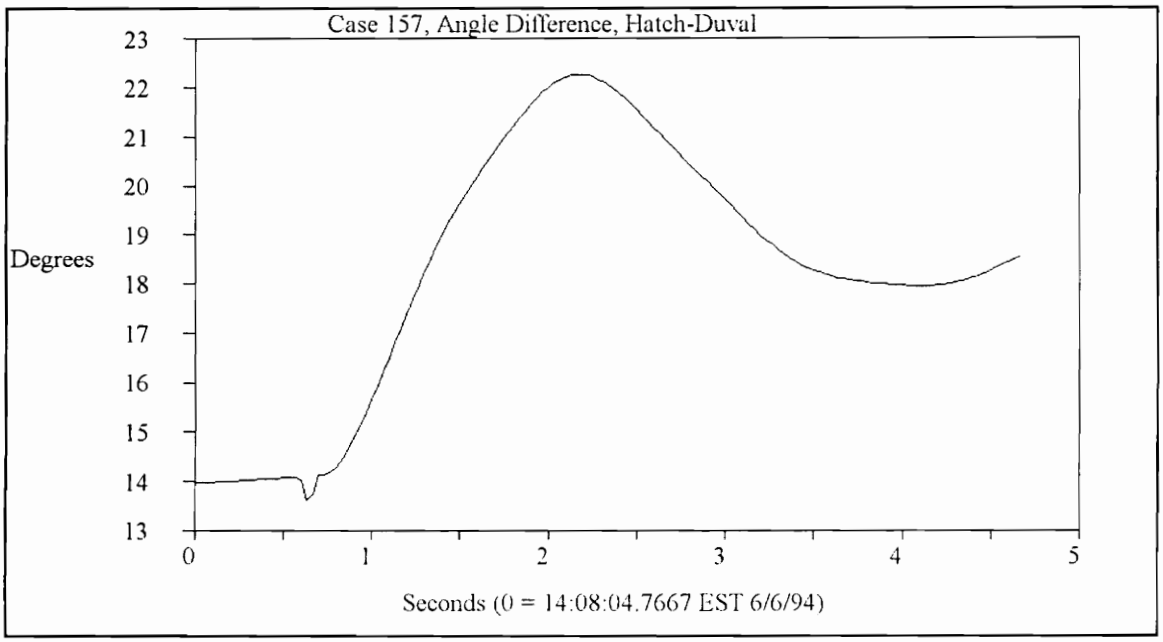

***Figure 6.20**. Measured Angle Swing, June 6, 1994*

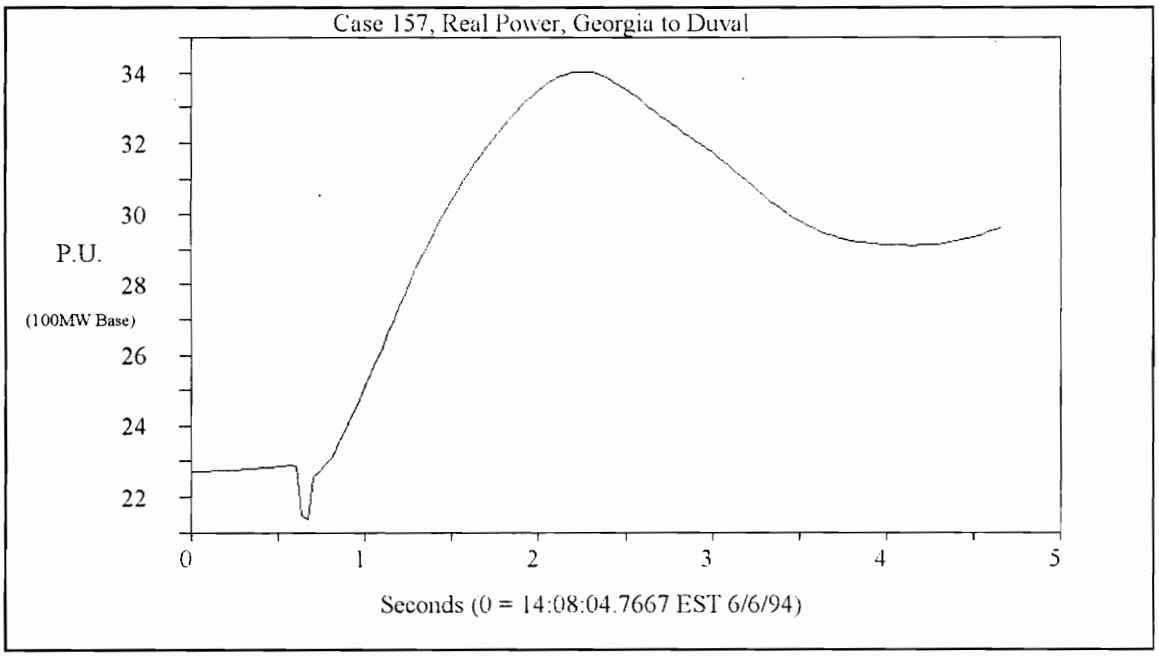

***Figure 6.21**. Measured Power Swing, June 6, 1994*

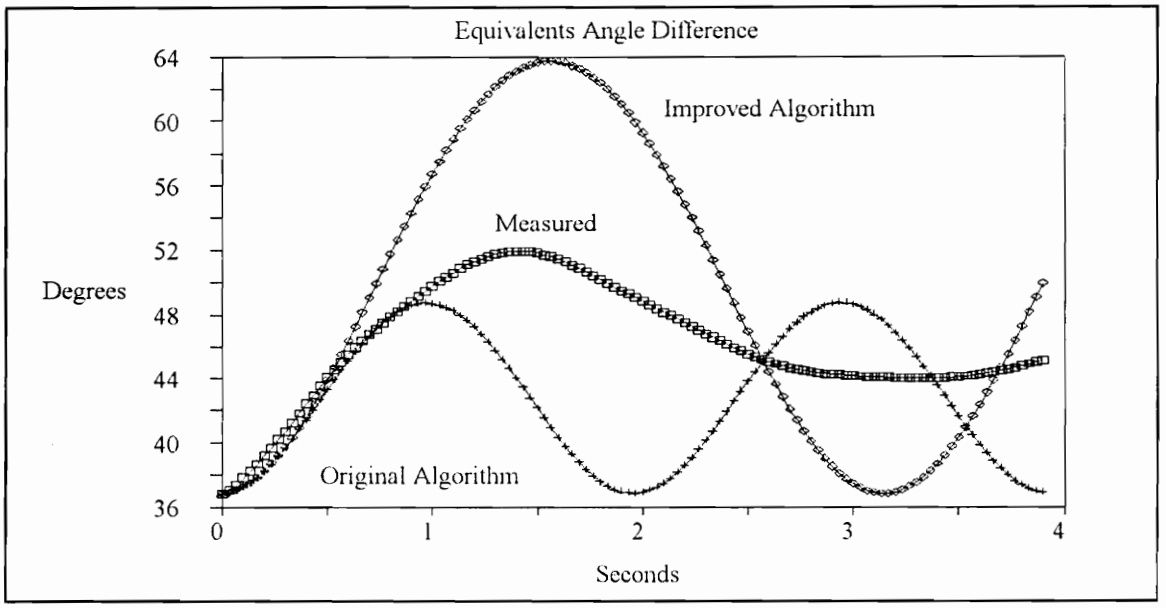

Figure 6.22. *Relay Predicted Angle Swing, June 6, 1994*

Table 6.8 Relay Outputs For Case 157:

	Original Algorithm	Improved Algorithm
Estimated Inertia Constant	NA	2657.31
Pre-fault Operating Power	-25.9416	-25.9416
Predicted New Power	-27.7717	-35.9079
Pre-fault Operating Angle	-36.7449	-36.7449
Predicted New Angle	-42.7234	-49.7253
Accelerating Area	6.0172	15.3526
Decelerating Area	204.0432	241.4935
Output	Stable	Stable

Comments:

The prediction of the improved algorithm is too high due to the large acceleration at the beginning of the swing. The acceleration changes at 0.5 seconds when the relay prediction has already been made. This changes can be seen in the shape of the angle swing and the angle velocity shown in Figure 6.23. This could be interpreted as a compound swing but the velocity has a single swing behavior.

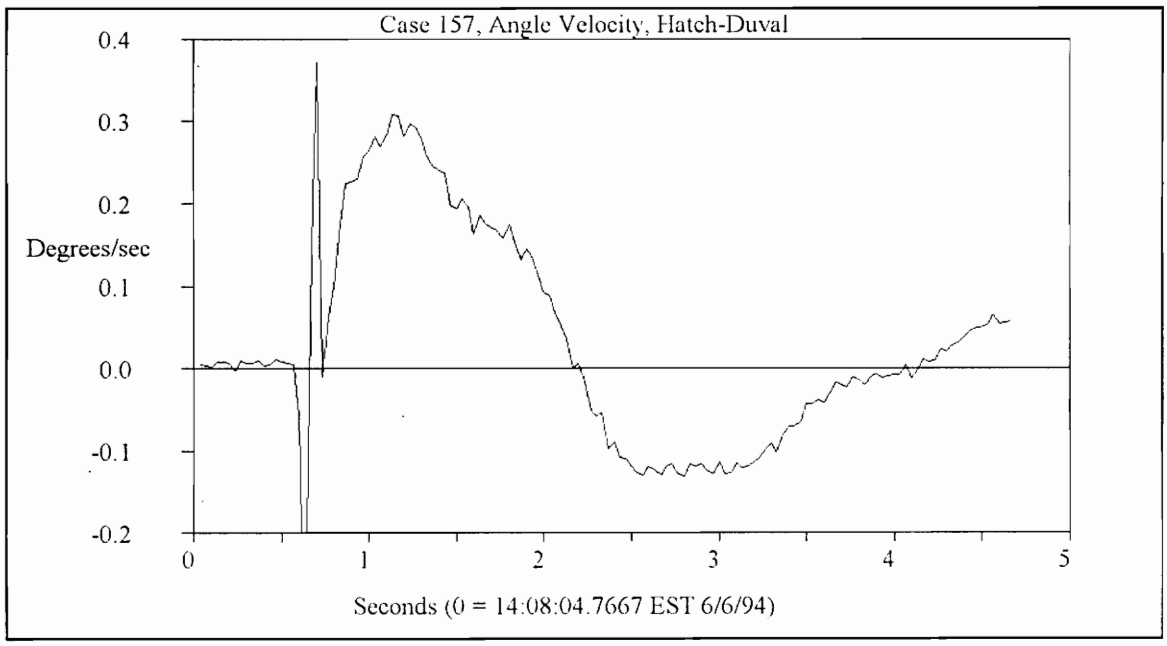

Figure 6.23. *Measured Angle Velocity, June 6, 1994*

Case 166:

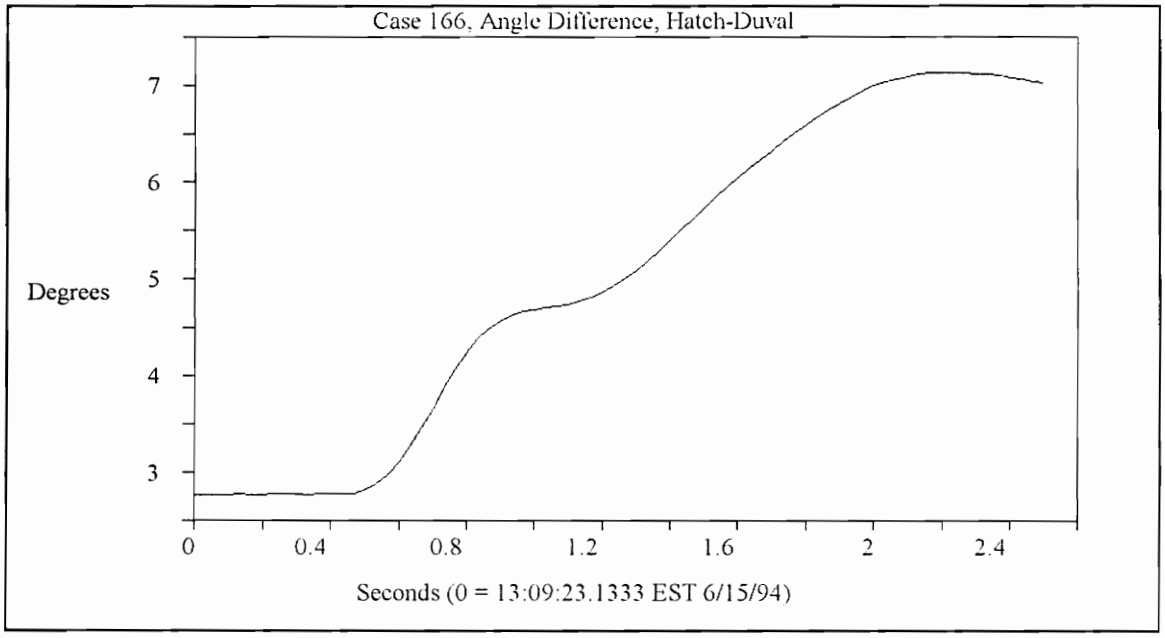

***Figure 6.24**. Measured Angle Swing, June 15, 1994*

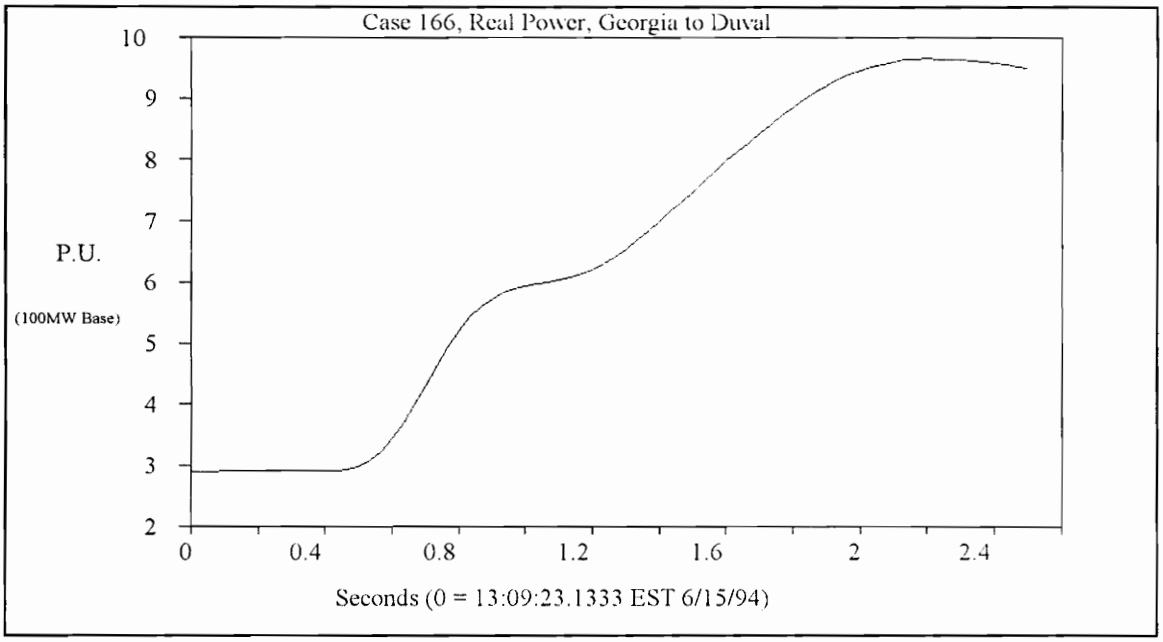

***Figure 6.25**. Measured Power Swing, June 15, 1994*

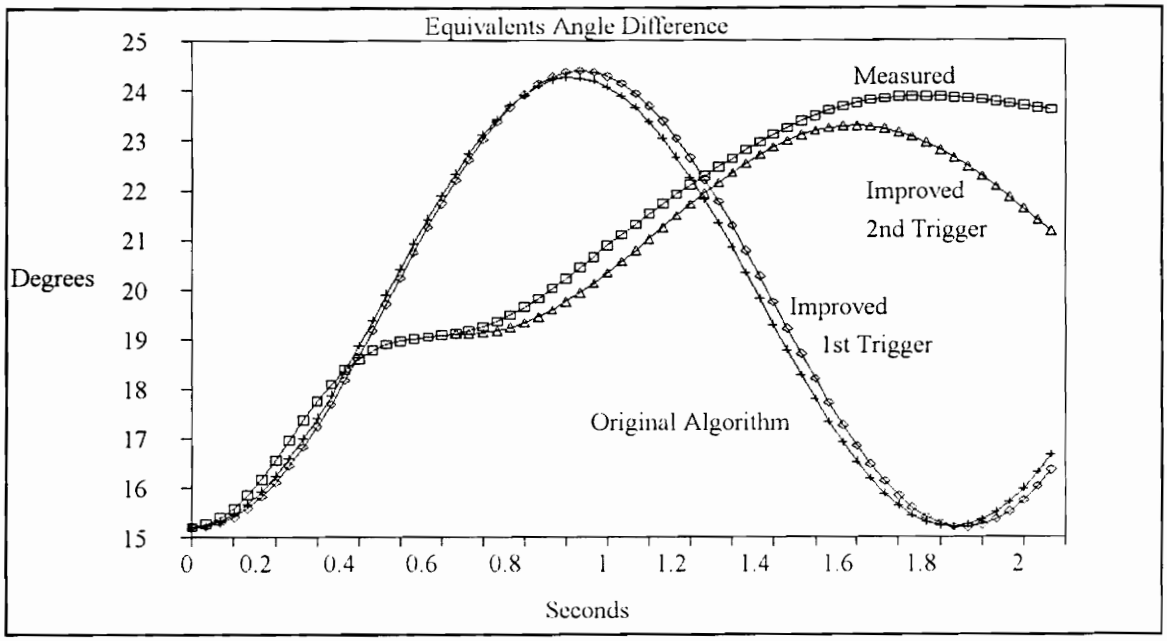

Figure 6.26. *Relay Predicted Angle Swing, June 15, 1994*

Table 6.9 Relay Outputs For Case 166:

Algorithm	Original	Improved 1st Trigger	Improved 2nd Trigger
Predicted Inertia Constant	NA	968.4923	1000.1730
Pre-fault Operating Power	-8.6911	-8.6911	-11.9550
Predicted New Power	-9.4127	-9.5408	-10.8799
Pre-fault Operating Angle	-15.2117	-15.2117	-19.1149
Predicted New Angle	-19.7240	-19.7885	-21.1932
Accelerating Area	1.3406	1.3720	0.7580
Decelerating Area	131.0766	131.5446	137.1361
Output	Stable	Stable	Stable

Comments:

The prediction for the original and improved algorithm are very close for the first swing. The prediction for the second trigger is much better than for the other compound swing cases. Figure 6.27 shows a different behavior for the acceleration during the second swing. The velocity shown in Figure 6.27 does not go to zero before increasing again but stops decreasing and starts increasing around the one second mark. The behavior of the velocity for the compound events is used by the improved algorithm to identify them and make a second prediction.

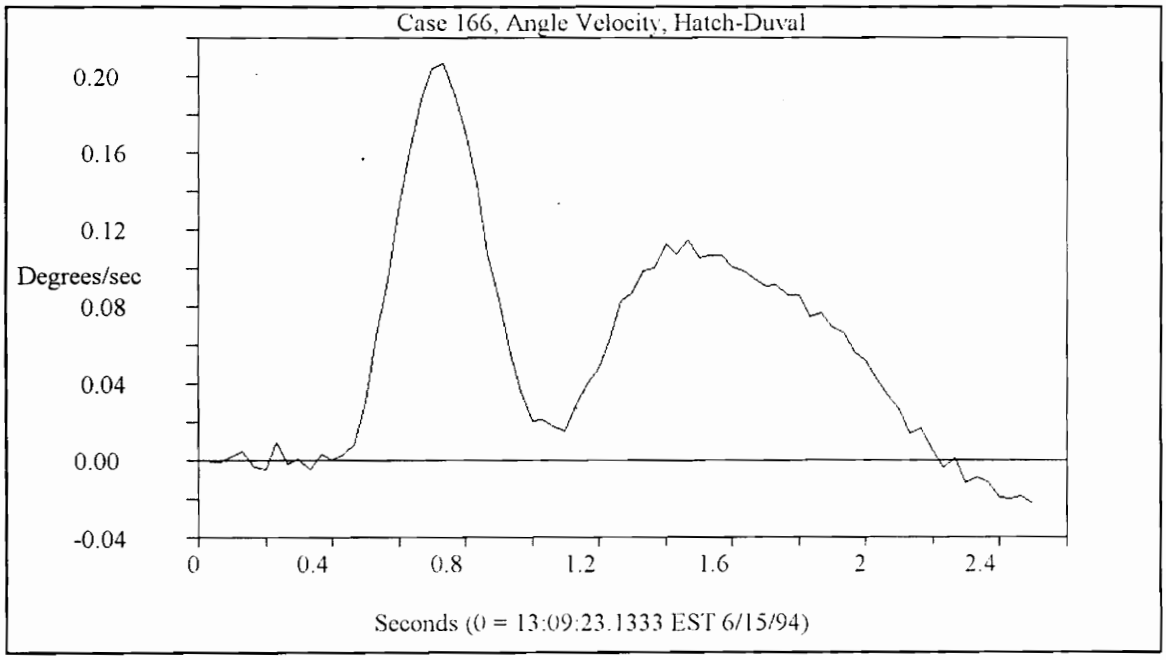

Figure 6.27. *Measured Angle Velocity, June 15, 1994*

Case 180:

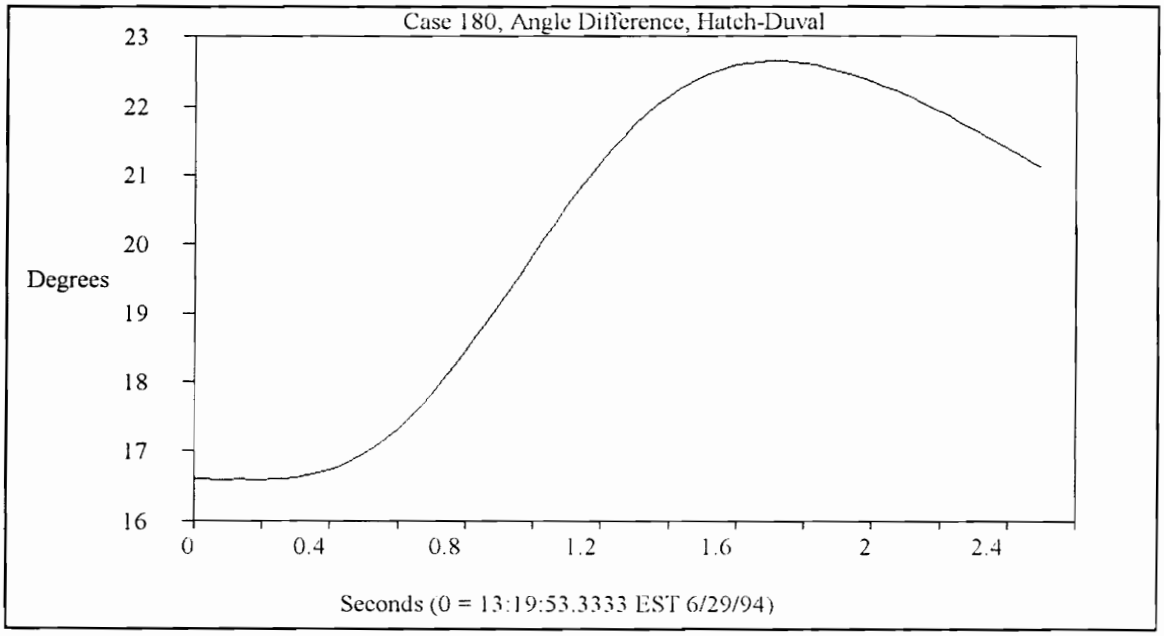

Figure 6.28. *Measured Angle Swing, June 29, 1994*

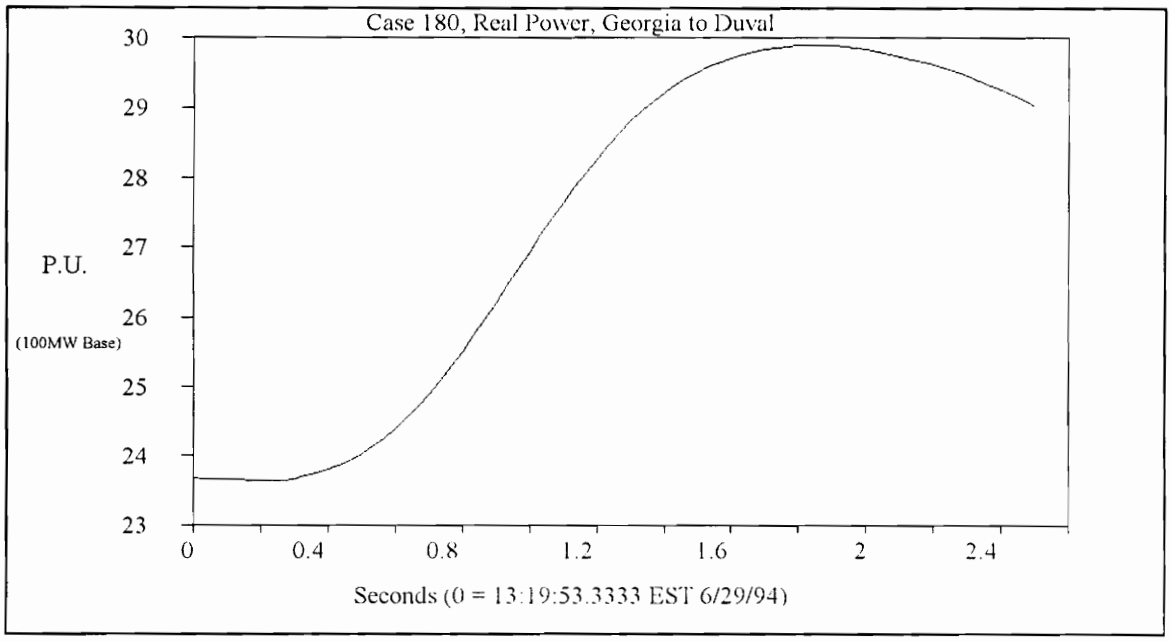

Figure 6.29. *Measured Power Swing, June 29, 1994*

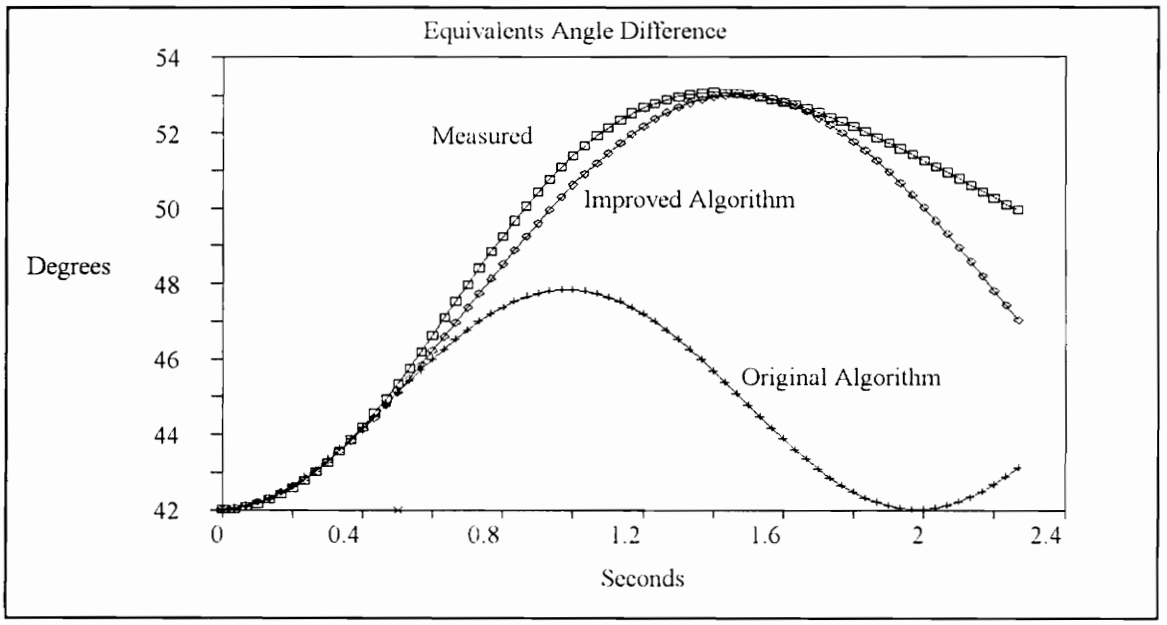

Figure 6.30. *Relay Predicted Angle Swing, June 29, 1994*

Table 6.10 Relay Outputs For Case 180:

	Original Algorithm	Improved Algorithm
Estimated Inertia Constant	NA	2472.06
Pre-fault Operating Power	-29.7048	-29.7048
Predicted New Power	-29.4785	-34.3562
Pre-fault Operating Angle	-41.9189	-41.9189
Predicted New Angle	-44.9138	-47.4274
Accelerating Area	3.2200	6.4397
Decelerating Area	212.2975	234.6562
Output	Stable	Stable

Comments:

The prediction for the improved algorithm is very close to the measured values. The acceleration is not smooth for the first swing as seen in Figures 6.28 and 6.29. The velocity shown in Figure 6.31 shows a single event behavior but does not have a smooth behavior.

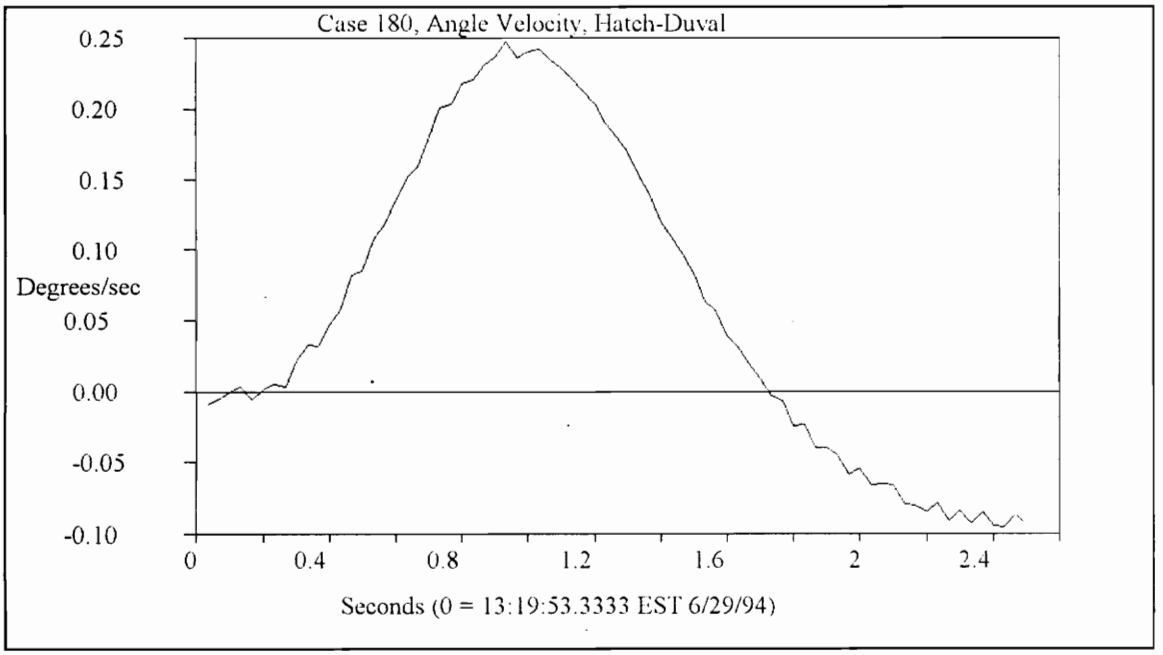

Figure 6.31. *Measured Angle Velocity, June 29, 1994*

Case 251:

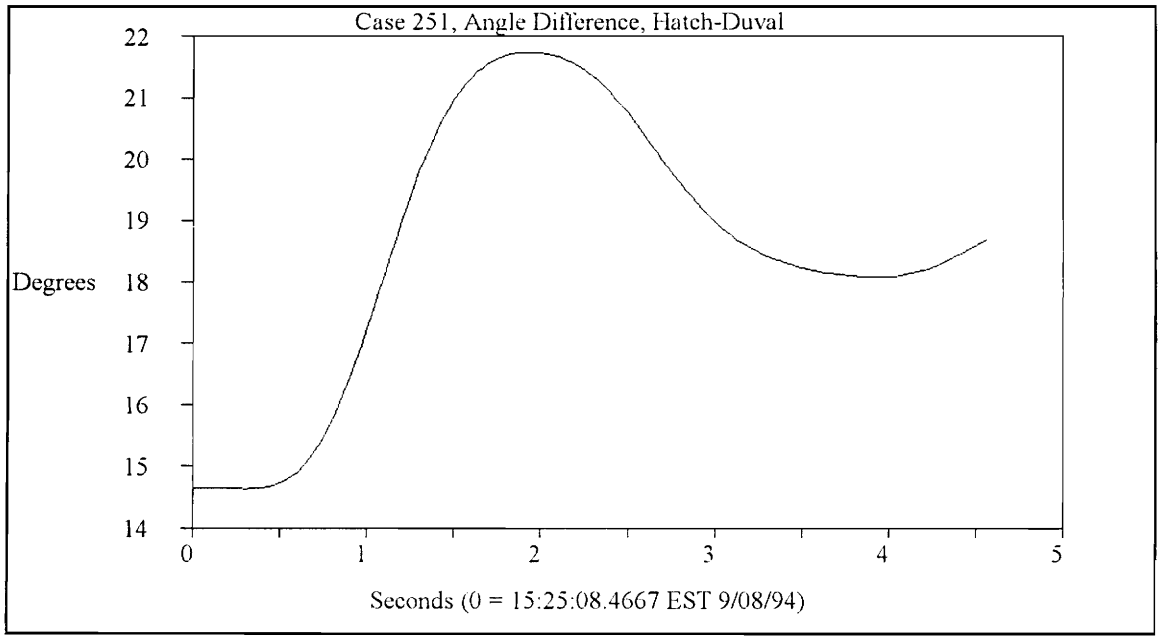

Figure 6.32. *Measured Angle Swing, September 8, 1994*

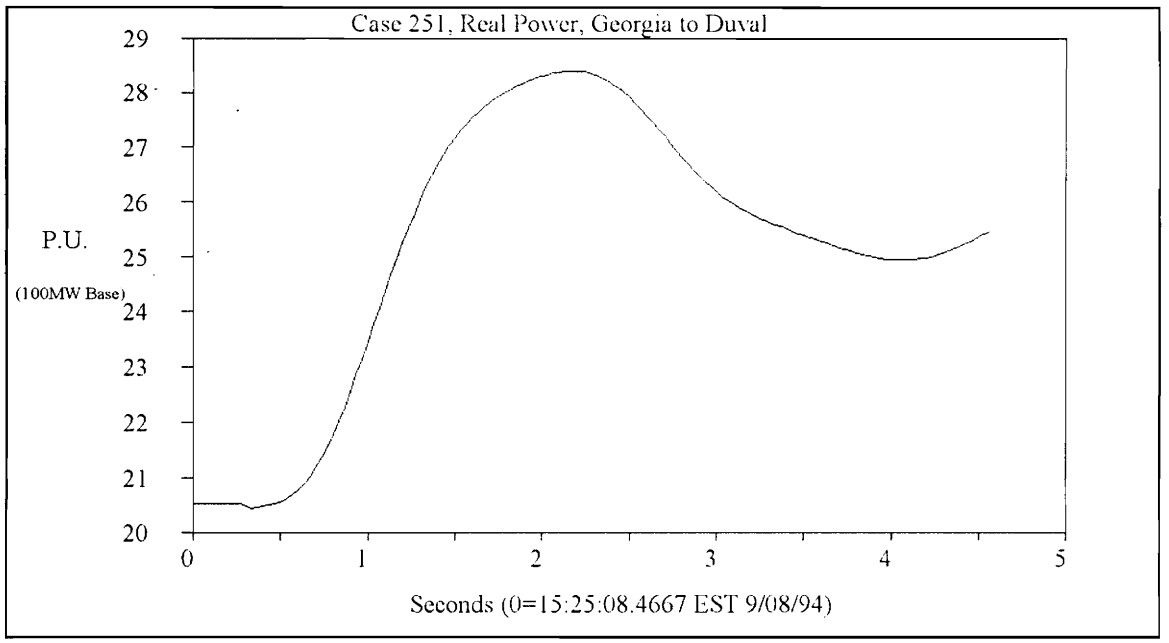

Figure 6.33. *Measured Power Swing, September 8, 1994*

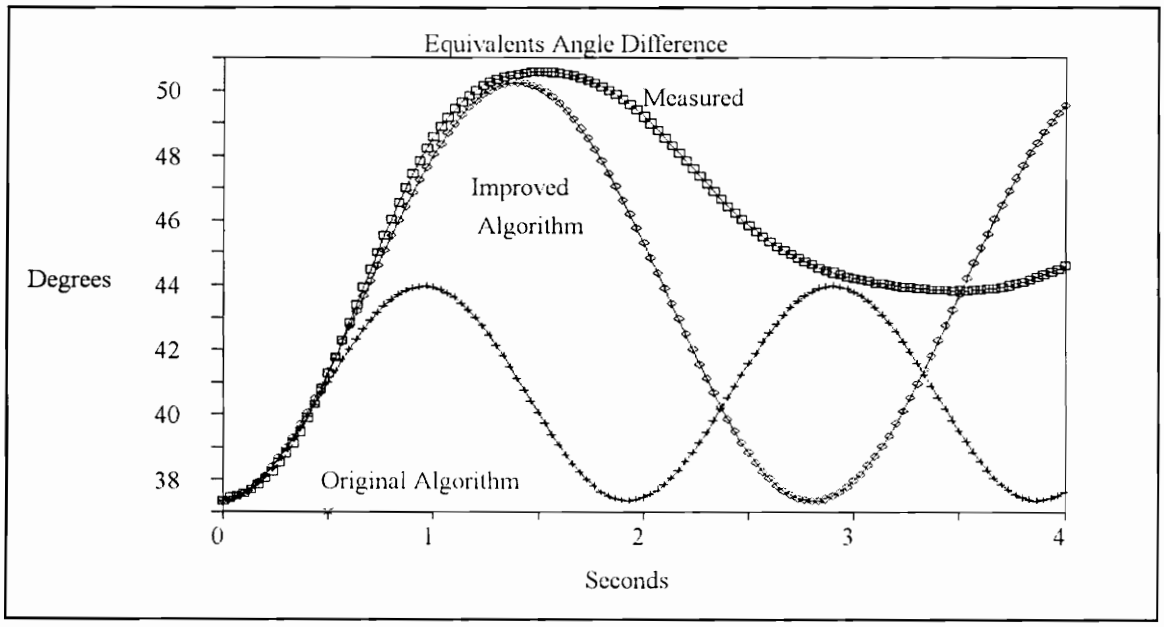

***Figure 6.34**. Relay Predicted Angle Swing, September 8, 1994*

Table 6.11 Relay Outputs For Case 251:

	Original Algorithm	Improved Algorithm
Estimated Inertia Constant	NA	2301.93
Pre-fault Operating Power	-26.4519	-26.4519
Predicted New Power	-26.3206	-31.6965
Pre-fault Operating Angle	-37.3610	-37.3610
Predicted New Angle	-40.6315	-43.6934
Accelerating Area	3.1466	6.7706
Decelerating Area	198.9474	222.8387
Output	Stable	Stable

Comments:

This is a clean swing with a very good prediction by the improved relay algorithm. There is a small glitch in the angle difference at the beginning of the swing which can be more easily seen in the angle velocity, Figure 6.35. This is almost a text book swing in the angle.

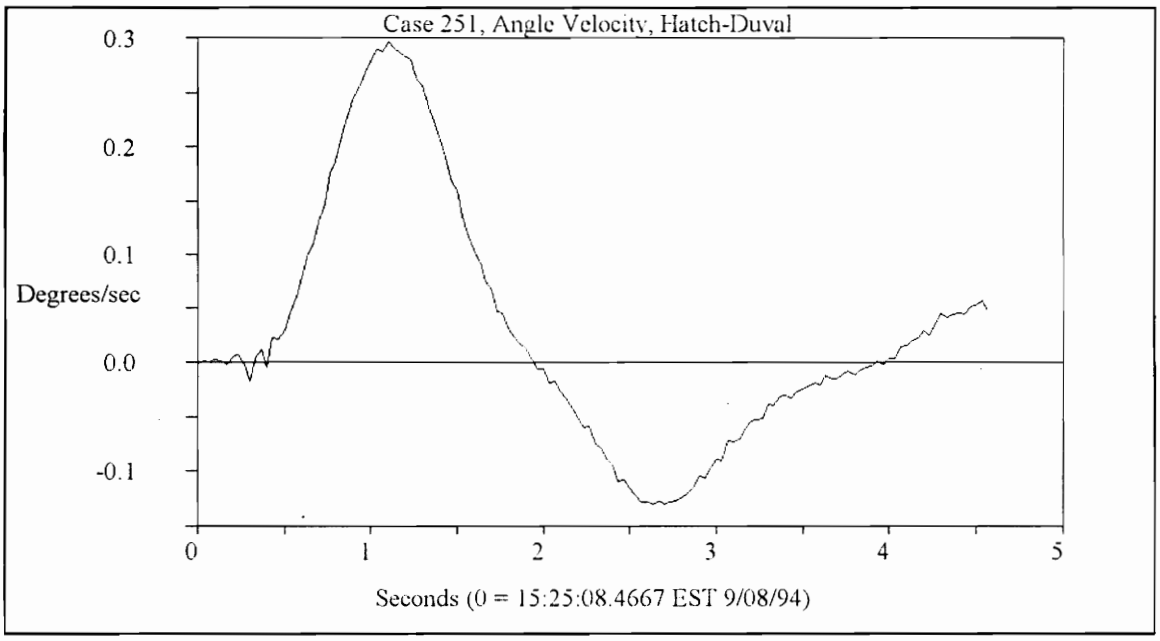

***Figure 6.35**. Measured Angle Velocity, September 8, 1994*

Case 266:

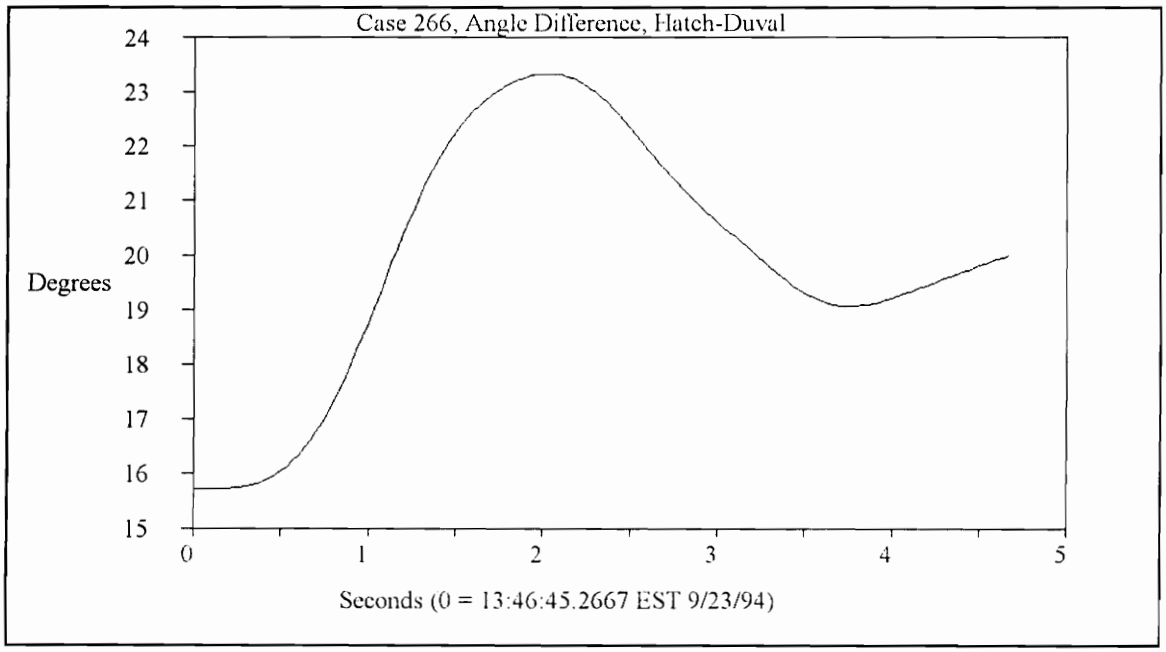

Figure 6.36. *Measured Angle Swing, September 23, 1994*

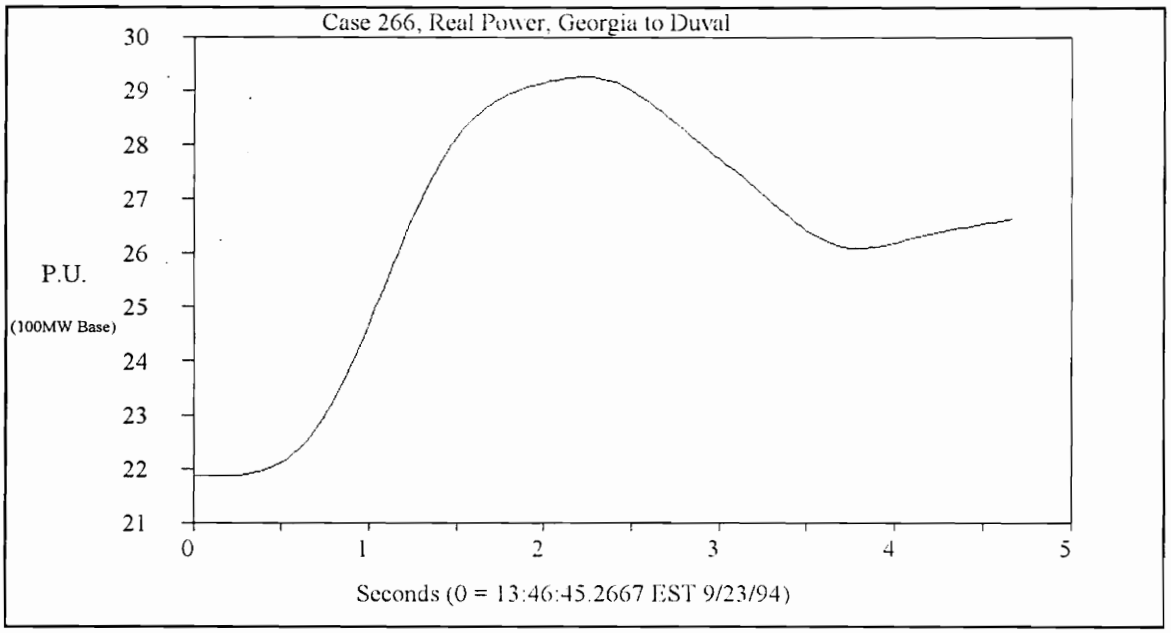

Figure 6.37. *Measured Power Swing, September 23, 1994*

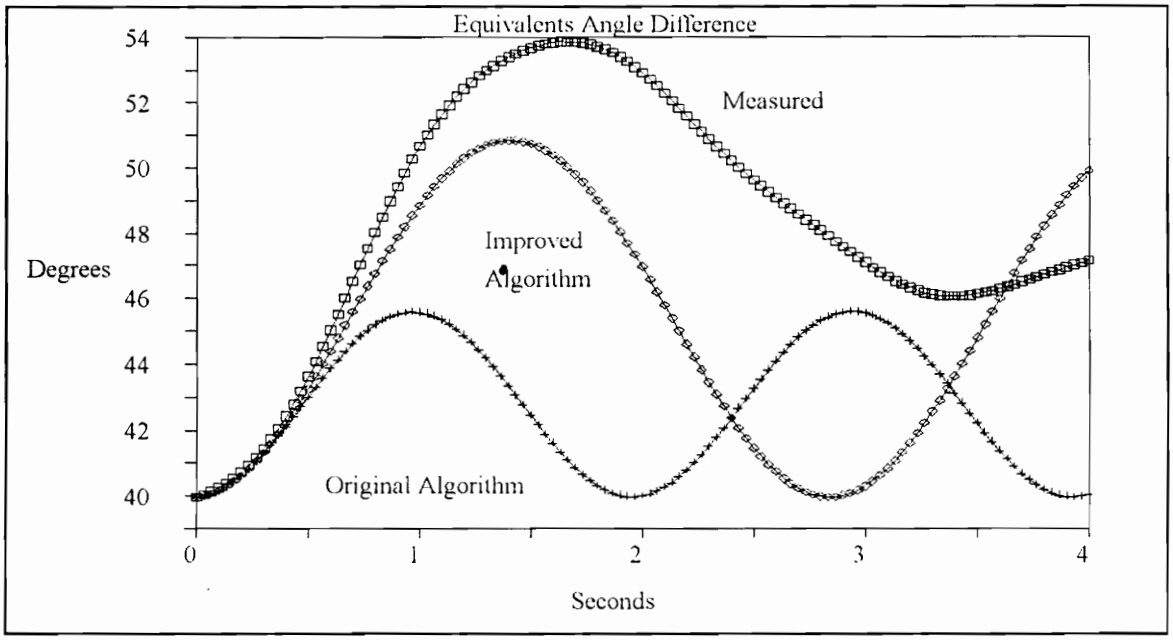

***Figure 6.38**. Relay Predicted Angle Swing, September 23, 1994*

Table 6.12 Relay Outputs For Case 266:

	Original Algorithm	Improved Algorithm
Estimated Inertia Constant	NA	2294.73
Pre-fault Operating Power	-28.0640	-28.0640
Predicted New Power	-27.7130	-32.5819
Pre-fault Operating Angle	-39.8211	-39.8211
Predicted New Angle	-42.7614	-45.3298
Accelerating Area	2.9728	6.0922
Decelerating Area	204.7695	226.6968
Output	Stable	Stable

Comments:

A better result was expected for this case using the improved algorithm. But the slow acceleration at the beginning of the swing results in a prediction of the new operating point that is lower than the actual operating point. The angle velocity in Figure 6.39 shows a change in the angle behavior at the beginning of the swing which affects the angle prediction.

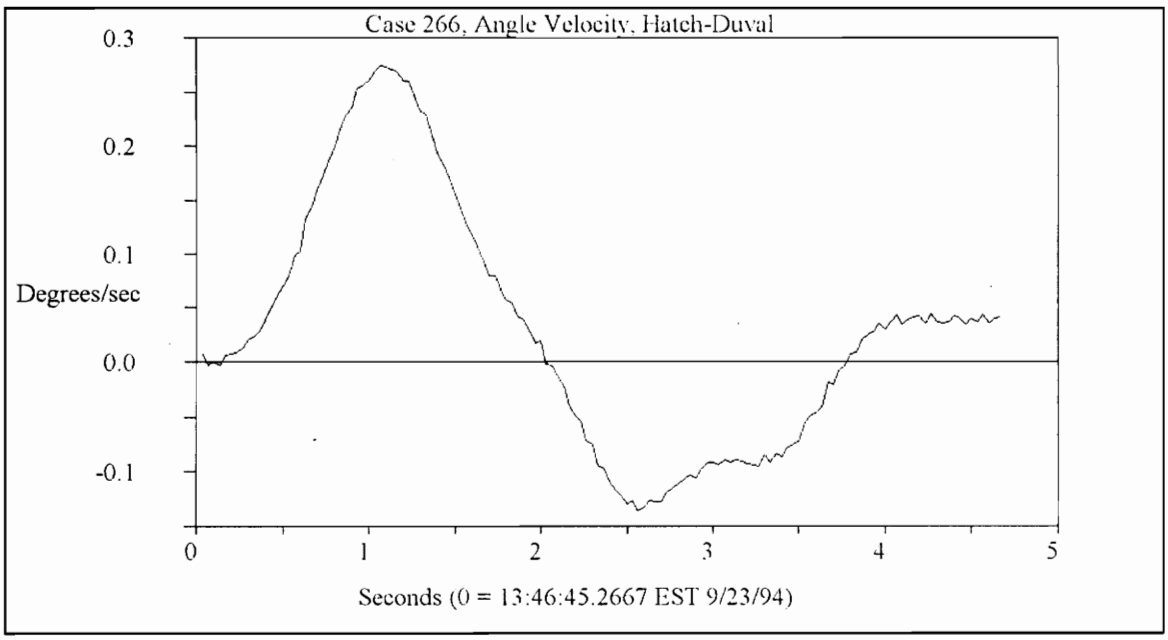

Figure 6.39. *Measured Angle Velocity, September 23, 1994*

Case 276:

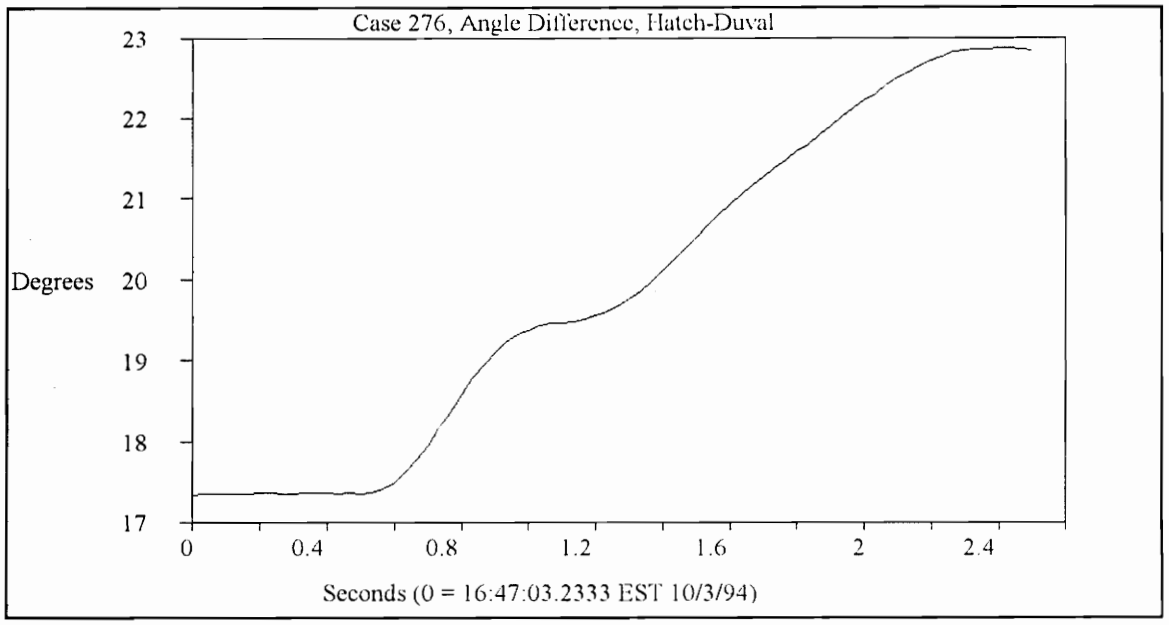

***Figure 6.40**. Measured Angle Swing, October 3, 1994*

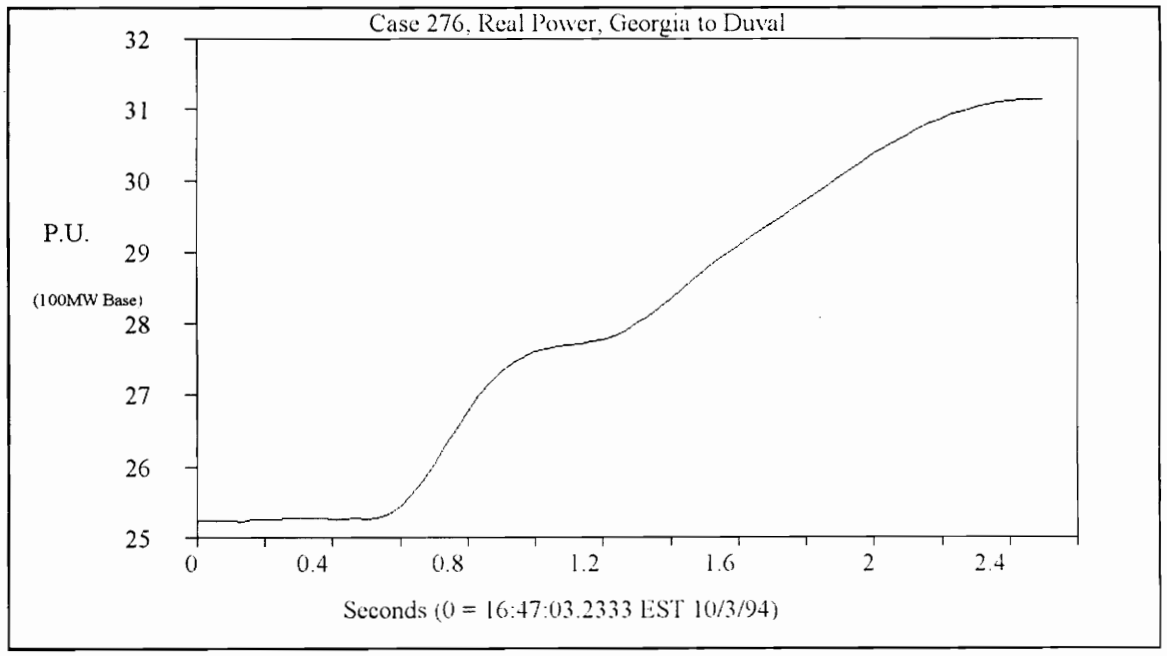

***Figure 6.41**. Measured Power Swing, October 3, 1994*

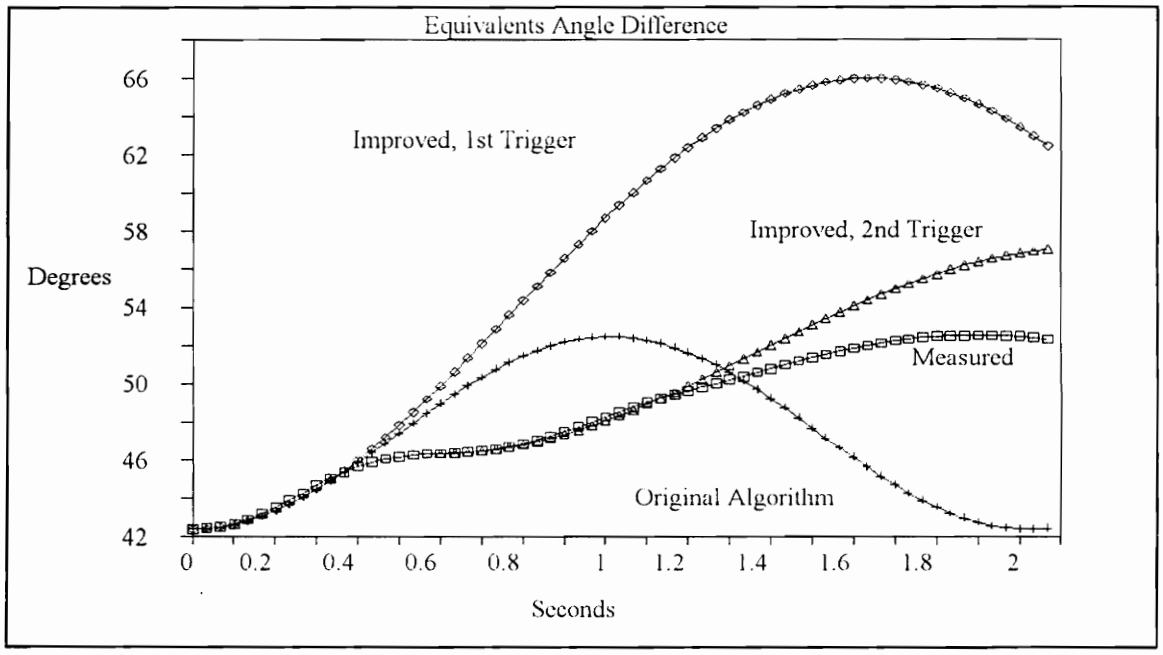

Figure 6.42. *Relay Predicted Angle Swing, October 3, 1994*

Table 6.13 Relay Outputs For Case 276:

Algorithm	Original	Improved 1st Trigger	Improved 2nd Trigger
Estimated Inertia Constant	NA	2670.92	2638.54
Pre-fault Operating Power	-30.3094	-30.3094	-32.7645
Predicted New Power	-31.4090	-38.6542	-37.2766
Pre-fault Operating Angle	-42.3672	-42.3672	-46.3267
Predicted New Angle	-47.3447	-53.6759	-51.6615
Accelerating Area	5.6623	14.6069	6.7970
Decelerating Area	221.4837	255.9008	248.7880
Output	Stable	Stable	Stable

Comments:

For this compound swing the prediction of the original algorithm for the first swing is very good. The improved algorithm estimates a value of the inertia constant that is too high for the observed swing. This may be due to the inertia constant assumed by the algorithm for the first estimate of the new operating point. The ragged peak of the angle velocity in Figure 6.43 must be considered for the detection of a second swing.

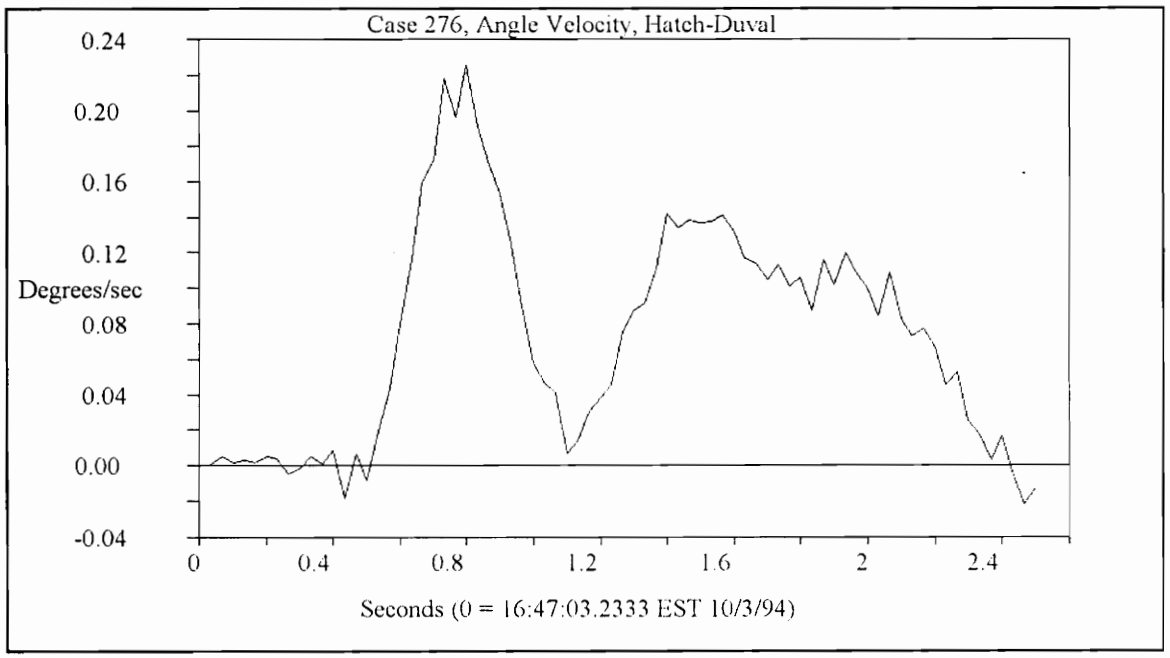

Figure 6.43. *Measured Angle Velocity, October 3, 1994*

Case 299:

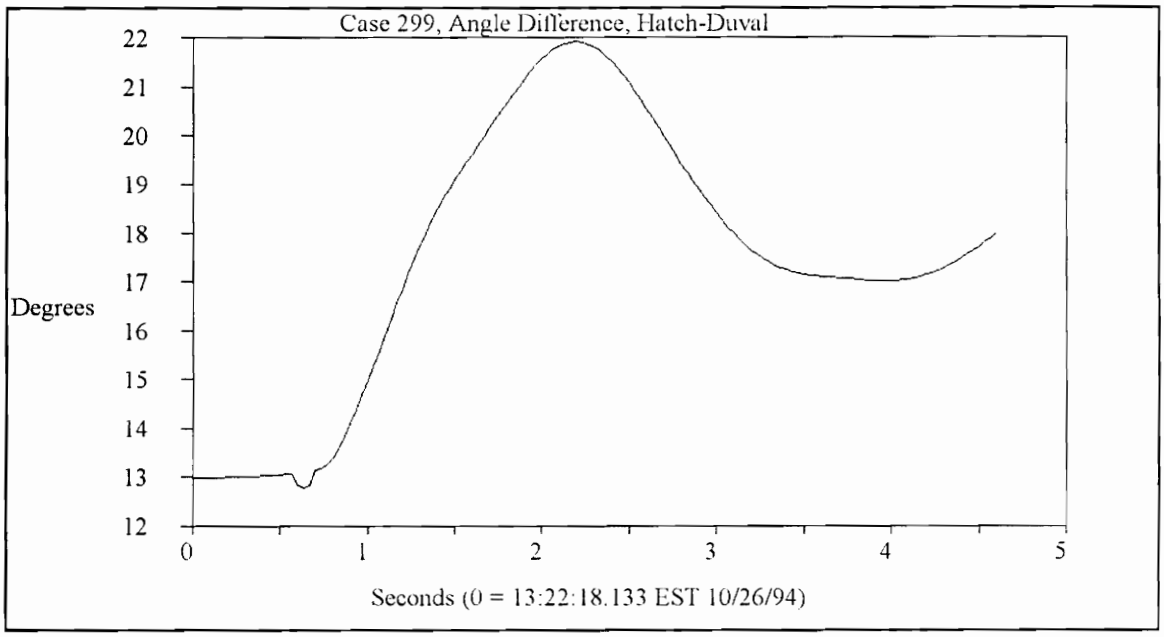

Figure 6.44. *Measured Angle Swing, November 26, 1994*

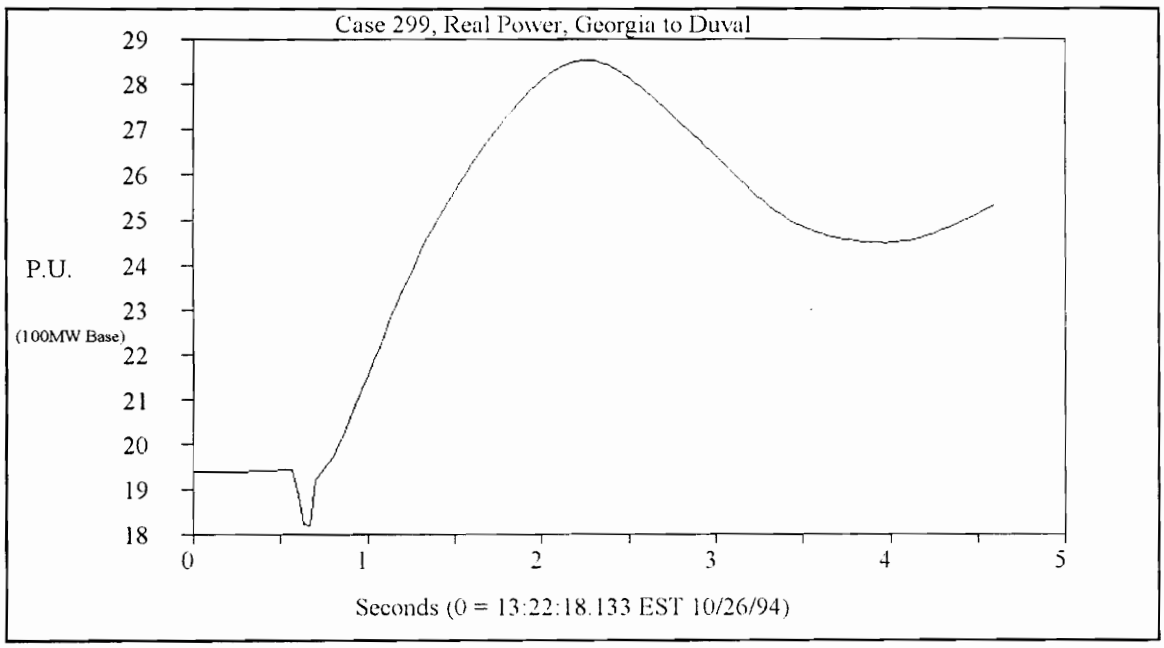

Figure 6.45. *Measured Power Swing, November 26, 1994*

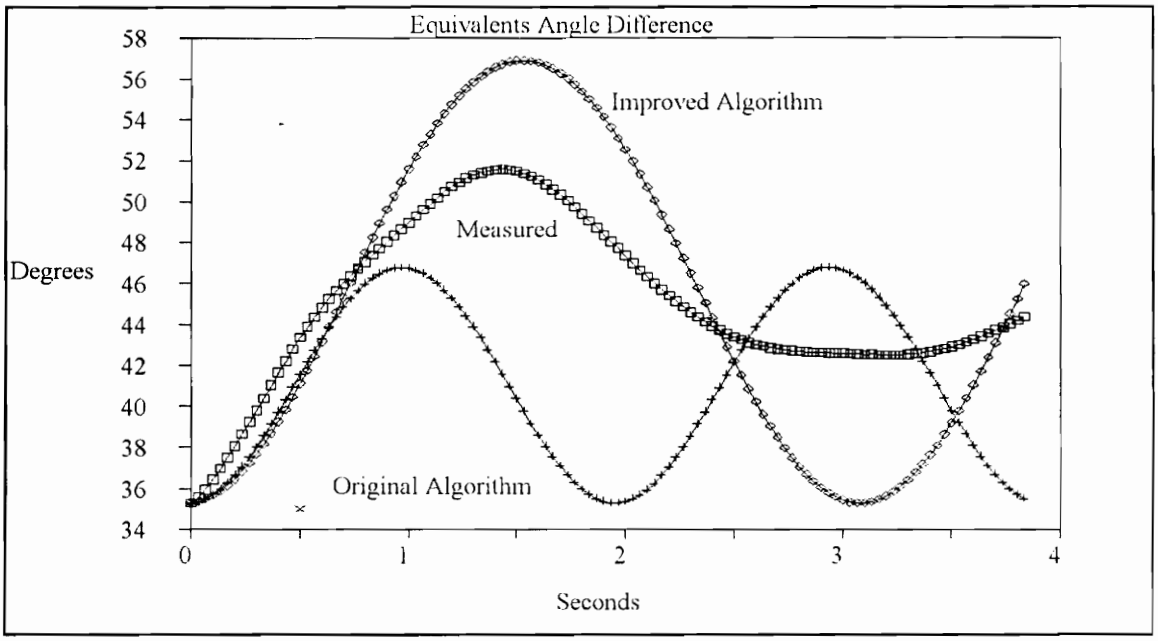

Figure 6.46. *Relay Predicted Angle Swing, November 26, 1994*

Table 6.14 Relay Outputs For Case 299:

	Original Algorithm	Improved Algorithm
Estimated Inertia Constant	NA	2755.41
Pre-fault Operating Power	-24.5788	-24.5788
Predicted New Power	-26.3424	-33.3144
Pre-fault Operating Angle	-35.1736	-35.1736
Predicted New Angle	-40.9802	-45.7836
Accelerating Area	5.5673	11.7056
Decelerating Area	196.3935	227.7840
Output	Stable	Stable

Comments:

The angle prediction is better with the improved algorithm but the swing is smaller than the prediction. Figure 6.47 shows changes in the velocity of the angle which suggest additional events contributing to changes in the angle swing. These changes are evident in the measured angle swing. This case is similar to case 157 and could also be considered a compound swing except for the lack of change in the angle velocity.

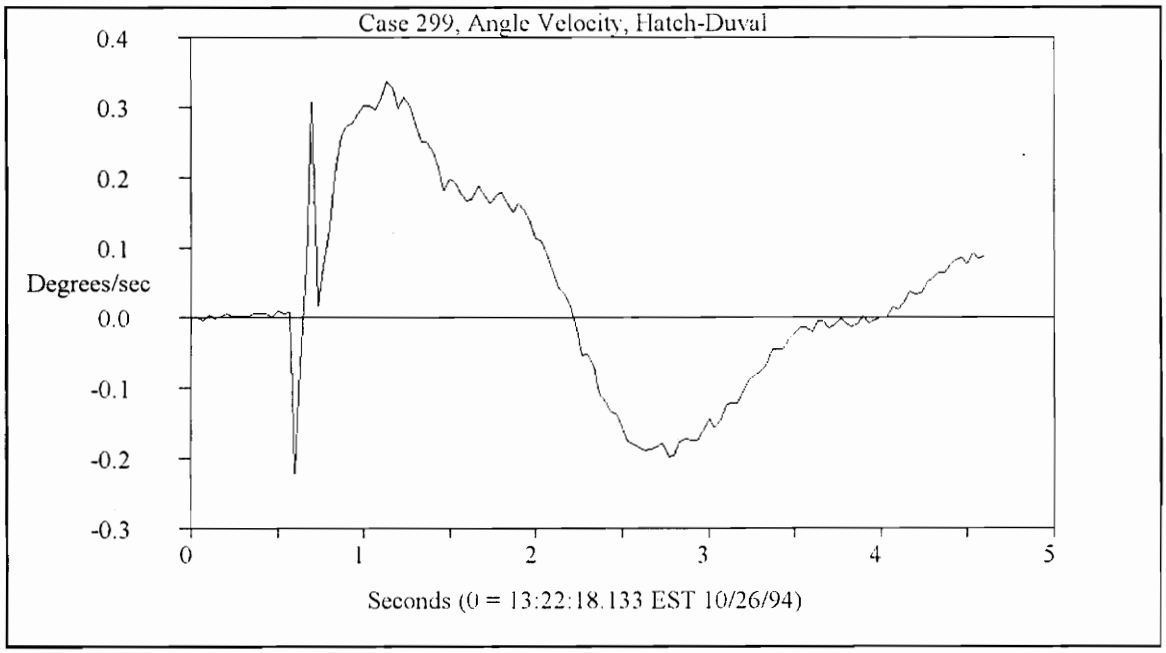

Figure 6.47. *Measured Angle Velocity, November 26, 1994*

Case 334:

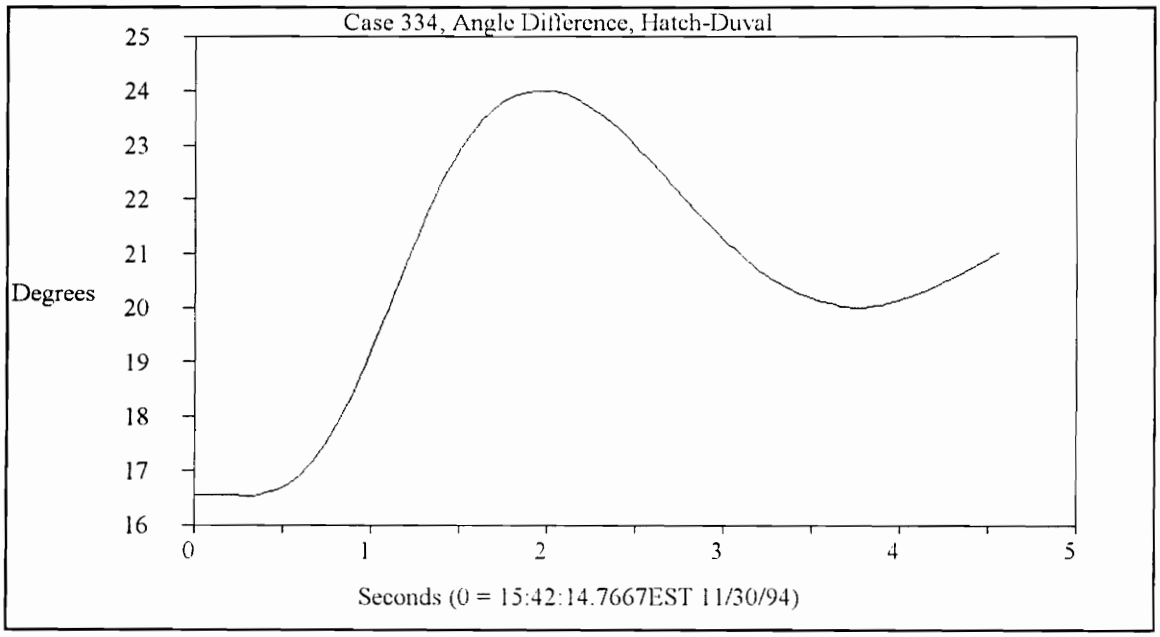

Figure 6.48. *Measured Angle Swing, November 30, 1994*

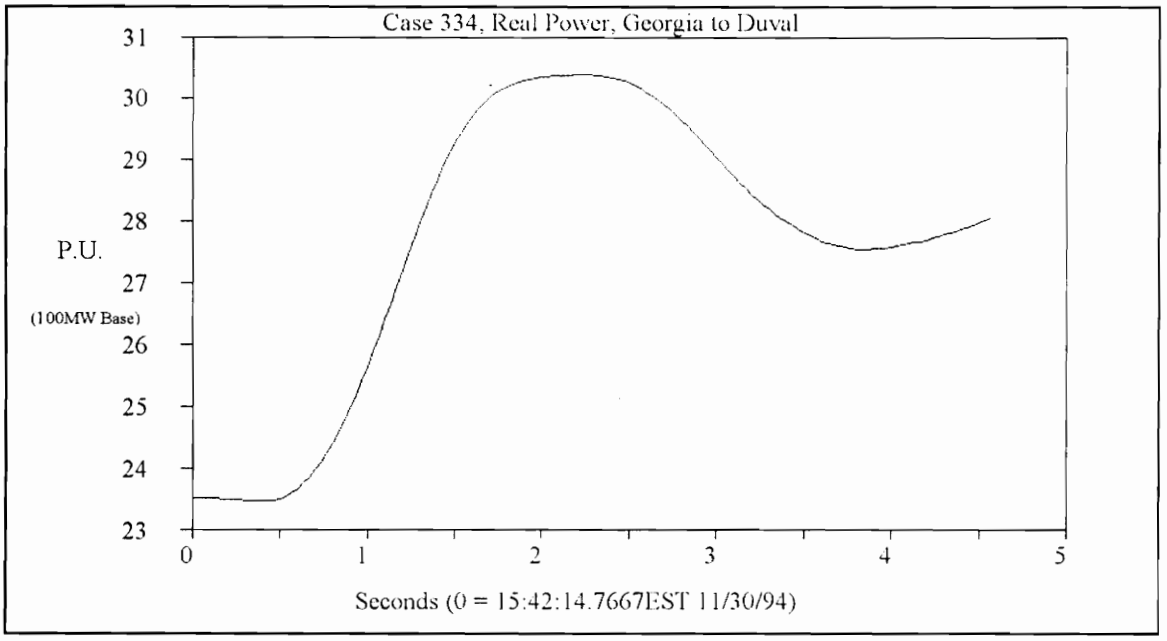

Figure 6.49. *Measured Power Swing, November 30, 1994*

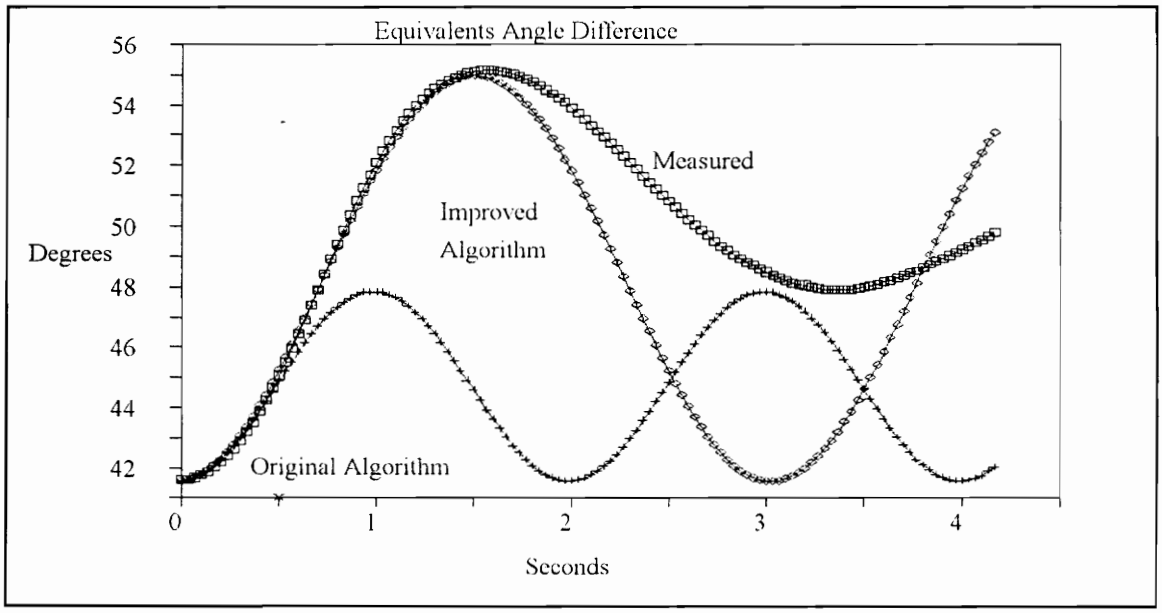

***Figure 6.50**. Relay Predicted Angle Swing, November 30, 1994*

Table 6.15 Relay Outputs For Case 334:

	Original Algorithm	Improved Algorithm
Estimated Inertia Constant	NA	2530.65
Pre-fault Operating Power	-29.2941	-29.2941
Predicted New Power	-29.1551	-34.6697
Pre-fault Operating Angle	-41.5650	-41.5650
Predicted New Angle	-44.6775	-48.1393
Accelerating Area	3.3135	7.7228
Decelerating Area	210.1551	235.5263
Output	Stable	Stable

Comments:

This shows a very good prediction for the improved algorithm. The angle velocity in Figure 6.51 shows an angle velocity with some noise at the beginning of the swing but not large enough to affect the angle.

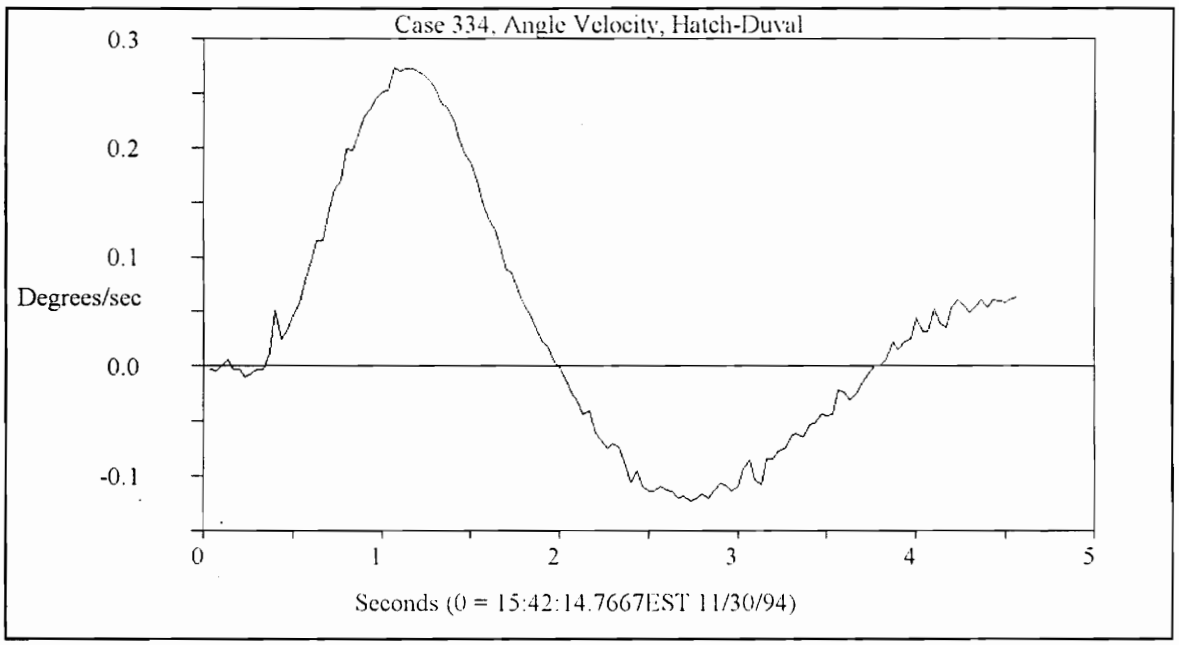

***Figure 6.51**. Measured Angle Velocity, November 30, 1994*

7

ALGORITHM CHANGES

7.1 Introduction

The original algorithm used by the out-of-step relay, described in section 3.2, showed poor results in the long term prediction of the angle swings for the loss of generation in Florida. Figure 7.1 shows a predicted angle swing where the predicted new operating point is too low and the frequency of oscillation is higher than the observed frequency. Figure 7.2 shows an angle swing where a second swing occurs half a second after the first one. The error in Figure 7.1 can be attributed to errors in the system model, described in section 2.3, and to the assumption of no damping, but these errors are not seen in Figure 7.2 where the same model seems to offer correct results for the first part of a compound swing. The second part of this swing was not expected by the relay and no action is taken to correct the prediction when the second swing occurs. An additional study is required to determine the cause of these two types of swings in the Florida system but the relay algorithms should be modified to adapt to and differentiate between these two types of swings.

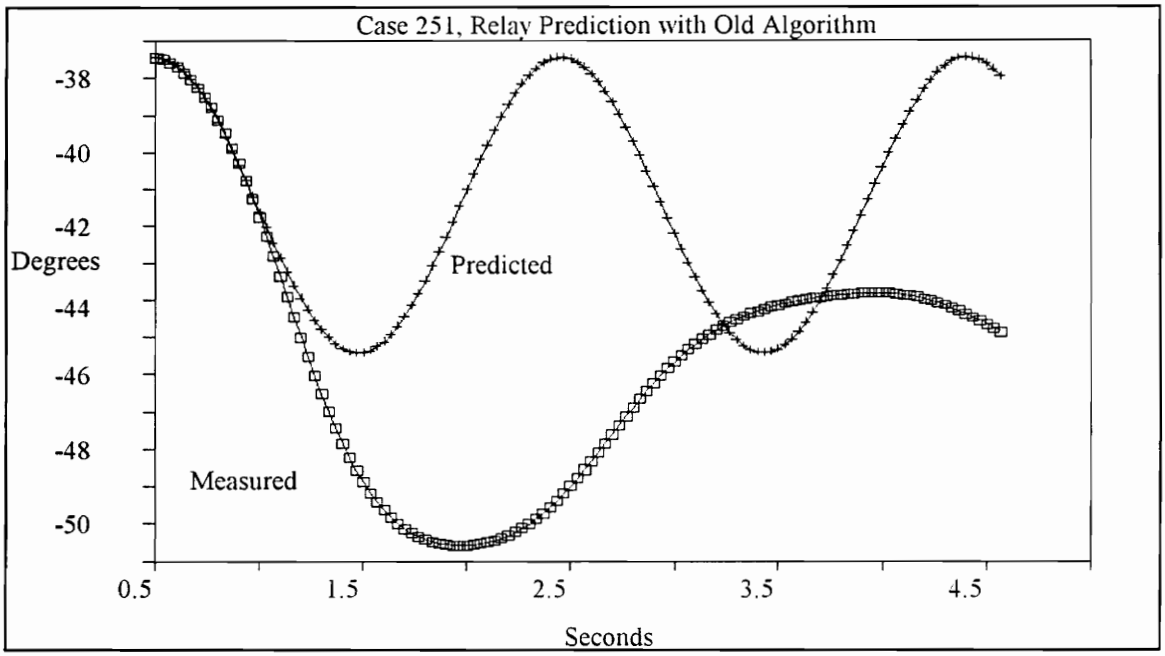

Figure 7.1. *Extended prediction for angle swing.*

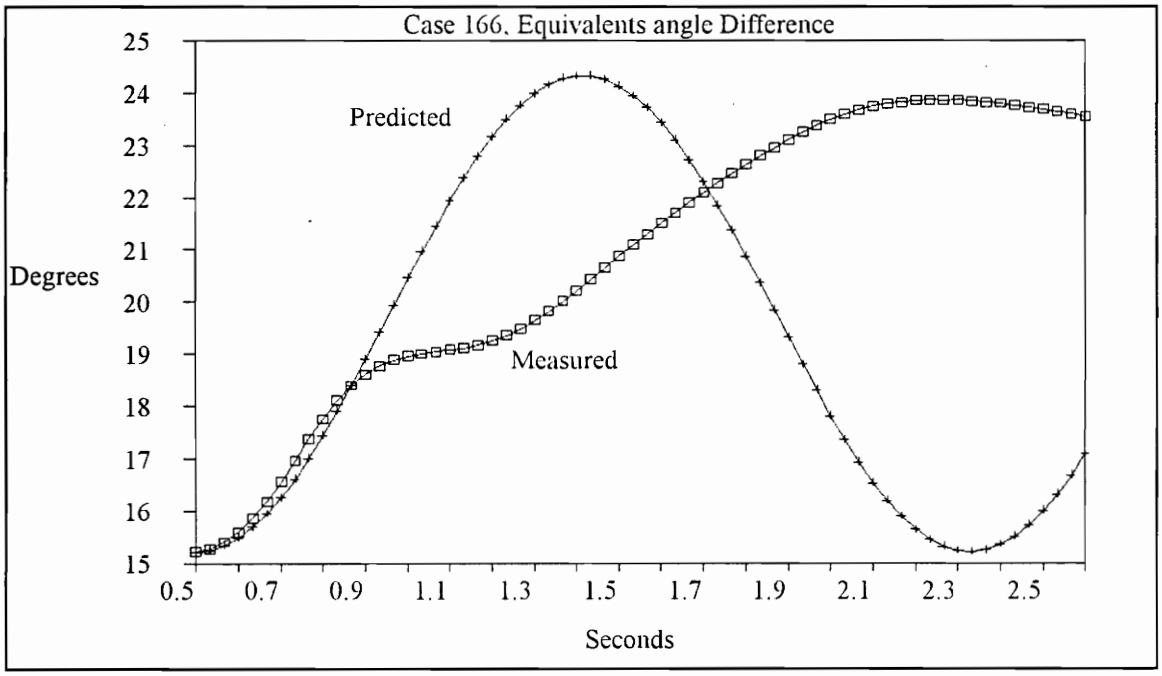

Figure 7.2. *Angle prediction for compound swing*

The following paragraphs describe how more parameters of the relay are made adaptable to obtain better angle predictions and how the triggering algorithm is changed to determine the occurrence of compound swings.

7.2 Model Changes

The error observed in figure 7.1 is due to incorrect values in the system model for that angle swing. The frequency of oscillation of the predicted angle swing is a function of the loads and the inertia constants of the model. Figures 7.3 and 7.4 show effect of the loads on the frequency of oscillation of the predicted angle swing. When the load values are increased the frequency of oscillation is reduced but very large changes in the loads would be required to correct for the error in the predicted oscillations.

The other parameter affecting the frequency of oscillation is the equivalent inertia constant which is a function of the inertia constant of the two equivalents, equation 7.1.

$$M_{eqv} = \frac{M_1 M_2}{M_1 + M_2} \tag{7.1}$$

From equation 7.1 it is clear that the effect of the smaller inertia constant is greater since the equivalent inertia has to be smaller than the lower inertia constant. This is also observed in Figures 7.5 and 7.6 where changes in the inertia constant of Florida, M_1, produce larger changes in the frequency of oscillation of the prediction.

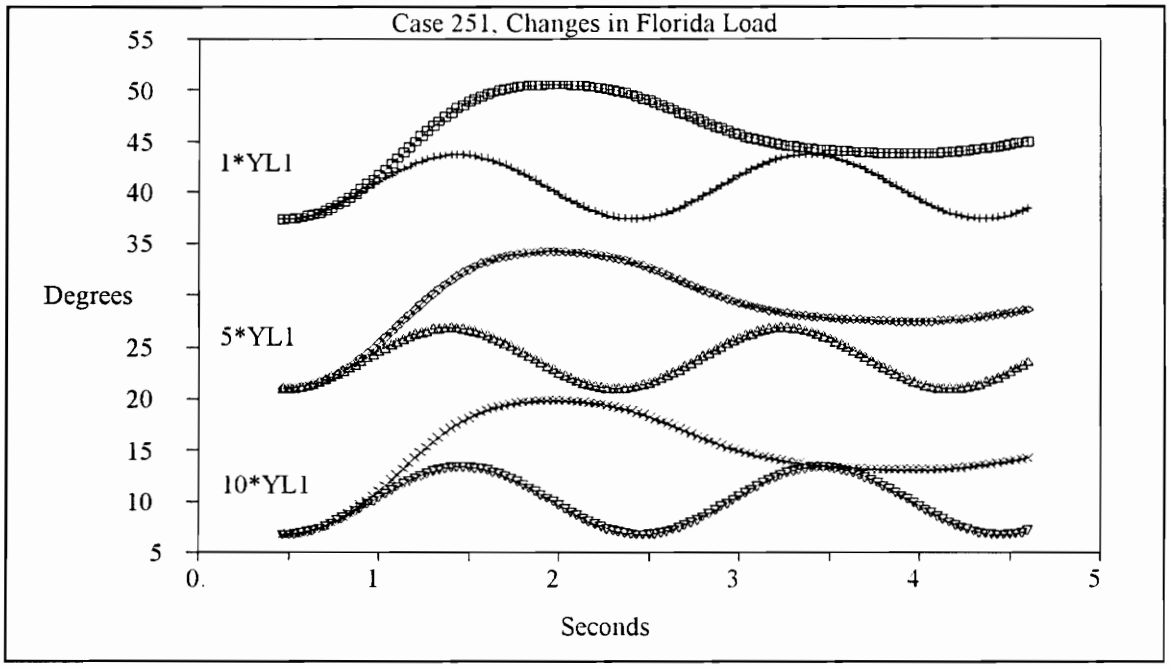

Figure 7.3. *Angle Prediction for changes in the Florida Load.*

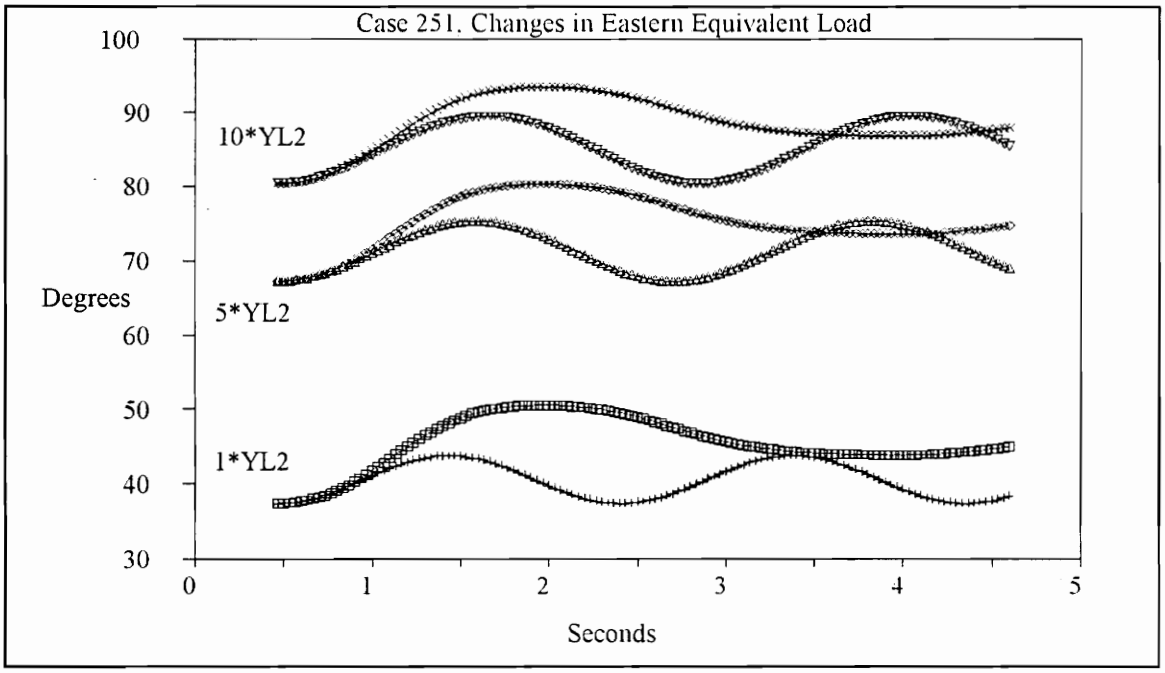

Figure 7.4. *Angle Predictions for Changes in Eastern Equivalent Load.*

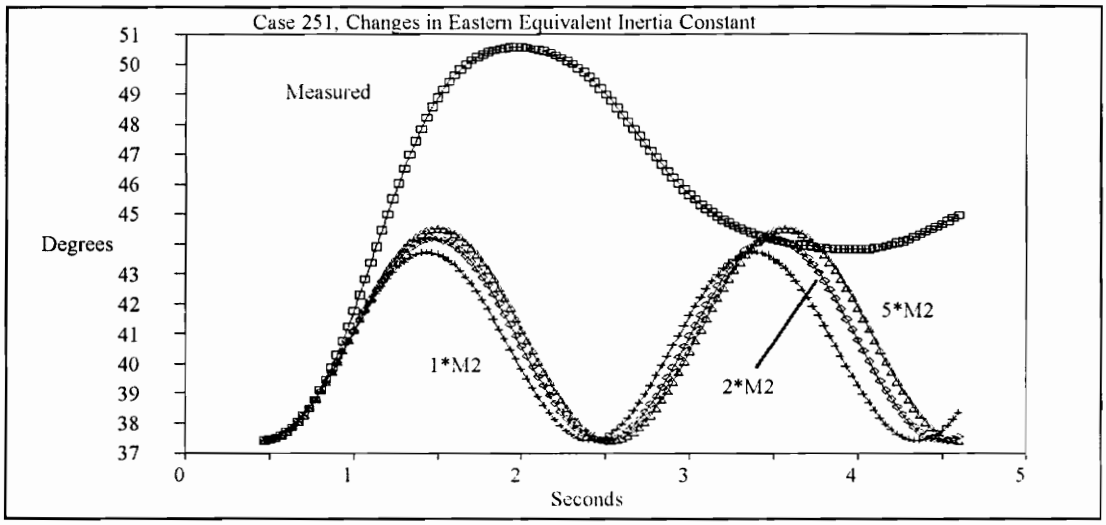

Figure 7.5. *Angle Predictions for Changes in Eastern Equivalent Inertia Constant.*

It was concluded from these tests that the effect of the loads on the frequency of oscillation is negligible compared to the effect of the inertia constants. Changes in the inertia constant of Florida alone could be used to correct the errors in the frequency of oscillation of the predicted angle swing.

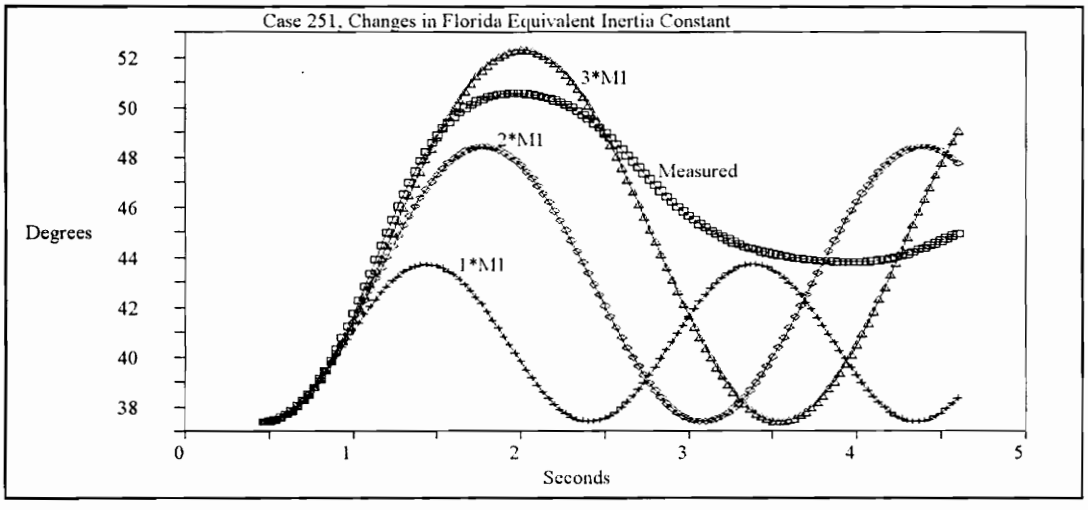

Figure 7.6. Angle Predictions for Changes in Florida Equivalent Inertia Constant.

7.2.1 Adaptive Inertia Constant for Florida Equivalent

For the new algorithm, the inertia constant of the Florida equivalent is considered variable and is estimated every time an angle swing is detected. To estimate the new inertia constant for the Florida equivalent the new operating point for the first swing must be known. Figure 7.7 shows the angle velocity for the example in Figure 7.1. The velocity of the angle difference reaches its maximum absolute value at time t_a when the acceleration becomes zero, which corresponds to the new operating point. Unfortunately this fact can not be used by the relay since it requires more than half a second to determine the new operating point. Therefore the new operating point has to be predicted from the measured data.

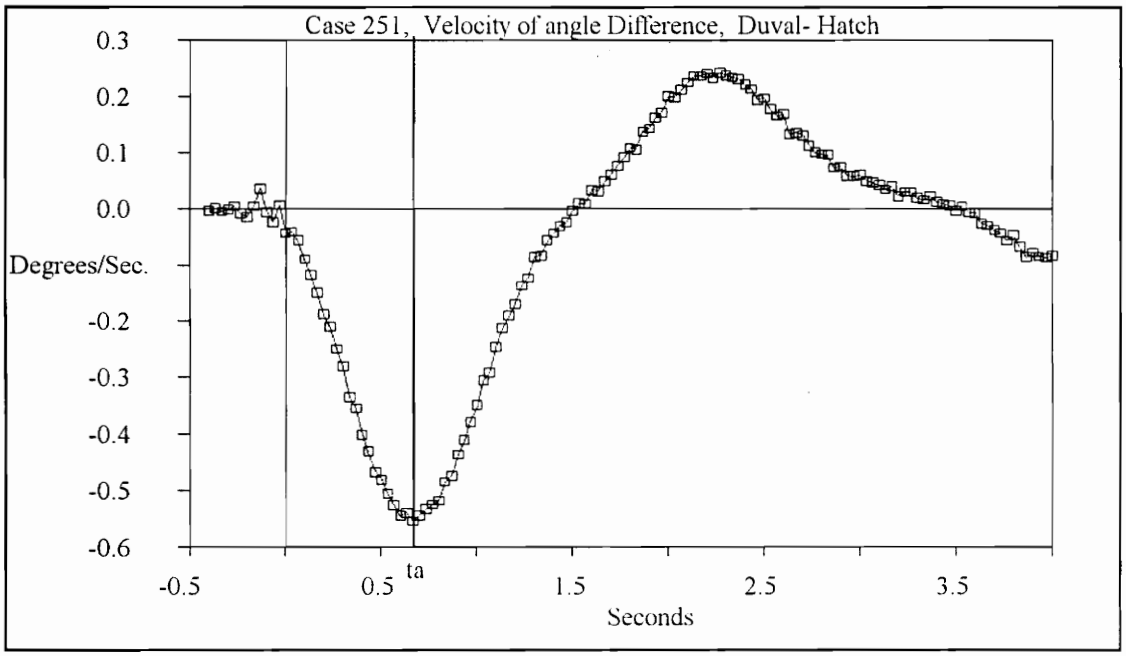

Figure 7.7. *Angle Velocity used to determine new operating point.*

The new algorithm predicts the new operating point as before assuming that the inertia constant value obtained in the post-disturbance analysis of the previous event is correct. Once the new operating point is determined the swing equation for a two machine system, equation 7.2, is used to estimate the value of M_1.

$$\frac{M_1 M_2}{M_1 + M_2}\frac{d^2\delta}{dt^2} = \frac{M_2 P_{a1} - M_1 P_{a2}}{M_1 + M_2} \tag{7.2}$$

Let M_1 be a percentage of M_2, $M_1 = rM_2$ then

$$\frac{rM_2}{r+1}\frac{d^2\delta}{dt^2} = \frac{P_{a1} - rP_{a2}}{r+1} \tag{7.3}$$

where $P_{a2} = P_m(\cos(\delta_{new} + \theta_{12}) - \cos(\delta - \theta_{12}))$

and $P_{a1} = P_m(\cos(\delta_{new} - \theta_{12}) - \cos(\delta - \theta_{12}))$

The value of δ_{new} is the angle for the estimated new operating point. By eliminating the common factor, 1+r, and applying the equal area relation to equation 7.3, the following equation is obtained:

$$\frac{rM_2}{2}\left(\frac{d\delta}{dt}\right)^2 = \int_{\delta_0}^{\delta}(P_{a1} - rP_{a2})d\delta \tag{7.4}$$

For discrete sampling in a slow moving angle it can be assumed that : $\frac{d\delta}{dt} \approx \frac{\Delta\delta}{\Delta t}$

Integrating 7.4 and using the approximation for angle velocity:

$$\frac{rM_2(\Delta\delta)^2}{2(\Delta t)^2} = k_1(\delta - \delta_0) + P_m \sin(\delta - \theta_{12}) - P_m \sin(\delta + \theta_{12}) - k_2 \qquad (7.5)$$

where $k_1 = [P_m \cos(\delta_{new} - \theta_{12})] - r[P_m \cos(\delta_{new} + \theta_{12})]$

and $k_2 = r[P_m \sin(\delta_0 + \theta_{12})] - P_m \sin(\delta_0 - \theta_{12})$

Grouping all 'r' terms, equation 7.6 is obtained:

$$r\left[\frac{M_2(\Delta\delta)^2}{2(\Delta t)^2} + a_1(\delta - \delta_0) + P_m(\sin(\delta + \theta_{12}) - a_2)\right] = b_1(\delta - \delta_0) - P_m(\sin(\delta - \theta_{12}) - b_2) \qquad (7.6)$$

where $a_1 = P_m \cos(\delta_{new} + \theta_{12})$ $\quad a_2 = \sin(\delta_0 + \theta_{12})$

and $b_1 = P_m \cos(\delta_{new} - \theta_{12})$ $\quad b_2 = \sin(\delta_0 - \theta_{12})$

Least squares is applied to equation 7.6 to estimate the value of 'r' which gives M_1 as a percentage of M_2. A new operating point is predicted using the estimated M_1 and equation 7.5. The least squares is performed with only 8 points to eliminate errors due to the effect of compound swings. Figure 7.8 shows the angle prediction given by the relay when the above algorithm is used to determine the system model.

7.2.2 Post Disturbance Update of Inertia Constant for Florida Equivalent.

After the event has occurred, a post disturbance estimation is performed to compute a value of the inertia constant to be used for the next angle swing. The value of the new operating point used for the post disturbance estimate of inertia is obtained by

tracking the velocity of the angle. The angle at which the velocity reaches its peak absolute value corresponds to the point of zero acceleration as shown in Figure 7.6. During the first swing the acceleration is zero when the angle crosses the new operating point. For compound cases determination of the new operating point is not possible and the inertia constant is not updated for these cases. Figure 7.9 shows the angle prediction obtained during post-disturbance analysis when the new operating point is known.

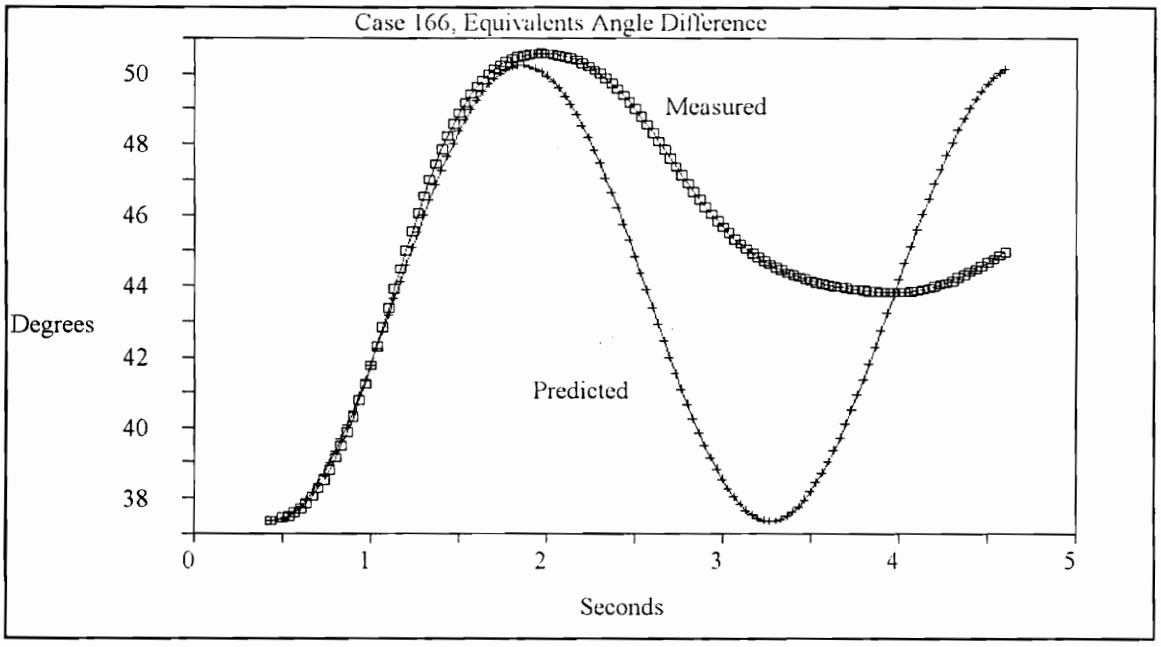

Figure 7.8. *Angle Prediction of New Relay Algorithm.*

The values obtained for the inertia constant of the Florida Equivalent from the collected cases for single swing average around 2500 seconds. The original value of this inertia constant was 948 seconds which is close to the value obtained for the first swing of the compound swing cases.

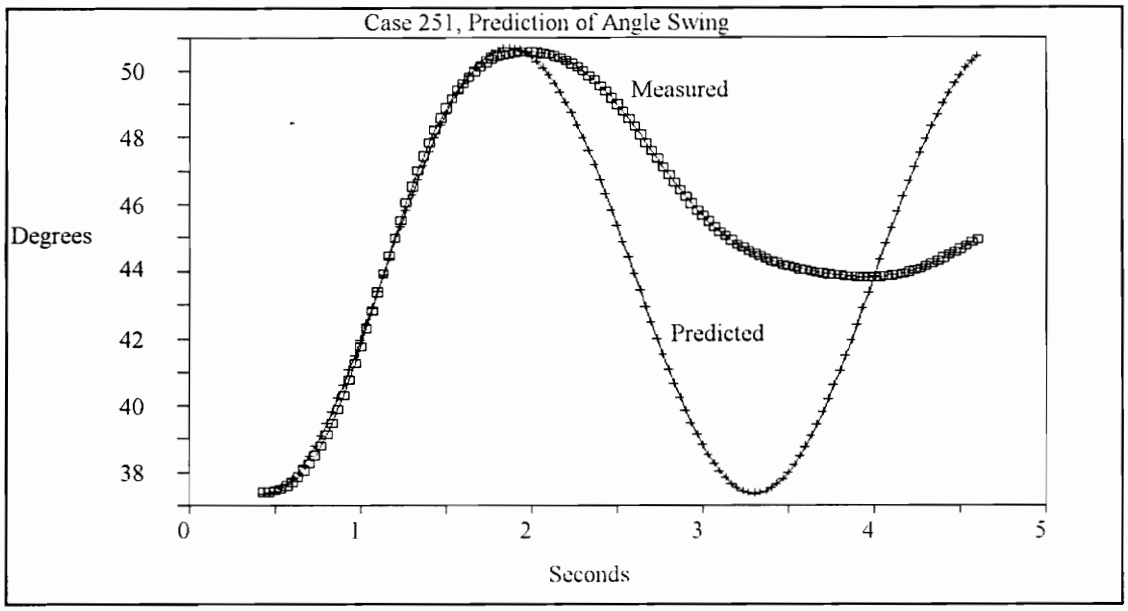

Figure 7.9. *Angle Prediction of post-disturbance Analysis.*

7.3 Compound Angle Swings

During compound angle swings, changes were observed about 0.5 seconds into the first swing causing a second swing on top of the first one, Figure 7.2. The cause of these swings is unknown but they could be due to modes of oscillation inside the Florida peninsula.

To account for this type of swing the triggering of the relay was modified to track the velocity of the angle difference and use it to determine when a second swing has occurred. Figure 7.10 shows the angle velocity of a compound swing. At time t_b the velocity of the swing changes indicating a new acceleration and therefore the start of a second swing. When this unexpected change is detected the relay does a second prediction on the angle swing, Figure 7.11.

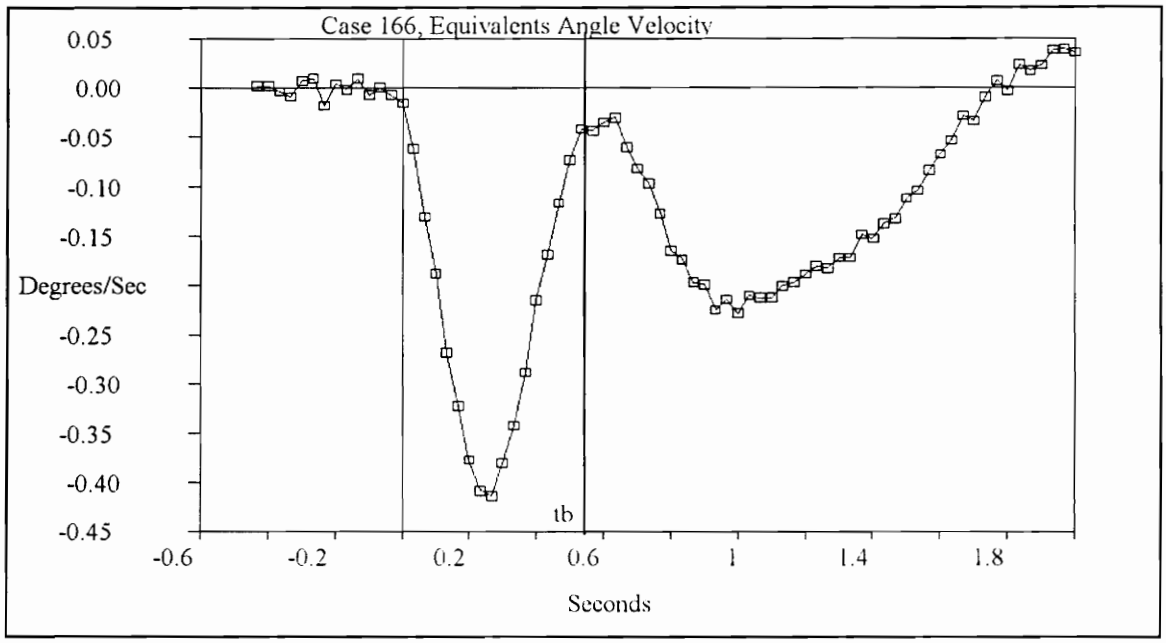

Figure 7.10. *Angle Velocity for Double Swing Case*

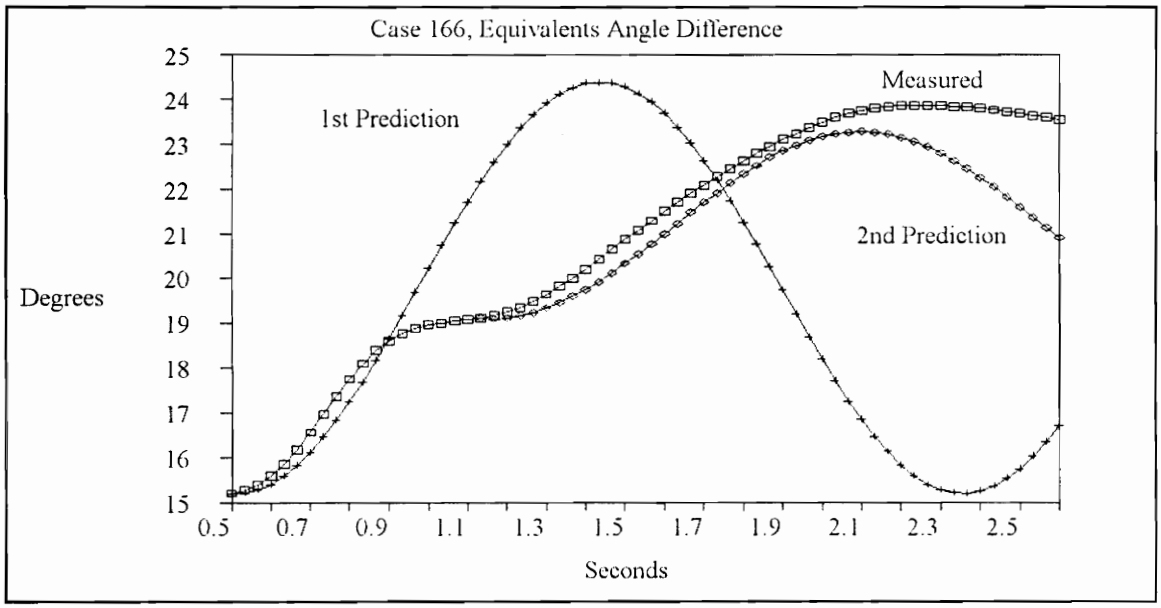

Figure 7.11. *Angle Predictions for Compound Swing.*

8

CONCLUSIONS AND FUTURE WORK

8.1 Introduction

The purpose of this project was to develop the necessary algorithms, implement the hardware and software for a relay prototype, use simulations to perform laboratory tests, and conduct a one-year-long field trial on an adaptive out-of-step relay system using synchronized phasor measurements. The concept of equal area criterion has been known for a long time but in this application it was used for the first time to determine system stability levels in real time. Most of the adaptive concepts used on the relay were implemented for the first time. A model with an adaptive inertia constant was specifically developed for this relay based on the information obtained from the field tests. Synchronized phasor measurement technology was applied successfully for the first time for protection applications, demonstrating the use of angle measurement for the detection of power swings and stability protection. The relay units were designed and implemented for this system with the capability of expansion to a three or four machine model of the system.

The fifteen month field testing revealed weaknesses in the equipment, original model, and some of the algorithms but it also provided the data required to improve the algorithms and solve the problems encountered with the relay system. This chapter lists

the major results, conclusions, and new ideas that resulted from the field testing of the out-of-step relay system.

8.2 Conclusions

a. The equal area criterion has traditionally been applied to determine the critical clearing time of generators as they swing against the rest of the system under the worst possible conditions. Although this provides good protection for generators it is a very limited use of the equal are criterion. For this project the equal area criterion is used to determine if the swings between Florida and the rest of the country are stable. The concepts as applied in this project not only differentiates between stable and unstable swings but provides a measurement of the degree of stability of the detected swings. The equal area criterion algorithms implemented for this project can also be used for the stability protection of an individual generator as it swings against the rest of the system, without the limitations of the worst case scenario established by the traditional critical clearing time techniques.

b. The ability of computer relays to receive information and modify their parameters and logic based on external information, has made them more adaptable to prevailing system conditions. In this project adaptive features were used successfully to update system load, based on pre-stored load curves, and to change the impedance matrix of the system model when changes were detected in critical transmission lines. These

adaptive techniques were not only proven to be possible and useful but necessary for the correct operation of the out-of-step relay system. The system model can be improved if actual load data from the control center is used instead of load curves to model the load in the relay system.

c. The original model used for the Florida system consisted of an equivalent inertia constant, system load, and transient reactance. This model was obtained using the machine data for the major generator units in Florida. As it was proven during the field testing the angle prediction of the relay are only as good as the model from which they are obtained. The seasonal variation in the equivalent inertia constant of the original model made the first angle predictions of the relay inaccurate for most of the detected angle swings. The data tables collected by the relay units and PMUs were used to determine an adaptive model for the inertia constant of the Florida system. The new inertia constant value for Florida is updated using a least square fit of the power flow and angle difference measurements for the first twelve cycles of the swing. The improved inertia constant value not only increases the adaptability of the model but proves the learning ability of the relay which results from the stored data tables. A more accurate model could be obtained if additional system information could be made available to the relay from the control center to make the base value of inertia constant more adaptable to seasonal variation and system changes.

d. Phasor measurement units have been available for several years and have been used successfully to collect swing data in large system. This was the first application of PMUs as transducer for relaying operation. During the fifteen months of field testing PMUs proved to be accurate and reliable transducers for relaying applications providing not only the required phase angle measurements but also status information on the state of key transmission lines used to update the impedance matrix used by the system model. No problems or failures were observed in the PMU's hardware or software during the operation of the out-of-step relay system. The additional data collected by the PMUs proved to be very useful for the update and improvement of the model used by the out-of-step relay system.

e. The detection of loss of generation in Florida depended on the ability to detect the angle swings between Duval and Hatch. All swings not generated by a fault on one of the critical lines were detected by tracking the changes in measured angle difference between the two PMU sites. It was demonstrated during the field tests that with the accuracy of measurement of the PMUs swings as small as 0.1 degree could be detected proving the usefulness of phasor angles for detection and analysis of system swings. The signature of angle swings agrees with that of the real power swings at Duval but angle difference only requires the angle between the two points while power flow requires the calculation of power on all connecting links, for this case only on links connecting Florida to Georgia but for complex systems the

calculation of real power swing may become computationally inefficient compared to angle swings.

f. The assumption of no damping was used for the applications of equal area and angle swing prediction. This assumption is valid for the equal area criterion as it applies to a two machine system where first swing stability is the only response required from the relay. A three or four machine model may require the introduction of damping in the derivations to determine second swing stability. For the angle prediction used by the relay for the validation of the two machine system model, damping is required to improve the prediction of the angle swing and allow a proper comparison between the predicted and measured angle difference. The prediction of the relay can be classified as adequate since for the first swing the damping effect is minimum but the effect increases with time and for the compound swing cases it is necessary to make the angle predictions as close as possible to the measured signal.

g. During the operation of the relay several compound swings were detected where a second swing occurred about 0.5 seconds after the first one. The relay operation for this swing was not correct due to the unpredictable nature of the second swing, and the speed of response required from the relay. More has to be learned about the nature and causes of this type of swing before its stability can be accurately determined by the out-of-step relay system. Two possible explanations are swing

modes inside the Florida system or a reaction of different system components to the system swing. A more exhaustive analysis has to be performed in this case studying the response to the swing of the different components of the system. This will require the installation of additional units in other areas of Florida. Several PMUs are presently installed in Southern and Eastern Florida but frequency triggers need to be set very low to detect some of these swings. This may saturate the PMU's memory with less significant events before a swing of interest occurs.

8.3 Future Work:

a. A faster data rate, once a cycle, would allow faster detection and more accurate prediction of angle swings. This increase in data rate will come at the expense of doubling the computational burden of the relay unit, but this can be easily overcome by a faster processor and more efficient programming. The new PMUs are capable of delivering data at this rate; the main delay will be in the communication channel between the relays which at 9600 baud will be pushed close to their limit. This possible source of problems could be eliminated with a faster baud rate through better modems. The communication board software in the relay units must be updated to handle communication between relay units independent of the main processor. At the present the decision of what data is sent to the remote relay is made by the main processor, but if this task is performed by the communications

board valuable time is saved for the relay algorithm and the re-transmission time to the remote unit is reduced.

b A three or four machine model will better represent the modes of oscillation in the Florida peninsula. The theory of operation for these models has been developed, tested with simulations, and proven to improve the ability of the out-of-step relay system. To implement such a system additional phasor measurement units are required in southern and western Florida to obtain the necessary angle measurements needed for the modeling of additional generators. The equal area criterion can not be applied to these models, but integration of the differential equations for three or four machines is possible with a faster processor.

c. System load for the out-of-step relay was modeled as a shunt admittance whose values were updated from pre-computed admittance values obtained from actual load curves of the Florida system. Improvements can be obtained if more sophisticated load models such as generation axis load flow are used. The normal seasonal changes and the influence of temperature on the load in Florida can be accounted for by creating temperature adaptable load curves.

d. Information from the control center could be used to update load models and improve the impedance matrix and inertia constant values used by the out-of-step relay specially for a three or four machine model. System information could be used

to update model information based on actual generation schedule and measured load values. The impedance matrix used by the model can be expanded and updated based on actual changes in the system's 500kV and 230kV lines. Due to the linear nature of the 500kV system opening of the lines inside Florida severely affect the model of the system. Having this information available to the relay will greatly increase the adaptability of the model for the Florida system.

e. The use of information from additional PMUs and from the control center will require that this information be available to all relay units and that the control signal could be sent to different locations. With an increase in the data rate the interchange of information and control signal for possible load shedding will be possible only if fiber optics are used to interconnect all the units in the system. Fiber optics are installed in some areas of the Florida system and plans are to install fiber optic through most of the system.

f. Integration of the phasor measurement unit, relay unit, and modems into a single unit will reduce the required hardware and cost of the system while increasing its dependability. Time will be saved on the data transfer from PMU to relay unit and between relay units. Tasks such as table storage and triggering are already performed by the PMUs, although additional code will be required to implement the equal area and angle prediction algorithms. The time necessary for the additional relay

computation can be obtained by eliminating some computations performed by the PMU which are not needed by the relay algorithms and by reducing the number of input channels to a maximum of twelve.

The data recorded during the field test period not only helped to prove and improve the adaptive relay algorithms and concepts used by the out-of-step relay system, but it also collected valuable field data which can be used for future improvement of the algorithms and to develop algorithms for other protective functions.

APPENDIX A

TWO MACHINE SWING CURVE

The equal area criterion applies to a one machine connected to an infinite bus. The application of this criterion to a two finite machine system requires that the swing equation for the two machine system be expressed as a single swing curve, similar to equation 4.21. From Chapter 4 the swing equation for a two machine system is:

$$P_{e,eqv} = P_c + P_{\max}\frac{M_2\cos(\delta-\theta_{12}) - M_1\cos(\delta+\theta_{12})}{M_1+M_2} \qquad \text{(A.1)}$$

where $P_c = \dfrac{M_2|E_1|^2 G_{11} - M_1|E_2|^2 G_{22}}{M_1+M_2}$ and $P_{\max} = |E_1||E_2||Y_{12}|$

To express equation A.1 as a single swing curve the two cosine terms must be combined into a single sine term as a function of the angle δ and θ_{12}. Figure A.1 shows the vectorial representation of the M_1 and M_2 terms in equation A.2. A vector with an angle of δ is shown as a reference.

$$M_2\cos(\delta-\theta_{12}) - M_1\cos(\delta+\theta_{12}) \qquad \text{(A.2)}$$

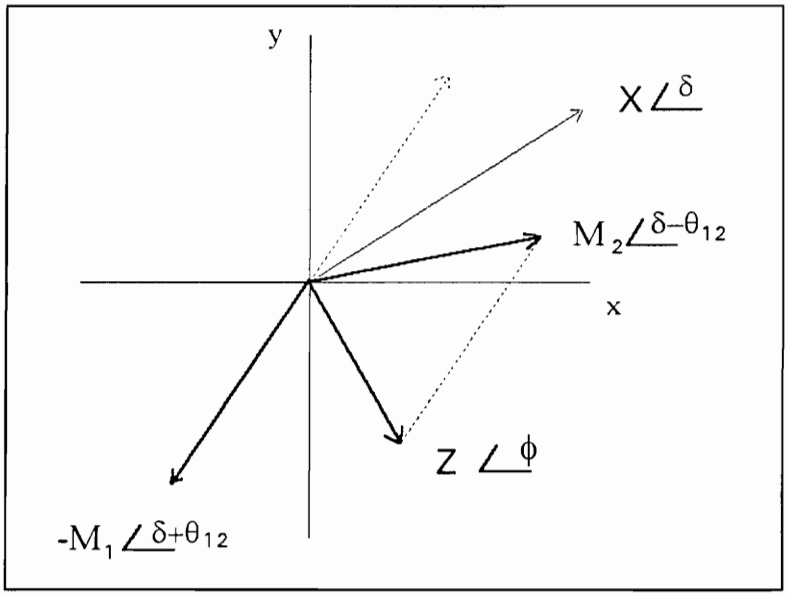

Figure A.1. *Vector Representation of Equation A.1*

To simplified the computations of magnitude and angle, it is better to change the reference axis from x-y in Figure A.1 to δ and δ+90 in Figure A.2.

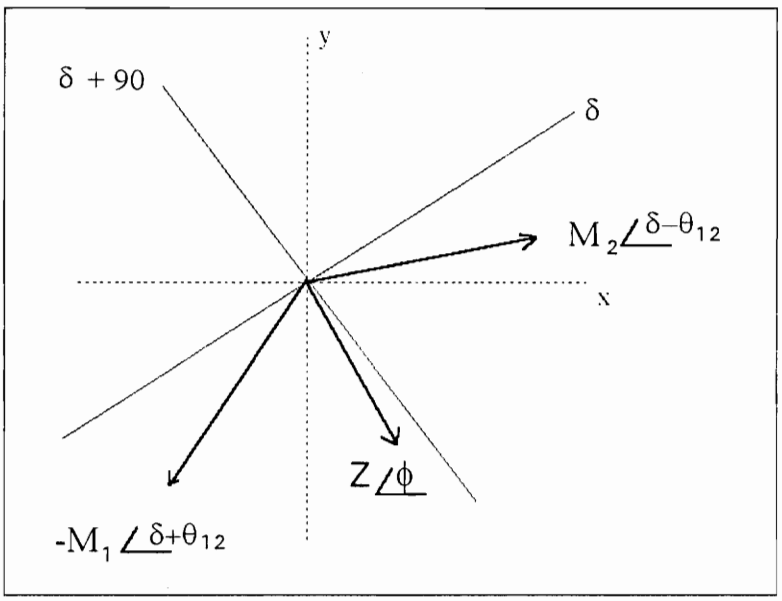

Figure A.2. *Vector Representation of Equation A.1 with δ Axis.*

With respect to the δ axis the horizontal component of the resulting vector, **Z**, is given by equation A.4.

$$(M_2 - M_1)\cos\theta_{12} \tag{A.3}$$

and the vertical component is given by equation A.5.

$$(M_2 - M_1)\sin\theta_{12} \tag{A.4}$$

The magnitude of the resulting vector is the square root of the sum of the square of the vertical and horizontal components, equation A.5.

$$|Z| = \sqrt{M_1^2 + M_2^2 - 2M_1M_2\cos(2\theta_{12})} \tag{A.5}$$

The angle of the resulting vector in the δ axis is the inverse tangent of the vertical component divided by the horizontal component, Equation A.6.

$$\phi_\delta = \arctan\left(\frac{M_2 - M_1}{M_2 + M_1}\tan\theta_{12}\right) \tag{A.6}$$

Equations A.5 and A.6 are used to represent A.2 in terms of a single sine term, equation A.7.

$$\sqrt{M_1^2 + M_2^2 - 2M_1M_2\cos(2\theta_{12})} * \sin(\delta - \gamma) \tag{A.7}$$

where $\gamma = \phi_\delta - 90°$

Substituting equation A.7 into equation A.1 gives the equivalent equation for the swing curve for a two machine system, equation A.8.

$$P_{e,eqv} = P_c + \frac{P_{\max}\sqrt{M_1^2 + M_2^2 - 2M_1M_2\cos(2\theta_{12})}}{M_1 + M_2}\sin(\delta - \gamma) \tag{A.8}$$

APPENDIX B

BIBLIOGRPAHY

B.1 General Knowledge

[1] O. Elgerd, "Electric Energy Systems Theory", 2nd Edition, New York, McGraw-Hill, 1982.

[2] L.W. Johnson, R.D. Riess, "Numerical Analysis", Reading MA,Second Edition, Addison-Wesley Publishing Company, 1982.

[3] W.D. Stevenson, "Elements of powers System Analysis", Fourth Edition, New York NY, McGraw-Hill Book Company, 1982.

[4] V. Del Toro, "Electric Power Systems", Englewood Cliffs NJ, Prentice Hall,1992.

B.2 Phasor Measurement

[5] A.G. Phadke, M. Ibrahim, T. Hlibka, "Fundamental Basis for Distance Relaying with Symmetrical Components", IEEE Transactions on Power Apparatus & Systems, Vol. PAS-96, No. 2, March/April 1977, pp. 635-646.

[6] B.G. Glazer, " GPS Receiver Operation", Global Positioning System Volume I, The Institute of Navigation Washington DC, 1980, pp. 81-86

[7] R.J. Milliken, C.J. Zoller, "Principle of Operation of NAVSTAR and System Characteristics", Global Positioning System Volume I, The Institute of Navigation Washington DC, 1980, pp. 1-14.

[8] J.J. Spilker, "GPS Signal Structure and Performance Characteristics", Global Positioning System Volume I, The Institute of Navigation Washington DC, 1980, pp. 29-54.

[9] P. Bonanomi, "Phase Angle Measurement With Synchronized Clocks - Principle and Applications", IEEE Transactions, Vol. PAS-100, No. 12, Dec. 1981,pp. 5036-5043.

[10] A.G. Phadke, J.S. Thorp, M.G. Adamiak, "A New Measurement Technique for Tracking Voltage Phasors, Local System Frequency, and Rate of Change of Frequency", IEEE Transactions on Power Apparatus and Systems, Vol. PAS-102, No. 5, May 1983, pp. 1025-1038.

[11] A. Phadke, M. Begovic, V. Centeno, A. Chaudhary, V. Phaniraj, "Coherent Sampling for System-Wide Digital Relaying", NSF/Virginia Tech Conference on Computer Relaying, Blacksburg, VA., October 1987, Paper III-5.

[12] R.P. Shultz, "Applications and Experience in Power System Monitoring with Phasor Measurements" Proceedings from The NSF/Virginia Tech Conference on Precise Measurements in Power Systems, Blacksburg, VA, October 1987, Paper IV-5.

[13] B. Fardanesh, "Multi-Functional Monitoring System for the New York State Transmission Network Using Synchronized Measurements" Proceedings from The NSF/Virginia Tech Conference on Precise Measurements in Power Systems, Blacksburg, VA, October 1987, Paper IV-6.

[14] A. Phadke, M. Begovic, V. Centeno, V. Phaniraj, "Clock Synchronization for Improved Monitoring, Protection and Control", Proceedings of IASTED Conference, Phoenix, AZ, March 1988, pp. 9-13.

[15] D.W. Allan, M. Granveaud, W.J. Klepczynski, W. Lewandowski, " GPS Time Transfer with Implementation of Selective Availability", Proceedings from the NASA 22nd Annual Precise Time and Time Interval Applications and Planning Meeting, Vienna, VA, 1990, pp. 145-156.

[16] P. Daly, "Current GPS/GLONASS Time References and UTC", Proceedings from the NASA 22nd Annual Precise Time and Time Interval Applications and Planning Meeting, Vienna Virginia, 1990, pp. 87-94.

[17] L. Mili, T. Baldwin, T. Adapa, "Phasor Measurement Placement for Voltage Stability Analysis of Power Systems", Proceedings of the 1990 IEEE Conference on Decision and Control, 90CH2917-3.

[18] W.G. Hartmann, "Automatic Synchronizing for Generation and Tie Lines", Proceedings of the Georgia Tech Protective Relaying Conference, Atlanta, GA, May 1991.

[19] R.E. Wilson, "Uses of Precise Time and Frequency in Power Systems", Proceedings of the IEEE, Vol. 79, No 7, July 1991, pp. 1009-1018.

[20] R.B. Langley, "The Mathematics of GPS", GPS World, Vol. 2, No. 7, July/August 1991, pp. 45-50.

[21] A.G. Phadke, L. Mili, and T. Baldwin, 'Real Time Phasor Measurement for Improved Monitoring and Control", EPRI Report, August 2, 1991.

[22] R.B Langley, 'The GPS Observable" GPS World, Vol. 4, No. 4, April 1993. pp 52-59.

[23] A.G. Phadke, 'Synchronized Phasor Measurements in Power Systems", IEEE Computer Applications in Power Systems, Vol. 6, No. 2, April 1993, pp. 10-15.

[24] J.F. Hauer, "An Application Perspective on Advanced Measurement Technology in Wide Area Monitoring and Control", Proceedings of the NSF/Virginia Tech Conference on Precise Measurements in Power Systems, Arlington, VA, October, 1993.

[25] P.W. Sauer, M.A. Pai, J. Zhao, 'Phasor Representations of Power Systems Transients", Proceedings of the NSF/Virginia Tech Conference on Precise Measurements in Power Systems, Arlington, VA, October 1993.

[26] Working Group H-7, 'Synchronized Sampling and Phasor Measurement for Relaying and Control", IEEE Transaction on Power Delivery, Vol. 9, No. 1, 1994, pp. 442-452.

[27] R. Burnett, M.M. Butts, P. Sterlina, 'Power System Applications for Phasor Measurement Units", IEEE Computer Applications in Power, Vol. 7, No. 1, January 1994, pp. 8-13.

[28] R.J. Murphy, R.O. Burnett, 'Phasor Measurement Hardware and Application", Proceedings of the Georgia Tech Protective Relay Conference, Atlanta, GA , May 1994.

[29] T.W. Cease, B. Feldhaus, 'Real-Time Monitoring of the TVA Power System", IEEE Computer Applications in Power, Vol. 7, No. 3, July 1994, pp. 47-51.

[30] R. Burnett, M.M. Butts, T.W. Cease, V. Centeno, G. Michel, R.J. Murphy, A.G. Phadke, 'Synchronized Phasor Measurements of A Power System Event", IEEE Transactions on Power Systems, Vol. 9, No. 3, August, 1994, pp. 1643-1649.

B.3 General Relaying

[31] C.R. Mason, "Art and Science of Protective Relaying", John Wiley and Sons, New York, 1956.

[32] G.D. Rockefeller, 'Fault Protection with a Digital Computer", Trans. IEEE, Power Apparatus and Systems, Vol. PAS-88, No. 4, April 1969, pp 438-461.

[33] J.S. Thorp, A.G. Phadke, S.H. Horowitz, J.E. Beehler, 'Limits to Impedance Relaying", IEEE Transactions on Power Apparatus and Systems, Vol. PAS-98, No. 1, Jan/Feb. 1979, pp. 246-260.

[34] T. Sakaguchi, "A Statistical Decision Theoretic Approach to Digital Relaying", IEEE Transactions on Power Apparatus and Systems, Vol. PAS-99, No. 5, Sept./Oct. 1980, pp. 1918-1926.

[35] 'Protective Relaying for Power Systems", Edited by S.H. Horowitz, IEEE Press, 1980.

[36] "Applied Protective Relaying", Westinghouse Electric Corporation, Coral Springs, FL, 1982.

[37] C.R. Heising, R.C. Patterson, "Reliability Expectations for Protective Relays", Proceedings of the Georgia Tech Protective Relaying Conference, Atlanta, GA, 1988.

[38] A.G. Phadke, J.S. Thorp, "Computer Relaying for Power Systems", John Wiley and Sons, New York, 1988.

[39] C.R. Heising, R.C. Patterson, "Digital Relay Software Quality", Proceedings of the Georgia Tech Protective Relaying Conference, Atlanta, GA, May 1989.

[40] G. Benmouyal, "Some Aspects of the Digital Implementation of Protection Time Functions", IEEE Transactions on Power Delivery, Vol. 5, No. 4, November 1990, pp. 1705- 1713.

[41] "Protective Relaying for Power Systems II", Edited by S.H. Horowitz, IEEE Press, 1992.

[42] S.H. Horowitz, A.G. Phadke, "Power System Relaying", John Wiley and Sons, New York, 1992.

[43] "Protective Relaying Theory and Applications", Edited by Walter A. Elmore, Marcel Dekker, Inc.; New York, 1994.

B.4 Adaptive Relaying

[44] T.E. Dy Liacco, "The Adaptive Reliability Control System", IEEE Transactions on Power Apparatus and Systems, Vol. PAS-86, No. 5, May 1967, pp. 517-531.

[45] A.G. Phadke, J.S. Thorp, S.H. Horowitz, "Study of Adaptive Transmission System Protection and Control", Oak Ridge National Laboratory, ORNL/SUB/85-2205C, US Department of Energy, 1985.

[46] G.D. Rockefelleer, C.L. Wagner, J.R. Linders, K.L. Hicks, D.T. Rizy, "Adaptive Power System Transmission Protection", Oak Ridge National Laboratory, RNL/SUB/85-2201C, US Department of Energy, 1985.

[47] J.S. Thorp, A.G. Phadke, S.H. Horowitz, M.M. Begovic, "Some Applications of Phasor Measurement to Adaptive Protection", Proceedings of the Fifteenth PICA Conference IEEE, Montreal, 1987, pp 467-474.

[48] A.G. Phadke, J.S. Thorp, S.H. Horowitz, "Impact of Adaptive Protection on Power System Control", Proceedings from Ninth Power Systems Computation Conference, Cascais, Portugal, Aug. 30 - Sept. 4, 1987, pp. 609-616.

[49] J.S. Thorp, W. Ma, "Adaptive Relaying Based on Stability Prediction", Blacksburg Conference on Computer Relaying, Blacksburg VA, October 1987, Paper III-6.

[50] A.A. Girgis, "A Note on Load Forecasting and Adaptive Protection", Blacksburg Conference on Computer Relaying, Blacksburg, VA, October 1987, Paper III-7.

[51] S.S Venkata, M.J. Damborg, A.K. Jumpala, "Concept of Adaptive Transmission Protection With Annotated Bibliography on Digital Relaying", Blacksburg Conference on Computer Relaying, Balcksburg, VA, 1987, October, Paper IV-5.

[52] S.H. Horowitz, A.G. Phadke, J.S. Thorp, "Adaptive Transmission System Relaying", IEEE Transactions on Power Delivery, Vol. 3, No 4, October 1988.

[53] G.D. Rockefeller, C.L. Wagner, J.R. Linders, K.L. Hicks, D.T. Rizy, "Adaptive Transmission Relaying Concepts for Improved Performance", IEEE Transactions on Power Delivery, Vol. 3, No. 4, October 1988, pp. 1446-1458.

[54] A.G. Phadke, S.H. Horowitz, " Adaptive Relaying", IEEE Computer Applications in Power, Vol. 3, No. 3, July 1990, pp. 47-51.

B.5 Out-of-Step Relaying

[55] R.D. Brown, K.R. McClymont, "A Power Swing Relay for Predicting Generation Instability." IEEE Transactions, Vol. PAS-84, No. 3, 1965, pp. 219-223.

[56] F.R. Schleif, L.W. Loyd, R.W. World, W.B. Gish, " A Swing Relay for the East-West Intertie.", IEEE Transactions, Vol. PAS-88, No. 6, 1969, pp. 821-825.

[57] W.R. Roemish, C.L. Clemans, L.W. Lloyd, F.R. Schleif, "An Acceleration Relay for Power Systems.", IEEE Transactions, Vol. PAS-90, No. 3, 1971, pp. 1150-1154.

[58] C.L. Clemans, W.R. Roemish, 'Power Rate Relay for System Applications", IEEE Transactions, Vol. PAS-92, No. 1, 1973, pp. 122-126.

[59] H.K. Lauw, 'Improvement in Critical Clearing Time Calculation by a New Equation of Motion in the On-Fault Condition", IEEE Transactions on Power Apparatus and Systems, Vol. PAS-94, No. 4, July/August 1975, pp. 1288-1293.

[60] IEEE Committee Report, "Out of Step Relaying for Generators" IEEE Transactions on Power Apparatus and Systems, Vol. 96, Sept./Oct. 1977. pp. 1556-1564.

[61] W.R. Roemish, E.T. Wall, "A New Synchronous Generator Out-Of-Step Relay Scheme Part I", IEEE Transaction on Power Apparatus and Systems, Vol. PAS-104, No. 3, pp. 563-582, March, 1985.

[62] W.R. Roemish, E.T. Wall, "A New Synchronous Generator Out-Of-Step Relay Scheme, Part II", IEEE Transaction on Power Apparatus and Systems, Vol. PAS-104, No. 3, March, 1985, pp. 572-583.

[63] E. Schweitzer, T. Newton, R. Baker, "Power Swing Relay Also Records Disturbances", Proceedings of the Georgia Tech Protective Relaying Conference, Atlanta GA, 1987.

[64] S. P. Turner, "Adaptive Out of Step Relay Algorithm", Master Thesis Virginia Polytechnic Institute and State University, Blacksburg, Virginia, 1990.

[65] S.L. Anderson, K. Kong, J. De La Ree, Y. Liu, A. G. Phadke, "Testing of An Adaptive Digital Out-of-Step Relay Using Real -Time EMTP Playback Techniques", Proceedings from the 1993 II Simposio Iberoamericano sobre Proteccion de Systemas Electricos de Potencia, Monterey Mexico, SIPSEP-93-26, 1993.

[66] D.W. Smaha, "Out-of-Step Relay Protection for Generators", IEEE Tutorial on The Protection of Synchronous Generators, 1995, 95-TP-102, pp. 45-51.

B.6 Florida-Georgia

[67] A.H. Darlington, "Response of Underfrequency Relays on The Peninsular Florida Electric System for Loss of Generation", Proceedings of the Georgia Tech Protective Relaying Conference, Atlanta GA, May 1978.

[68] W.E. Lester, "Florida Power Corporation Out-of-Step Relay Application", Proceedings from the Georgia Tech Protective Relaying Conference, Atlanta, GA, May 1980.

[69] P.B. Winston, R.O. Burnett, "Impact of Disturbances on Weak Intercompany Transmission Ties", Proceedings from the Georgia Tech Protective Relaying Conference, Atlanta, GA, May 1980.

[70] T.A. Pruitt, R.O. Burnett, P.B. Winston, "Response of Plant Hatch Nuclear Power Units to Grid Disturbances", Proceedings of the Georgia Tech Protective Relaying Conference, Atlanta GA, 1981.

[71] R.W. Ohnesorge, T.A. Pruitt, "Operational Aspects of the Southern-Florida Interface, Past, Present and Future", Proceedings of the Georgia Tech Protective Relaying Conference, Atlanta, GA, 1984.

[72] A.A. Fouad, V. Vittal, J.G. Raine, T. Oh, "Investigation of Loss of Generation Disturbance in the Florida Power and Light Company Network by the Transient Energy Function Method" IEEE Transactions on Power Systems, Vol. 1, No. 3, Aug.1986, pp. 60-66.

[73] North American Electric Reliability Council, 1987 System Disturbances, Princeton, 1988.

[74] North American Electric Reliability Council, 1989 System Disturbances, Princeton, 1990.

[75] S. Steven, A. Nirenberg, K.D. Sparks, D.A. McInns, 'Load-Shedding Program Safeguards Network", Electrical World, Vol. 206, No 3, March 1992.

B.7 Stability

[76] W.V. Lyon, H.E. Edgerton, 'Transient Torque-Angle Characteristics of Synchronous Machines", Transactions of AIEE, Vol. 49, April 1930, pp. 686-699.

[77] H.H. Skilling, M.H. Yamakawa, "A Graphical Solution of Transient Stability", Electrical Eng. 59, 1940, pp. 462-465.

[78] E.W. Kimbark, 'Power System Stability Volume I" , John Witley and Sons, Inc., New York, 1948.

[79] Task Force on Terms and Definitions, 'Proposed Terms and Definitions for Power System Stability", IEEE Transactions, Vol. PAS-101, No. 7, July 1982, pp. 1894-1898.

[80] A.A Fouad, V. Vittal, 'Power System Response to a Large Disturbance: Energy Associated with Separation", Proceedings from the IEEE 1983 Power Industry Computer Applications Conference, pp. 116-122.

[81] B. Toumi, R. Dhifaoui, Th. Van Custem, M. Pavella, 'Fast Transient Stability Assessment Revisited", IEEE Transactions on Power Systems, Vol. PWRS-1, No. 2, May 1986, pp. 211-220.

[82] F.J. Al Azzawi, F.F. Al Baldawi, "A Comparative Study of Fast Assessment Methods Used for Multimachine Power System Transient Stability", Proceedings of the Ninth Power Systems Computation Conference, Cascais, Portugal, Aug. 30-Sept. 4, 1987, pp. 633-638.

[83] Y. Xue, Th. Van Cutsem, M. Pavella, " A Simple Direct Method for Fast Transient Stability Assesment of Large Power Systems", IEEE Transactions on Power Systems, Vol. 3, No. 2, May 1988, pp. 400-412.

[84] Y. Xue, Th. Van Cutsem, M. Pavella, "Extended Equal Area Criterion Justifications, Generalizations, Applications", IEEE Transactions on Power Systems, Vol. 4, No. 1, February 1989, pp. 45-52.

[85] Y. Tamura, T. Motoyoshi, T. Ogata, Y. Tayama' 'Proposal of A New Voltage-Monitoring Scheme of Phase Difference Contours to Identify Weak Areas During Voltage Instability", Proceedings form the Tenth Power Systems Computational Conference, Graz Austria, August 19-24, 1990, pp. 1244-1251.

[86] J. Arrillaga, C.P. Arnold, 'Computer Analysis of Power Systems", John Wiley and Sons, New York, 1990.

[87] M. Klein, G.J. Rogers, P. Kundur, "A Fundamental Study of Inter-Area Oscillations in Power Systems", IEEE Transactions on Power Systems, Vol. 6, No. 3, March 1991, pp. 914-921.

[88] V. Vittal, N. Bhatia, A.A. Fouad, "Analysis of the Inter-Area Mode Phenomenon in Power Systems Following Large Disturbances", Transactions on Power Systems, Vol. 6, No. 4, November 1991. pp. 1515-1521.

[89] Y. Xue, l. Wehenkel, R. Belhomme, P. Rousseaux, M. Pavella, E.Euxibie, B. Heilbronn, J.F. Lesigne, 'Extended Equal Area Criterion Revisited", Transaction on Power Systems, Vol. 7, No. 3, 1992, pp. 1012-1022.

[90] C. Chang, A. Liu, C. Huang, 'Oscillatory Stability Analysis Using Real Time Measured Data", IEEE Transactions on Power Systems, Vol. 8 , No. 3, 1993, pp. 823-829.

[91] P.M. Anderson, A.A. Fouad, 'Power System Control and Stability", IEEE Press, New York, 1993.

[92] P. Kundur, 'Power System Stability and Control", McGraw-Hill, New York, NY, 1994.

[93] M. Pavela, P.G. Murthy, "Transient Stability of Power Systems Theory and Practice", John Wiley and Sons, New York, 1994.

[94] Jin Lu, James S. Thorp, "A Method for Fast Stability Prediction of One-Machine Infinite Bus Power System Using Real-Time Phasor Measurements", School of Electrical Enginnering, Cornell University, Ithaca, Ny 14853, (607)-255-3586.

B.8 System Model

[95] M.H. Kent, W.R. Schmus, F.A. McCrackin, L.M. Wheeler, "Dynamic Modeling of Loads in Stability Studies", Proceedings from the 1968 ASME/IEEE Joint Power Generation Conference, San Francisco California, September 15-19, 1968. 68TP 705-PWR.

[96] J. Robert, Y. Robichaud, "Load Behavior and Transient Stability", IEEE Conference Paper, PES Winter Power Meeting, January 1970, Paper 70CP149-PWR.

[97] T.G. Deville, F.C. Schweppe, "On Line Identification of Interconnected Network Equivalents from Operating Data", IEEE Conference Paper, PES Summer Meeting, July 1972, Paper C72 464-6.

[98] K.E. Bollinger, A.K. Laha, R.A. Winsor, "System Models From Transient Stability Programs", Proceedings from the 9th Conference on Power Industry Computer Applications, New Orleans, LA, June 2-4 1975, pp. 330-334

[99] W.W. Price, D.N. Ewart, E. m. Gulachenski, R.F. Silva, "Dynamic Equivalents from On-Line Measurements", IEEE Transaction on Power Apparatus and Systems, Vol. PAS-94, No. 4, July/August 1975.

[100] O.A. Agarkov, V.P. Kychakov, N.I. Voropai, 'Transient Stability Studies of Bulk Power Systems Using the Simplified and Detailed Mathematical Models", Proceedings from the Ninth Power Systems Computation Conference, Cascais Portugal, Aug. 30 - Sept. 4, 1987, pp. 617-621.

[101] A. Edstrom, K. Walve, J.A. Bubenko, 'Dynamic Equivalents for Large Scale Interconnected Power Systems", Proceedings from the Ninth Power Systems Computational Conference, Cascais Portugal, Aug. 30-Sept. 4, 1987, pp. 609-616.

[102] E. Handschin, A. Kubbe, Th. Reibing, 'Electric Load Modelling: Analysis, Identification and Validation", Proceedings from the Ninth Power Systems Computation Conference, Cascais Portugal, Aug. 30- Sept. 4, 1987, pp. 549-555.

[103] C. Rajagopalan, B. Lesieutre, P.W. Sauer, M.A. Pai, 'Dynamic Aspects of Voltage/Power Characteristics", IEEE Transaction on Power Systems, Vol. 7, No. 3, August 1992, pp.990-1000.

[104] V. Atarod, P.L. Dandeno, M.R. Iravani, 'Impact of Synchronous Machine Constants and Models on the Analysis of Torsional Dynamics", IEEE Transactions on Power systems, Vol. 7, No. 4, November 1992, pp. 1456-1463.

[105] IEEE Task Force, 'Load Representation For Dynamic Performance Analysis", IEEE Transactions on Power Systems, Vol. 8, No. 2, May 1993, pp. 472-482.

[106] 'Electrical World Directory of Electric Power Producers", 103rd Edition, New York, McGraw Hill, 1995.

[107] K. Kong, 'Real Time Simulations of EMTP Results", Master Thesis, Virginia Tech, Blacksburg, VA, Novemeber 1993.

[108] S.L. Anderson, 'Reduced Order Power System Models for Transient Stability Studies" ", Master Thesis, Virginia Tech, Blacksburg, VA, December 1993.

APPENDIX C

EVENT LOG

C.1 Introduction

For each filename, the name begins with "h" if the file was retrieved from Hatch, "d" if the file was retrieved from Duval. The date and time that the file was captured form the rest of the name. For example, **h3355754.dat** was collected at Hatch on day 33 of 1994, at 5:57:54 EST. Because the year is not included in the file notation the files collected on 1993 have a letter "a" following the first letter of the file and include only the day of the year hour and first digit of minutes. For Example, **da289181.dat** was trigger on day 289 of 1993 at 18 hours between minutes 10 and 19. Files were collected at Virginia Tech through the remote port in the relay units.*

C.2 October 1993

2 files collected for 2 events both swings

16 October 1993
da289181.dat; trigger = swing
18 October 1993
da2911414.dat; trigger = swing

C.3 November 1993

2 files collected for 2 event both swings

5 November 1993
da309095.dat; trigger = swing
19 November 1993
da323113.dat; trigger = swing

* Files were Collected by Nora Castro from February 1994 through February 1995.

C.4 December 1993

3 files collected for 3 events all swings

2 December 1993
da336075.dat; trigger = swing
5 December 1993
da339013.dat; trigger = swing
10 December 1993
da344061.dat; trigger = swing

C.5 January 1994

3 files collected for 2 event all swings

21 January 1994
d210619.dat; trigger = swing
29 January 1994
d292024.dat; trigger = swing
h292024.dat; trigger = swing

C.6 February 1994

20 files collected for 12 events: 11 swings and 1 external trigger

3 February 1994
h3355754.dat; trigger = swing
h3355756.dat; trigger = swing
h3355757.dat; trigger = swing
5 February 1994
h3517174.dat; trigger = external
6 February 1994
h378244.dat; trigger = swing
7 February 1994
h386853.dat; trigger = swing
8 February 1994
h3918261.dat (was dated 39:18:26:10); trigger = swing
h391826a.dat (was dated 39:18:26:11); trigger = swing
h391826b.dat (was dated 39:18:26:13); trigger = swing
h391826c.dat (was dated 39:18:26:14); trigger = swing
9 February 1994
h4093620.dat; trigger = swing

13 February 1994
h4413452.dat (was dated 44:13:45:27); trigger = swing
h441345a.dat (was dated 44:13:45:28); trigger = swing
h4413468.dat; trigger = swing
h4413469.dat; trigger = swing
14 February 1994
d4522332.dat; trigger = swing
d4522331.dat; trigger = swing
15 February 1994
d461257.dat; trigger = swing
16 February 1994
d4711106.dat; trigger = external
22 February 1994
h5217955.dat; trigger = swing

C.7 March 1994

26 files collected for 18 events: 16 swings and 2 external triggers.

3 March 1994
h612041.dat; trigger = swing
d612041.dat; trigger = swing
6 March 1994
h6515030.dat; trigger = swing
d6515030.dat; trigger = swing
13 March 1994
h721356.dat; trigger = external
15 March 1994
h74853.dat (t_0=74:8:53:50:432); trigger = swing
h74853a.dat (t_0=74:8:53:52:48); trigger = swing
h741125.dat; trigger = swing
19 March 1994
h771717.dat; trigger = swing
26 March 1994
d851010.dat; trigger = swing
d851010a.dat; trigger = swing
28 March 1994
d871329.dat; trigger = swing
d87155.dat; trigger = swing
d871811.dat; trigger = swing
d871811a.dat; trigger = swing
d871811b.dat; trigger = swing

29 March 1994
h82814.dat; trigger = swing
h831534.dat; trigger = swing
h851010.dat; trigger = swing
h851010a.dat; trigger = swing
h851753.dat; trigger = swing
h8517533.dat; trigger = swing
30 March 1994
d89033.dat; trigger = swing
d898047.dat; trigger = swing
d89152.dat; trigger = external
31 March 1994
d90652.dat; trigger = swing

C.8 April 1994

24 files collected for 19 events all swings.

2 April 1994
d911822.dat; trigger = swing
d91200.dat; trigger = swing
d91200a.dat; trigger = swing
d91200b.dat; trigger = swing
d912258.dat; trigger = swing
d92842.dat; trigger = swing
3 April 1994
d9329.dat; trigger = swing
h93957.dat; trigger = swing
h931122.dat; trigger = swing
4 April 1994
h932156.dat; trigger = swing
h932331.dat; trigger = swing
h94622.dat; trigger = swing
12 April 1994
h101195a.dat; trigger = swing
h101195b.dat; trigger = swing
h101195c.dat; trigger = swing
14 April 1994
d104140.dat; trigger = swing
d104448.dat; trigger = swing

19 April 1994
d1091314.dat; trigger = swing
21 April 1994
d111645.dat; trigger = swing
22 April 1994
d1111638.dat; trigger = swing
d111163b.dat; trigger = swing
d1111659.dat; trigger = swing
d112537.dat; trigger = swing
25 April 1994
d1151135.dat; trigger = swing

C.9 May 1994

36 events for 21 events: 1 external , 3 fault , 4 false faults and 13 swing triggers.

3 May 1994
d123419.dat; trigger = fault
d123942.dat; trigger = swing
d123943.dat; trigger = swing
d123944.dat; trigger = swing
d12394c.dat; trigger = swing
d123945.dat; trigger = swing
4 May 1994
d123163.dat; trigger = swing
5 May 1994
h1231132.dat; trigger = external
h123163.dat; trigger = swing
h1231614.dat; trigger = swing
h1231748.dat; trigger = swing
h1231749.dat; trigger = swing
h1231821.dat; trigger = swing
h123198.dat; trigger = swing
h1242245.dat; trigger = fault
6 May 1994
h125225.dat; trigger = fault
7 May 1994
d127120.dat; trigger = swing
h127120.dat; trigger = swing
14 May 1994
h13396.dat; trigger = swing
h134835.dat; trigger = swing
h134133.dat; trigger = swing

16 May 1994
d134133.dat; trigger = swing
d1351745.dat; trigger = swing
d135174b.dat; trigger = swing
h1351745.dat; trigger = swing
h135174b.dat; trigger = swing
h136124.dat; trigger = swing
17 May 1994
d136124.dat; trigger = swing
d137130.dat; trigger = swing
h1362239.dat; trigger = false fault trigger
h137130.dat; trigger = swing
18 May 1994
h137220.dat; trigger = False fault trigger
28 May 1994
h1472226.dat; trigger = false fault trigger
31 May 1994
d1502228.dat; trigger = swing
h1502213.dat; trigger = false fault trigger
h1502228.dat; trigger = swing

C.10 June 1994

46 files for 39 events: 2 external, 13 false faults and 24 swing triggers.

4 June 1994
h1551253.dat; trigger = swing
h1551422.dat; trigger = swing
h1551637.dat; trigger = swing
h1551724.dat; trigger = swing
h1551727.dat; trigger = swing
5 June 1994
h1552147.dat; trigger = false fault trigger
6 June 1994
d157148.dat; trigger = swing
h157148.dat; trigger = swing
h157148b.dat; trigger = swing
h1571638.dat; trigger = swing
h1571812.dat; trigger = swing
7 June 1994
h1572239.dat; trigger = false fault trigger

12 June 1994
h1621734.dat; trigger = swing
h1622253.dat; trigger = false fault trigger
13 June 1994
d1631928.dat; trigger = swing
h1632032.dat; trigger = swing
h1632322.dat; trigger = false fault trigger
14 June 1994
d1642155.dat; trigger = swing
h1642139.dat; trigger = swing
h1642155.dat; trigger = swing
h1642159.dat; trigger = swing
h1642311.dat; trigger = false fault trigger
15 June 1994
d1651751.dat; trigger = external
h1651754.dat; trigger = external
d166139.dat; trigger = swing
d1661514.dat; trigger = swing
h166139.dat; trigger = swing
h1661514.dat; trigger swing
h1661543.dat; trigger = false fault trigger
20 June 1994
h1711045.dat; trigger = false fault trigger
h1711931.dat; trigger = false fault trigger
21 June 1994
h172107.dat; trigger = false fault trigger
23 June 1994
h1741457.dat; trigger = false fault trigger
24 June 1994
h1741841.dat; trigger = swing
h1742316.dat; trigger = swing
25 June 1994
h1751643.dat; trigger = swing
h176032.dat; trigger = false fault trigger
h1761311.dat; trigger = swing
h1761318.dat; trigger = swing
h1761337.dat; trigger = swing

26 June 1994
h1762241.dat; trigger = swing
h1762355.dat; trigger = swing
h17709.dat; trigger = false fault trigger
h177212.dat; trigger = false fault trigger
29 June 1994
h1801319.dat; trigger = fault
h180159.dat; trigger = fault
30 June 1994
d1801319.dat; trigger = swing
h1802337.dat; trigger = false fault trigger

C.11 July 1994

33 files collected for 28 events: 1 external, 5 fasle faults and 22 swing triggers.

2 July 1994
d1821152.dat; trigger = swing
h1821820.dat; trigger = swing
h1821842.dat; trigger = swing
h1822222.dat; trigger = false fault trigger
4 July 1994
h1841959.dat; trigger = swing
h1842129.dat; trigger = false fault trigger
6 July 1994
h187110.dat; trigger = swing
h1871415.dat; trigger = fale fault trigger
h1871518.dat; trigger = external
9 July 1994
h1901348.dat; trigger = swing
11 July 1994
d1901348.dat; trigger = swing
d1911849.dat; trigger = swing
d1911851.dat; trigger = swing
13 July 1994
d19457.dat; trigger = swing
h19457.dat; trigger = swing
h194947.dat; trigger = swing
14 July 1994
d194947.dat; trigger = swing
d1941838.dat; trigger = swing
15 July 1994
d195127.dat; trigger = swing

17 July 1994
d198165.dat; trigger = false fault trigger
d199641.dat; trigger = swing
h199641.dat; trigger = swing
21 July 1994
h202110.dat; trigger = swing
23 July 1994
h2041417.dat; trigger = swing
24 July 1994
h2051238.dat; trigger = swing
26 July 1994
h2071851.dat; trigger = swing
28 July 1994
d202_a.dat; trigger = swing
d204_a.dat; trigger = swing
d207_a.dat; trigger = swing
29 July 1994
h210.dat; trigger = swing
30 July 1994
h211.dat; trigger = swing

C.12 August 1994

26 files for 19 events all swings.

1 August 1994
h213_a.dat; trigger = swing
3 August 1994
h215856.dat; trigger = swing
5 August 1994
h217150.dat; trigger = swing
6 August 1994
h218010.dat; trigger = swing
9 August 1994
h2211144.dat; trigger = swing
13 August 1994
h225039.dat; trigger = swing
h225730.dat; trigger = swing

17 August 1994
h2282039.dat; trigger = swing
h229252.dat; trigger = swing
h229519.dat; trigger = swing
h22979.dat; trigger = swing
h2291230.dat; trigger = swing
20 August 1994
h231a.dat; trigger = swing
h232a.dat; trigger = swing
23 August 1994
h2341713.dat; trigger = swing
d2341713.dat; trigger = swing
26 August 1994
h2381446.dat; trigger = swing
d2381446.dat; trigger = swing
28 August 1994
h2401344.dat; trigger = swing
d2401344.dat; trigger = swing
30 August 1994
h242537.dat; trigger = swing
d242537.dat; trigger = swing
31 August 1994
h2422026.dat; trigger = swing
d2422026.dat; trigger = swing
h2431450.dat; trigger = swing
d2431450.dat; trigger = swing

C.13 September 1994

28 files collected for 17 events: 1 false fault and 16 swing triggers.

8 September 1994
h2511525.dat; trigger = swing; to = 0 = 251:15:25:9:96
h25115b.dat; trigger = swing (multiple triggered event)
d2511525.dat; trigger = swing
d25115b.dat; trigger = swing
10 September 1994
h252204.dat; trigger = swing to = 0 = 252:20:4:24:48
d252204.dat; trigger = swing
12 September 1994
h2541935.dat; trigger = swing; to = 0 = 254:19:35:30:48
d2541935.dat; trigger = swing

13 September 1994
h256532.dat; trigger = swing; to = 0 = 256:5:32:52:120
16 September 1994
h259153.dat; trigger = swing; to = 0 = 259:15:3:30:384
h2591740.dat; trigger = swing; to = 0 = 259:17:40:49:144
17 September 1994
h2601248.dat; trigger = swing; to = 0 = 260:16:22:50:48
h2601622.dat; trigger = swing; to = 0 = 260:16:22:50:48
18 September 1994
h261935.dat; trigger = swing; to = 0 = 261:9:35:3:624
21 September 1994
h2632150.dat; trigger = swing; to = 0 = 263:21:50:7:624
23 September 1994
ht_265a.dat; trigger = swing; to = 0 = 265:7:30:48:384
ht_266b.dat; trigger = swing; to = 0 = 266:13:46:45:672
ht_266a.dat; trigger = swing; continuation of ht_266b.dat
dv 266_a.dat; trigger = swing; to = 0 = 266:13:46:45:696
25 September 1994
ht_268a.dat; trigger = swing; to = 0 = 268:8:11:56:96
dv_268a.dat, trigger = swing
26 September 1994
h269828.dat; trigger = swing; to = 0 = 269:8:28:3:600
d269828.dat; trigger = swing
27 September 1994
h270816.dat; trigger = swing; to = 0 = 270:8:16:32:192
d270816.dat; trigger = swing
28 September 1994
h271846.dat; trigger = swing; to = 0 = 271:8:46:42:576
d2711041.dat; trigger = false fault trigger; to = 0 = 271:10:41:27:96
30 September 1994
h273658.dat; trigger = swing; to = 0 = 273:6:58:30:696

C.14 October 1994

50 files for 29 events: 2 false fault and 27 swing triggers.

4 October 1994
h2761647.dat; trigger = swing; to = 0 = 276:16:47:3:648
5 October 1994
d273658.dat; trigger = swing (refer to Hatch table, 30 Sept.)
d2761647.dat; trigger = swing (refer to Hatch table, 4 Oct.)
h2781018.dat; trigger = swing; to = 0 = 278:10:18:58:504
d2781018.dat; trigger = swing

6 October 1994
h27910.dat; trigger = swing; to = 0 = 279:1:0:28:552
h279534.dat; trigger = swing; to = 0 = 279:5:34:8:312
h279811.dat; trigger = false fault trigger; to = 0 = 279:8:11:0:480
7 October 1994
d27910.dat; trigger = swing (refer to Hatch table 6 Oct.)
d279534.dat; trigger = swing (refer to Hatch table 6 Oct.)
12 October 1994
d284824.dat; trigger = false fault trigger; to = 0 = 284:8:24:56:288
14 October 1994
h287744.dat; trigger = swing; to = 0 = 287:7:44:20:216
h287744b.dat; trigger = swing; to = 0 = 287:7:44:32:624
h287147.dat; trigger = swing; to = 0 = 287:14:7:6:288
15 October 1994
h287214.dat; trigger = swing; to = 0 = 287:21:4:40:168
d287214.dat; trigger = swing
17 October 1994
h2901554.dat; trigger = swing; to = 0 = 290:15:54:26:240
19 October 1994
h292538.dat; trigger = swing; to = 0 = 292:5:38:12:696
20 October 1994
h293141.dat; trigger = swing; to = 0 = 293:1:41:34:72
h293528.dat; trigger = swing; to = 0 = 293:5:28:18:648
d293141.dat; trigger = swing
d293528.dat; trigger = swing
21 October 1994
h294521.dat; trigger = swing; to = 0 = 294:5:21:37:384
d294521.dat; trigger = swing
22 October 1994
h2942129.dat; trigger = swing; to = 0 = 294:21:29:31:288
h295726.dat; trigger = swing; to = 0 = 295:7:26:14:528
h295165.dat; trigger = swing; to = 0 = 295:16:5:16:144
h2951627.dat; trigger = swing; to = 0 = 295:16:27:14:504
d2942129.dat; trigger = swing
d295726.dat; trigger = swing
d295165.dat; trigger = swing
d2951627.dat; trigger = swing
23 October 1994
h296724.dat; trigger = swing; to = 0 = 296:7:24:52:288
d296724.dat; trigger = swing

24 October 1994
h29759.dat; trigger = swing; to = 0 = 297:5:9:33:216
d29759.dat; trigger = swing
26 October 1994
h299545.dat; trigger = swing; to = 0 = 299:5:45:1:600, CDT
h2991322.dat; trigger = swing; to = 0 = 299:13:22:18:576, CDT
h299132a.dat; multiple table event
d299545.dat
d2991322.dat
d299132a.dat
27 October 1994
h300154.dat; trigger = swing; to = 0 = 300:1:54:10:456, CDT
h300515.dat; trigger = swing; to = 0 = 300:5:15:44:288, CDT
d300154.dat
d300515.dat
28 October 1994
d3002323.dat; trigger = swing; to = 0 = 300:23:23:24:600, CDT
d301211.dat; trigger = swing; to = 0 = 301:2:11:47:336, CDT
d301515.dat; trigger = swing; to = 0 = 301:5:15:28:96, CDT
d301550.dat; trigger = swing; to = 0 = 301:5:50:19:696, CDT

C.15 November 1994

53 files for 23 events all swings.

3 November 1994
h3062318.dat; trigger = swing; to = 0 = 306:23:18:10:48, EDT
h307611.dat; trigger = swing; to = 0 = 306:6:11:39:600, EDT
d3062318.dat
d307611.dat
8 November 1994
h3121324.dat; trigger = swing; to = 0 = 312:13:24:13:480, EDT
h3121326.dat; trigger = swing; to = 0 = 312:13:26:13:288, EDT
10 November 1994
d313236.dat
14 November 1994
h3181136.dat; trigger = swing; to = 0 = 318:11:36:42:72, EDT
h3181230.dat
d3181136.dat
d3181230.dat

15 November 1994

h319142.dat; trigger = swing; to = 0 = 319:1:42:17:360, EDT
h319185.dat; trigger = swing; to = 0 = 319:18:5:48:312. EDT
d319142.dat
d319185.dat

18 November 1994

h320A.dat; trigger = swing; to = 0 = 320:14:31:32:240
h321A.dat; trigger = swing; to = 0 = 321:23:33:45:72
h322A.dat; trigger = swing; to = 0 = 322:6:19:39:408
h322B.dat; trigger = swing; to = 0 = 322:13:35:14:24
d320A.dat; trigger = swing
d321A.dat; trigger = swing
d322A.dat; trigger = swing
d322B.dat; trigger = swing

19 November 1994

h323A1.dat; trigger = swing; to = 0 = 323:0:5:7:672
h323A.dat; trigger = swing; to = 0 = 323:7:47:57:696
h323B1.dat; trigger = swing; to = 0 = 323:18:33:32:360
d322C.dat; trigger = switch; to = 0 = 322:23:1:51:288
d323A.dat; trigger = swing; to = 0 = 323:7:47:57:24

20 November 1994

h324A.dat; trigger = swing; to = 0 = 324:2:5:8:600
h324B.dat ; trigger = swing; to = 0 = 324:8:27:20:312
d324A.dat; trigger = swing; to = 0 = 324:2:5:8:648
d324B.dat; trigger = swing; to = 0 = 324:8:27:20:360

21 November 1994

h324C.dat; trigger = swing; to = 0 = 324:16:3:14:360
h325A.dat ; trigger = swing; to = 0 = 325:6:1:34:96
h325B.dat ; trigger = swing; to = 0 = 325:6:51:29:624

23 November 1994

h326A.dat; trigger = swing; to = 0 = 326:5:57:3:264
h327A.dat; trigger = swing; to = 0 = 327:6:28:55:576
d327A.dat; trigger = swing; to = 0 = 327:6:28:55:648

24 November 1994

h328A.dat; trigger = swing; to = 0 = 328:8:40:14:456
d328A.dat; trigger = swing; to = 0 = 328:8:40:14:480

25 November 1994

h328B.dat; trigger = swing; to = 0 = 328:22:15:20:96
h329A.dat; trigger = swing; to = 0 = 329:7:49:51:24

26 November 1994

h330A.dat; trigger = swing; to = 0 = 330:9:1:48:648

27 November 1994
h331101.dat; trigger = swing; to = 0 = 331:10:1:45:576
d331101.dat; trigger = swing; to = 0 = 331:10:1:45:600
28 November 1994
h33264.dat; trigger = swing; to = 0 = 332:6:4:59:600
30 November 1994
h3341542.dat; trigger = swing; to = 0 = 334:15:42:15:312
h334154a.dat; multiple table event.
d334123.dat; trigger = swing; to = 0 = 344:12:3:44:600
d334123a.dat; multiple table event.
d334123b.dat; multiple table event.
d3341542.dat; trigger = swing; to = 0 = 334:15:42:15:312
d334154a.dat; multiple table event.

C.16 December 1994

61 files for 25 events: 3 faults and 22 swings

1 December 1994
h3342217.dat; trigger = swing; to = 0 = 334:22:17:27:144
d3342217.dat; trigger = swing
2 December 1994
d336018.dat; trigger = swing; to = 0 = 336:0:18:12:384
4 December 1994
d3381140.dat; trigger = fault; to = 0 = 338:11:40:14:288
d3381321.dat; trigger = fault; to = 0 = 338:13:21:24:600
d338132a.dat; trigger = swing; to = 0 = 338:13:21:27:528
d338132b.dat; trigger = swing; to = 0 = 338:13:21:34:480
d338132c.dat; trigger = swing; to = 0 = 338:13:21:41:504
d3381322.dat; trigger = swing; to = 0 = 338:13:21:11:216
7 December 1994
h341612.dat; trigger = swing; to = 0 = 341:6:12:16:408
8 December 1994
h342032.dat; trigger as fault - work being done on line; to = 0 = 342:0:32:49:552
h342039.dat; trigger = swing; to = 0 = 342:0:39:8:168
h342041.dat; trigger = swing; to = 0 = 342:0:41:42:96
h342147.dat; trigger = swing; to = 0 = 342:1:47:20:432
h342215.dat; trigger = swing; to = 0 = 342:2:15:10:576
h342658.dat; trigger = swing; to = 0 = 342:6:58:5:456
d342032.dat; trigger = swing; to = 0 = 342:0:32:49:624
d34203a.dat; trigger = swing; to = 0 = 342:0:32:56:96
d342033.dat; trigger = swing; to = 0 = 342:0:33:0:240
d342033a.dat; multiple table event

d342033b.dat; trigger = swing; to = 0 = 342:0:33:5:24
d342033c.dat; trigger = swing; to = 0 = 342:0:33:21:600
d342033d.dat; trigger = swing; to = 0 = 342:0:33:27:96

9 December 1994

h3422332.dat; trigger = swing; to = 0 = 342:23:32:40:48
h3422338.dat; trigger = swing; to = 0 = 342:23:38:32:456
h3422340.dat; trigger = swing; to = 0 = 342:23:40:33:240
h343057.dat; trigger = swing; to = 0 = 343:0:57:18:528
h3430b.dat; trigger = swing; to = 0 = 343:0:57:28:456
h34313.dat; trigger = swing; to = 0 = 343:1:3:41:240
d3422332.dat; trigger = swing; to = 0 = 342:23:32:40:384
d34223b.dat; trigger = swing; to = 0 = 342:23:32:42:96
d34223c.dat; trigger = swing; to = 0 = 342:23:32:44:120
d34223d.dat; trigger = swing; to = 0 = 342:23:32:46:192
d34223e.dat; trigger = swing; to = 0 = 342:23:32:48:216
d34223f.dat; trigger = swing; to = 0 = 342:23:32:50:240
d34223g.dat; trigger = swing; to = 0 = 342:23:32:52:264

10 December 1994

h3432123.dat; trigger = swing; to = 0 = 343:21:23:59:600
d3432123.dat; trigger = swing
d3442159.dat; trigger = swing; to = 0 = 344:21:59:49:216

11 December 1994

h345658.dat; trigger = swing; to = 0 = 345:6:58:44:72
h345659.dat; trigger = swing; to = 0 = 345:6:59:31:504
h345659b.dat; trigger = swing; to = 0 = 345:6:59:55:360
d345658.dat; trigger = swing
d345659.dat; trigger = swing
d345659a.dat; trigger = swing

13 December 1994

h347618.dat; trigger = swing; to = 0 = 347:6:18:12:144
h3471142.dat; trigger = swing; to = 0 = 347:11:42:5:576
d347618.dat; trigger = swing
d3471142.dat; trigger = swing

15 December 1994

h3482311.dat; trigger = swing; to = 0 = 348:23:11:26:144
h349620.dat; trigger = swing; to = 0 = 349:6:20:9:144
d3482311.dat; trigger = swing
d349620.dat; trigger = swing

17 December 1994

h3501855.dat; loss of GPS time. Not plotted.

18 December 1994

h352844.dat; trigger = swing; to = 0 = 352:8:44:53:600
h3521316.dat; trigger = swing; to = 0 = 352:13:16:7:576
d3521316.dat; trigger = swing; to = 0 = 352:13:16:7:648

19 December 1994

h35369.dat; trigger = swing; to = 0 = 353:6:9:22:336
h353639.dat; trigger = swing; to = 0 = 353:6:39:56:216
h353640.dat; trigger = swing; to = 0 = 353:6:40:20:552
h3531614.dat; trigger = fault; to = 0 = 353:16:14:6:168

C.17 January 1995

26 files for 20 events: 1 false fault, 6 loss of sync and 13 swing triggers.

3 January 1995

h3_2336.dat, relay loss of sync

4 January 1995

h4_816.dat, trigger = swing, to = 0 = 4:8:16:6:336

6 January 1995

h6_723.dat, trigger = swing, to = 0 = 6:7:23:36:672
h6_1625.dat, trigger = swing, to = 0 = 6:16:25:14:120
h6_1629.dat, trigger = swing, to = 0 = 6:16:29:25:696

7 January 1995

h7_228.dat, trigger = swing, to = 0 = 7:2:28:55:192
h7_440.dat, trigger = swing, to = 0 = 7:4:40:52:264
d7_440.dat, see Hatch, 7 January
d7_440a.dat, relay loss of sync
d7_1812.dat, trigger = swing, to = 0 = 7:18:12:55:408

8 January 1995

d8_85.dat, trigger = swing, to = 0 = 8:8:5:47:24

9 January 1995

h91322.dat, trigger = swing, to = 0 = 9:13:22:57:456
h91554.dat, trigger = swing, to = 0 = 9:15:54:56:168
d91322.dat, trigger = swing, to = 0 = 9:13:22:58:264
d91554.dat, see Hatch, 9 January

11 January 1994

h11737.dat, trigger = swing, to = 0 = 11:7:37:44:696
d11737.dat, trigger = swing, to = 0 = 11:7:27:43:624
d111821.dat, trigger = false fault trigger, relay loss of sync

13 January 1995

h13619.dat, trigger = swing, to = 0 = 13:6:19:33:240
h13810.dat, trigger = swing, to = 0 = 13:8:10:52:120

25 January 1995

h25659.dat, trigger = swing, to = 0 = 25:6:59:35:264

h352844.dat; trigger = swing; to = 0 = 352:8:44:53:600
h3521316.dat; trigger = swing; to = 0 = 352:13:16:7:576
d3521316.dat; trigger = swing; to = 0 = 352:13:16:7:648

19 December 1994

h35369.dat; trigger = swing; to = 0 = 353:6:9:22:336
h353639.dat; trigger = swing; to = 0 = 353:6:39:56:216
h353640.dat; trigger = swing; to = 0 = 353:6:40:20:552
h3531614.dat; trigger = fault; to = 0 = 353:16:14:6:168

C.17 January 1995

26 files for 20 events: 1 false fault, 6 loss of sync and 13 swing triggers.

3 January 1995

h3_2336.dat, relay loss of sync

4 January 1995

h4_816.dat, trigger = swing, to = 0 = 4:8:16:6:336

6 January 1995

h6_723.dat, trigger = swing, to = 0 = 6:7:23:36:672
h6_1625.dat, trigger = swing, to = 0 = 6:16:25:14:120
h6_1629.dat, trigger = swing, to = 0 = 6:16:29:25:696

7 January 1995

h7_228.dat, trigger = swing, to = 0 = 7:2:28:55:192
h7_440.dat, trigger = swing, to = 0 = 7:4:40:52:264
d7_440.dat, see Hatch, 7 January
d7_440a.dat, relay loss of sync
d7_1812.dat, trigger = swing, to = 0 = 7:18:12:55:408

8 January 1995

d8_85.dat, trigger = swing, to = 0 = 8:8:5:47:24

9 January 1995

h91322.dat, trigger = swing, to = 0 = 9:13:22:57:456
h91554.dat, trigger = swing, to = 0 = 9:15:54:56:168
d91322.dat, trigger = swing, to = 0 = 9:13:22:58:264
d91554.dat, see Hatch, 9 January

11 January 1994

h11737.dat, trigger = swing, to = 0 = 11:7:37:44:696
d11737.dat, trigger = swing, to = 0 = 11:7:27:43:624
d111821.dat, trigger = false fault trigger, relay loss of sync

13 January 1995

h13619.dat, trigger = swing, to = 0 = 13:6:19:33:240
h13810.dat, trigger = swing, to = 0 = 13:8:10:52:120

25 January 1995

h25659.dat, trigger = swing, to = 0 = 25:6:59:35:264

26 January 1995

d261838.dat, relay loss of sync

28 January 1995

d281007a.dat, relay loss of sync

d281007b.dat, relay loss of sync

29 January 1995

h290850.dat, trigger = swing, to = 0 = 29:8:50:9:120

h291656.dat, relay loss of sync

C.18 February 1995

2 files for two events: 1 loss of sync. and 1 swing trigger.

1 February 1995

h320817.dat, trigger = swing, to = 0 = 32:8:17:38:696

h321908.dat, relay loss of sync.